IDENTIFICATION AND MANIPULATION OF KEY REGULATORS IN LACE PLANT PROGRAMMED CELL DEATH

by

Adrian Noble Dauphinee

Submitted in partial fulfilment of the requirements
for the degree of Doctor of Philosophy

at

Dalhousie University
Halifax, Nova Scotia
May 2017

To my parents, John and Suzanne, and my brother Richard. Thank you for all of your understanding, support, and for teaching me the importance of hard work and chasing dreams.

TABLE OF CONTENTS

LIST OF TABLES

LIST OF FIGURES

ABSTRACT

The lace plant (*Aponogeton madagascariensis*) is an aquatic monocot species that has emerged as a model for studying developmental programmed cell death (PCD). In multicellular eukaryotes, PCD plays vital roles in development and survival through the targeted deletion of compromised or superfluous cells. PCD occurs as part of normal leaf development in the lace plant and results in perforations throughout the lamina, thereby creating the lattice-like appearance from which its common name was derived. The lace plant provides an excellent model system due to: the predictability of PCD, the suitability of its leaves for live cell imaging, and availability of axenic cultures allowing for efficient propagation and pharmacological experimentation. Taking advantage of the lace plant system features, the cellular dynamics and time-course analysis of lace plant PCD has been described, however little is known about the regulation of this rarely observed type of developmentally regulated cellular death in leaves. The objective of this study is to identify the key regulators of lace plant PCD and to develop a genetic transformation protocol that will allow for greater control and understanding of the process. The regulators investigated include the phytohormone ethylene, antioxidants and reactive oxygen species (ROS), and the autophagic "self-eating" intracellular degradation pathway. Data indicate that ethylene and ROS are positive regulators of lace plant PCD, while antioxidants and autophagy function in cell survival and confer tolerance to the induction of cell death. Additionally, we show that the lace plant is amenable to *Agrobacterium tumefaciens*- mediated genetic transformation. The work shown here provides a model for lace plant PCD signaling and a framework to advance the system moving forward. Elucidating the mechanisms controlling cellular death in the lace plant contributes to the PCD literature. The ability to regulate PCD has a wide range of applications from agriculture to medicine. Understanding of plant PCD regulation can be employed to reduce postharvest losses or to develop crops more resistant to environmental stressors, and potential medicinal applications may arise due to the functional conservation observed among eukaryotic lineages for this vital process.

LIST OF ABBREVIATIONS USED

1-MCP	1-methylcyclopropene
3MA	3-methyladenine
AA	Ascorbic acid
ABTS	2,2′-azino-bis-3-ethylbenzothiazoline-6-sulfonic acid
ACC	1-aminocyclopropane-1-carboxylic acid
AdoMet	S-adenosyl methionine
Akt	Protein kinase B
ANOVA	Analysis of variance
AOA	Aminooxyacetic acid
APX	Ascorbate peroxidase
ATG	Autophagy related
AVG	Aminoethoxyvinyl glycine
AVI	Audio video interleave
BAP	6-benzylaminopurine
C3RE	Cyanidin-3-rutinoside equivalents
CAT	Catalase
Cys	Cysteine
Cyt c	Cytochrome c
CV	Central vacuole
DISC	Death-inducing signaling complex
DIC	Differential interference contrast
EPCD	Early-programmed cell death
ER	Endoplasmic reticulum
ERF	Ethylene response factors
FDA	Food and drug administration
GFP	Green fluorescent protein
GLM	General linear model
GPX	Glutathione peroxidase
HR	Hypersensitive response

HRP	Horseradish peroxidase
HTS	High throughput screening
IMS	Intermembrane space
LPCD	Late-programmed cell death
MDC	Monodansylcadaverine
MS	Murashige and Skoog
mTOR	Mammalian target of rapamycin
mTORC	Mammalian target of rapamycin complex
MTSB	Microtubule stabilization buffer
NAA	1-napthaleneacetic acid
NBT	Nitro blue tetrazolium
NCCD	Nomenclature Committee on Cell Death
nDNA	Nuclear deoxyribonucleic acid
NPCD	Non-programmed cell death
NPP	Normal probability plot
PCD	Programmed cell death
PCR	Polymerase chain reaction
PI3K	Phosphoinositide 3-kinase
PIC	Picloram
PM	Plasma membrane
PTC3	Plant tissue culture contamination control
Ri	Root-hair inducing
ROS	Reactive oxygen species
SAM	Shoot apical meristem
SOD1	Superoxide dismutase 1
T-DNA	Transfer-DNA
TDZ	Thidiazuron
Ti	Tumour-inducing
TUNEL	Terminal deoxynucleotidyl transferase-mediated dUTP nick end-labeling
TBS	Tris-buffered saline
TBS-T	Tris-buffered saline with tween 20

TEM	Transmission electron microscopy
VALAP	Vaseline lanolin paraffin wax
ZPCK	Z-L phe chromethyl ketone

ACKNOWLEDGEMENTS

My deepest thanks to Arunika Gunawardena, for your mentorship and dedication throughout this journey. Whatever challenges arose, I knew that we would persevere. I am truly grateful for all of the paths and opportunities you have made for me. Thank you Christian Lacroix for always being there to offer support, guidance and share your wisdom. A special thanks to Tom MacRae for always providing assistance, access to equipment and advice when I needed it, and to both Tom and Mark Johnston for serving on my committee. The support, training and guidance I received from Keiko Yoshioka and Ron Qu were instrumental transformation experiments. To all the Gunawardena lab members that I've had the pleasure to work with over the years: unravelling the mysteries of the lace plant with all of you has been an incredible and unpredictable experience that I will never forget. Thank you to all my friends, family and Stephanie Connors for her support.

I am extremely grateful for the funding from Dalhousie University, The Natural Sciences and Engineering Research Council of Canada, and The Killam Trusts that provided support and allowed me to pursue this work to the fullest.

CHAPTER 1

INTRODUCTION

Large portions of this introduction are published as:

Dauphinee AN, Gunawardena AHLAN (2015) An overview of programmed cell death research: from canonical to emerging model species. In: Gunawardena AHLAN, McCabe PF, editors. Plant programmed cell death. Springer International, Switzerland. p 1–31.

1.1. PROGRAMMED CELL DEATH

Programmed cell death (PCD) is an active intracellular-mediated form of destruction that allows for the precise removal of cells as part of development and homeostasis (Green 2011). Due to the intrinsic nature of PCD to multicellular life, it has been intensively studied in a wide array of processes, primarily in eukaryotes. More recently however, apparent forms of PCD have been discovered in a diverse range of microbial organisms including yeast and bacteria, where it helps the development of populations and the survival of communities (Deponte 2008; Bayles 2014; Allocati et al. 2015). Although there are functional similarities between eukaryotic and bacterial PCD, the evolutionary origins of regulated cell death processes remain unclear (Rice and Bayles 2003; Deponte 2008). Regardless of the origins, it is evident that PCD has been refined to serve specific

developmental roles and to allow organisms to adapt to various harmful environmental stimuli.

1.2. CLASSES OF ANIMAL CELL DEATH

Cellular death is best understood in animals and was initially categorized into three major types primarily based on morphology: apoptosis (Type I), autophagy or autophagic cell death (Type II), and necrosis (Type III; Green 2011 Galluzzi et al. 2012; Galluzzi et al. 2015). Apoptosis is the most commonly observed form of programmed cell death (Green 2011). Kerr et al. (1972) coined the usage of the term apoptosis, which is a Greek derivation for the dropping or falling off of petals or leaves from flowers or trees, respectively. Kerr et al. (1972) observed that apoptosis was an active phenomenon with a complementary, although opposing role to mitosis in the homeostasis of animal cell populations. The morphological features of this process include: a reduction of cellular volume, chromatin condensation, nuclear fragmentation, no (or few) modifications to the ultrastructure of cytoplasmic organelles, plasma membrane (PM) blebbing and an intact PM until advanced stages (Kroemer et al. 2005). Cellular contents are packaged into apoptotic bodies, which are then engulfed and digested by phagocytes and, thus, an immune response is not triggered (Green 2011). The biochemical pathways and molecular interactions that carry out apoptosis, are well-understood.

In order to facilitate comparisons of cell death mechanisms amongst the kingdoms, the vertebrate apoptotic regimes known as the intrinsic and extrinsic pathways will be

discussed in brief. In both of these apoptotic pathways, the irreversible destruction of the cell is executed by cysteine-aspartic proteases (caspases). The differences between the two pathways are in the activation of the executioner caspases. In the intrinsic pathway, Bcl-2 family proteins are key pro- and anti-apoptotic regulators that affect the release of the mitochondrial intermembrane space (IMS) protein cytochrome c (cyt c). Cyt c goes on to trigger intermediates (which vary among animals) prior to caspase activation. In the extrinsic pathway, caspase activation occurs after the formation of a death-inducing signaling complex (DISC), which follows the ligation of a death receptor found on the surface of the cell (Kroemer and Reed 2000; Klener 2006). Additionally, it should be pointed out that among animal systems there is diversity in the numbers and types of caspases present, as well as a myriad of induction signals and pro/anti-apoptotic regulatory proteins involved. It appears as though apoptosis has been fine-tuned in various species through the course of evolution leading to the wide diversity of pathways which have been identified to date (Oberst et al. 2008; Green 2011; Fuchs and Steller 2011).

Type II, or autophagic cell death is driven by autophagy ("self-eating") and is the other classically defined form of PCD that occurs in animals, but it is not well understood in comparison to apoptosis (Green 2011). Similarities exist in the two types in that: i) neither trigger an inflammatory response in tissues and ii) like apoptosis, autophagy can exhibit DNA laddering and caspase activation. However, both of these features occur late, if at all (Levine and Yuan 2005; Kroemer 2009; van Doorn 2011). Autophagic cell death is primarily distinguishable from apoptosis by morphology, the presence of

autophagosomes, and involvement of autophagy proteins (Tsujimoto and Shimizu 2005; Green 2011). Autophagosomes are double-membrane vesicles that sequester cytoplasmic contents and deliver them to a lytic compartment for degradation. Autophagy itself, not to be confused with autophagic cell death, is primarily a survival mechanism that allows for the remobilization of resources and it can inhibit and/or precede apoptosis (Mariño et al. 2014). Whether or not autophagy actually contributes to cellular death has been debated as there is little evidence suggesting it is responsible for PCD induction. It appears as though in many cases, autophagy contributes to the cell's effort to stay alive, suggesting that the term autophagic cell death may be a misnomer (Levine and Yuan 2005; Tsujimoto and Shimizu 2005; Kroemer and Levine 2008; Liu and Bassham 2012).

Necrosis (or Type III cell death), is triggered following severe injury to the cell and can be viewed as an accidental form of death with swelling and bursting of the cell (Galluzi et al. 2015). The lack of control and haphazard release of cellular contents can elicit an immune response within an animal body, which is in sharp contrast to PCD via apoptosis and autophagic cell death (Green 2011). Necrotic death is usually initiated by an early rupture of the plasma membrane from a given stressor that triggers sudden physical damage to the plasma membrane, decreased energy levels, or loss of function of ion channels (Zong and Thompson 2006). There is evidence suggesting that necrosis is also a form of PCD; however, this notion is still contested. Intermediate classifications such as necroptosis or aponecrosis (Zong and Thompson 2006; Vandenabeele et al. 2010) have also been used to define categories of cellular death but these terms are not yet widely accepted (Green 2011). There has been extensive research on animal cell death over the

last four decades and many aspects of the signaling and regulatory pathways of these cell death types have been discovered (Zong and Thompson 2006; Vandenabeele et al. 2010; Green 2011; Mariño et al. 2014). It should be pointed out that, as biochemical and molecular evidence accumulates, it is apparent that apoptosis and autophagy affect each other (Edinger and Thompson 2004; Mariño et al. 2014), however the ability of autophagy to cause cell death is in doubt (Shen et al. 2012). In light of advancements in the field, the Nomenclature Committee on Cell Death (NCCD) recently proposed classifications based on well-defined subroutines that allow for their detection (Galluzzi et al. 2012). The subroutines are: extrinsic and intrinsic apoptosis, regulated necrosis, autophagic cell death and finally, mitotic catastrophe (Galluzzi et al. 2012). However, for the purposes of this chapter, henceforth we will draw comparisons between cell death in plants and the characteristics of the three classical forms of animal cell death outlined above.

1.3. PCD PROCESSES AND SIGNALING IN PLANTS

Plant cells, like those of animals can be destroyed via PCD or necrosis; the latter being originally defined as an uncontrolled, accidental death. PCD is critical for proper development and survival of plants (Greenberg 1996) and is activated during a myriad of life processes (Lam 2004). Putative examples of PCD in higher plants include: the deletion of the embryonic suspensor, aleurone degeneration (in monocots), tracheary element and trichome development, shedding of root cap cells, aerenchyma formation, leaf morphogenesis, abortion of floral organs, megaspore development and the

hypersensitive response (HR) (Gray 2004; Gunawardena 2008; Kacprzyk et al. 2011). Through the study of PCD processes in various plant systems, similarities to animal apoptosis have been found including: a reduction of cellular volume (or cell shrinkage), nuclear condensation, nDNA fragmentation, release of cyt c, and the involvement of caspase-like proteases such as vacuolar processing enzymes (VPEs) and metacaspases (Hara-Nishimura et al. 2005; Kacprzyk et al. 2011; Tsiatsiani et al. 2011; Lord and Gunawardena 2012).

Despite the overlap of some features, there are marked differences between plant and animal PCD, some of which can be attributed directly to characteristics inherent to plants. Examples include plant hormones such as: ethylene (Bouchez et al. 2007; Trobacher 2009), jasmonic acid, abscisic acid (Young and Gallie 1999), and gibberellic acid (Trobacher et al. 2013), which have all been implicated in PCD signaling pathways. Chloroplasts are also suspected of playing key regulatory roles in cellular death signaling primarily due to their role in energy production and ability to produce reactive oxygen species (ROS), which are known to trigger PCD in many animal and plant systems (Doyle et al. 2010; Ambastha et al. 2015). Other major sources of ROS production in plants include mitochondria, peroxisomes and cell walls (Mignolet-Spruyt et al. 2016). The plant vacuole is a large hydrolytic compartment contributing up to 90% of a cells volume and it plays a major role in the degradation of cellular constituents (Hedrich and Neher 1987; Marty 1999). The vacuole appears to play a central role in plant PCD and the autolysis of the cell during autophagy, breaking down contents delivered for degradation (Marty 1999; Bassham 2007).

1.4. CLASSES OF PLANT PCD

There are two broad categories of plant PCD: environmentally induced and developmentally regulated (Gunawardena 2008). In terms of specific forms of plant PCD, studies and classifications have historically drawn heavily upon comparisons to animal cell death pathways (Bozhkov and Lam 2011). For instance, terminology such as apoptotic-like cell death and autophagic cell death has been widely used in the past. Due to lack of consistency in the literature regarding the specific forms of PCD, Bozhkov and Lam (2011) called for the development of clear morphological classification system for plant PCD. As a result, two forms of plant PCD were proposed: vacuolar and necrotic cell death (van Doorn et al. 2011). Vacuolar cell death involves autophagy-like processes along with the release of hydrolases from lytic vacuoles to produce a cell corpse that is largely cleared. In contrast, necrotic death can be differentiated as there is an early rupture of the PM, shrinkage of the protoplast, swelling of various organelles, a lack of autophagy, and a cell corpse that is more or less unprocessed. Additionally, the authors convincingly argue that apoptosis, or apoptosis-like terminology should not be applied to plant PCD systems since the formation of apoptotic bodies is not observed following blebbing of the plasma membrane, which, as mentioned above, is a primary morphological indicator of Type I cell death (or apoptosis) in animals. Moreover, it is also noted by van Doorn et al. (2011) that cases exist of either mixed or “atypical” cell death forms that do not neatly fall into the proposed categories. The authors emphasize that their classification is not meant to be static and should be changed if necessary as

more evidence is gathered. Although there has been some debate regarding the classification of plant PCD (van Doorn 2011; Reape and McCabe 2013), there appears to be a consensus that more biochemical and molecular data is necessary to gain a clearer picture of the pathways and diversity of cell death in plants. Studying PCD in a variety of plant systems outside of the canonical models such as *Arabidopsis thaliana* will also help to characterize the forms of this process.

1.5. THE LACE PLANT: A PCD MODEL SYSTEM

1.5.1. The Aquatic Lace Plant

Lace plant [*Aponogeton madagascariensis* (Mirb.) H. Bruggen] is a member of the cape pond-weed family, or Aponogetonaceae, which consists of a single genus of aquatic monocots (van Bruggen 1985). The monograph of the family described 43 species (van Bruggen 1985), but a recent phylogenetic study suggests there are at least 52 *Aponogeton* species (Les and Tippery 2013). Lace plants are endemic to the Comoros Islands and Madagascar and naturalized in Mauritius. They are submerged freshwater plants found in stagnant and running waters, including rapids and torrents (van Bruggen 1985). Lace plants (Figure 1.1) have a spherical corm bearing roots and helically arranged leaves and inflorescences with white or violet flowers on two spikes, which are exposed above water after peduncle growth (van Bruggen 1985). The leaves have a distinct perforated leaf morphology which has led to its cultivation as an aquarium ornamental for over a century, although its cultivation has long been viewed as difficult and the plant is known

to rarely flower outside of its natural habitat (Sergueff 1907; van Bruggen 1985). Lace plant is the only aquatic vascular plant known to produce holes during leaf morphogenesis. Outside of the Aponogetonaceae, only a few genera of the Araceae family are known to contain species with leaf perforations (Gunawardena 2008; Nowak et al. 2011). Both the Aponogetonaceae and the Araceae belong to the monocot order Alismatales, but it is unknown whether the formation of perforations during leaf morphogenesis in the two families has a common evolutionary origin. The function of perforations in leaf lamina remains unknown, although several hypotheses have been proposed. The perforations may aid contribute to: thermoregulation, reduce drag in flowing waters, camouflage, or protection against herbivory (Gunawardena and Dengler 2006).

Figure 1.1 The lace plant (*Aponogeton madagascariensis*). (A) Habitus of the lace plant, which consists of: a spherical corm (1) bearing roots (2) and shoots. The first 3-4 leaves to grow in culture typically do not perforate (3). Leaves that develop later contain anthocyanins (4) and do perforate as they progress towards maturity (5). (B) Lace plant growing in magenta box culture (black arrow = window stage leaf, where PCD is actively occuring). (C) Aquarium-grown plant producing inflorescences (white arrows). (D) Mature inflorescence that has emerged from the water. Bars = 2 cm.

1.5.2. Perforation Formation: A Unique Gradient of PCD

PCD in the lace plant occurs in a spatio-temporally predictable manner between longitudinal and transverse veins and results in a lattice-like pattern in the mature leaves (Gunawardena et al. 2004). Typically, the first 3-4 leaves to form have a simple, non-perforated morphology and are the smallest leaves that are produced (Figure 1.1A). Leaves that develop afterwards contain anthocyanins and produce perforations. The process is broken-down into five stages: preperforation, window, perforation formation, perforation expansion, and mature (Figure 1.2; Gunawardena et al. 2004). Preperforation leaves are those which have newly emerged from the corm, are tightly furled, and have an abundance of anthocyanins. Based on light and scanning electron microscopy observations, there are no morphological indications that PCD will occur in these leaves (Figure 1.2A). PCD is active during the window stage (Figure 1.2B), which exhibits a distinct coloration gradient within areoles (framed by longitudinal and transverse veins) due to cells at different stages of PCD (discussed below). Next, during perforation formation (Figure 1.2C), a hole forms at the center of the areole and the zone of cell death extends outwards. The size of the perforation significantly increases by the perforation expansion stage, but halts 4-5 cell layers from the vasculature (Figure 1.2D). At the mature stage of development (Figure 1.2E), perforation formation is complete and there are no longer any cells undergoing PCD. Additionally, mesophyll cells at the perforation border transdifferentiate into epidermal cells and a layer of suberin is produced to prevent nutrient loss and limit pathogen invasion (Gunawardena et al. 2007).

A unique gradient of cell death is visible within areoles of the window stage (Figure 1.2F, Appendix A: Online Resource 1.1). Lord et al. (2011) identified three distinct cell phases along this gradient: non-, early- and late-PCD (N-, E-, and LPCD, respectively). NPCD cells (Figure 1.2G) are those which retain their chlorophyll and anthocyanin pigmentation (which is in mesophyll cells) throughout perforation formation and persist throughout maturity. These cells maintain regular functions, unlike EPCD stage cells (Figure 1.2H) which are green due to chlorophyll pigmentation but have lost their anthocyanin and are fated to die. LPCD cells (Figure 1.2I) are on the brink of death and are distinguishable as being nearly transparent, with little to no chlorophyll pigmentation left. The fascinating gradient of PCD in the lace plant window stage is easily accessible and can be observed within a single field of view. This provides a distinct advantage over many other systems as cellular observations can be made simultaneously among control cells (NPCD) and those in the early and later phases of developmental cell death. The lace plant has emerged as a model system to study developmental PCD due to the predictability of perforation formation, its suitability for live cell imaging, and the availability of axenic cultures.

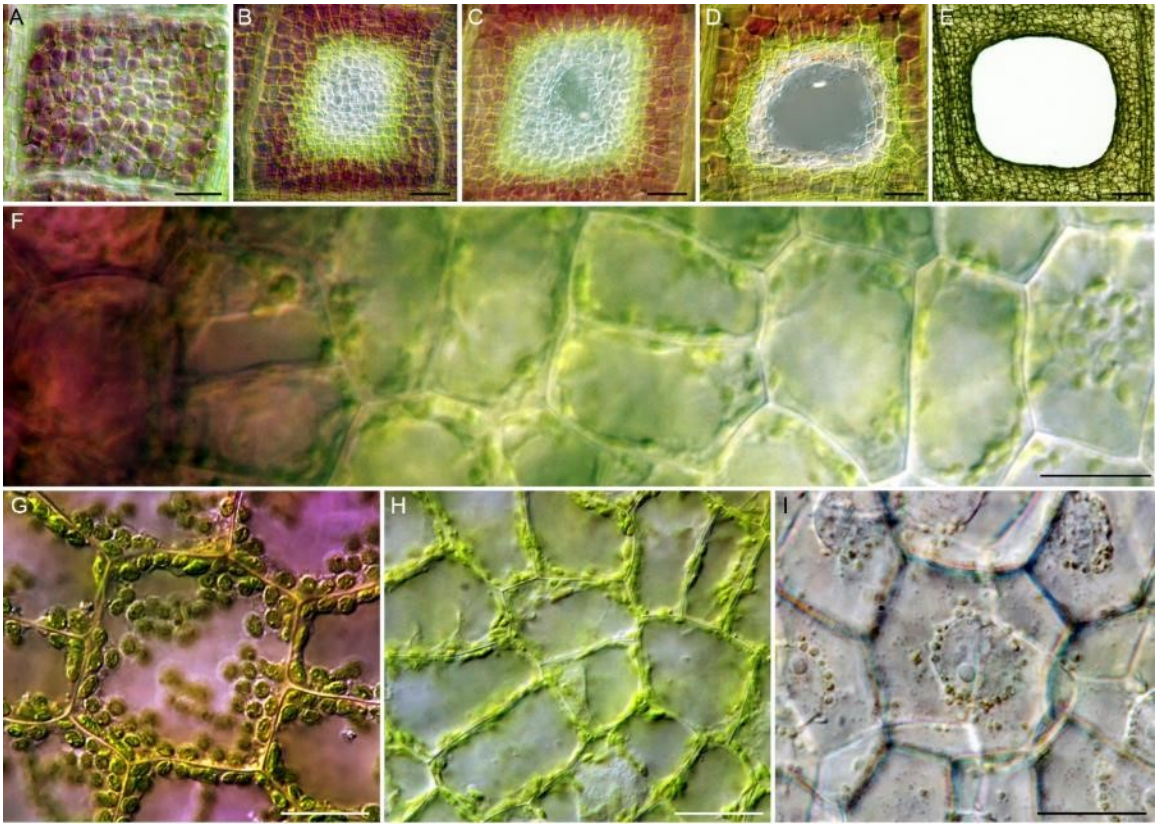

Figure 1.2. Stages of lace plant perforation formation and the PCD gradient. (A) There are no visible signs that PCD will occur in preperforation stage areoles (space between longitudinal and transverse veins). (B) During the window stage of development, PCD is actively occurring. (C) The perforation formation stage occurs when a physical tear is visible in the areole. (D) Cell death then radiates outward, and the hole widens significantly before the perforation expansion stage. (E) PCD halts 4–5 cell layers from the veins by the mature stage. (F) Within the window stage there is a gradient of cell death (see also, Appendix A: Online Resource 1.1). (G) Non-PCD, or NPCD cells do not die as the perforation forms, (H) Early-PCD, or EPCD cells have lost anthocyanins and are slated for death. (I) Late-PCD, or LPCD stage cells have lost most of their pigmentation and are near death. Bars: A = 50 µm; B-C = 75 µm; D = 100 µm; E = 300 µm; F = 30 µm; G = 40 µm; H = 50 µm; I = 40 µm.

1.5.3. The Dynamics of Lace Plant Developmental PCD

Lace plant developmental PCD detailed by Wertman et al. (2012) is described below. The work featured the unique gradient of PCD in combination with compound light, scanning electron, and laser scanning confocal microscopy techniques. In addition, the

authors made a custom slide as part of a novel live cell imaging assay that allowed for the observation of PCD during the formation of perforations in whole leaves (Wertman et al. 2012). The disappearance of anthocyanin pigmentation and an increase in vesicle formation (which continues to the very late stages of PCD) are among the first visible cues indicating that cells are fated to die. Following this, chlorophyll degradation begins along with actin microfilament bundling (visualized using Alexa Fluor 488 phalloidin staining) and an increase in organelle movement on transvacuolar strands. The aggregation of mitochondria and the perinuclear accumulation of mitochondria and chloroplasts is next. Later in the cell death process, nuclei are positive for terminal deoxynucleotidyl transferase-mediated dUTP nick end-labeling (TUNEL; indicating nDNA fragmentation), the breakdown of the actin cytoskeleton, and early changes in the cell wall are observed. Prior to cell death, there is a visible swelling of the vacuole followed by the tonoplast collapse. The cessation of vacuolar aggregate movement, nuclear shrinkage, and the complete loss of mitochondrial membrane potential occur in the time between tonoplast and plasma membrane collapse. The visible dissolution of the cell wall takes place after the condensation of the cell (Wertman et al. 2012). A previous study concerning the cell wall revealed that cell wall degradation begins early in the cell death process and the walls are significantly weakened by the time perforations form, thereby facilitating the mechanical rupture (Gunawardena et al. 2007). Long-term live cell imaging experiments (lasting > 72 hours) that captured continuous video as the perforation developed revealed that during lace plant leaf morphogenesis, it takes approximately 48 h from the point of chlorophyll reduction to the collapse of the PM (Wertman et al. 2012).

1.5.4. Comparisons of Developmental and Environmentally Induced PCD

The characteristics of the lace plant also facilitates the study of cell death induced by environmental stimuli. The live cell imaging technique developed by Wertman et al. (2012) highlighted the unique gradient of PCD in the lace plant and the advantages of using this model system. The assay was modified to view the effects of various stressors (heat-shock, NaCl, HCL and NaOH) at various intensities on leaves as well as leaf sections (Dauphinee et al. 2014). Video analysis was used to compare the timeframe and dynamics of developmental PCD as described by Wertman et al (2012) versus induced cell death (Figure 1.3A, B; Appendix A: Online Resource 1.2). As mentioned earlier, in lace plant developmental PCD, the vacuole plays a central role, and there is a retraction of the PM at death. Regardless of the intensity or form of stressor, similar vacuolar dynamics were observed (Dauphinee et al. 2014), suggesting the vacuole plays a central role in all forms of death in the lace plant. Significant differences were also observed among the treatments, most notably in cell volume reduction or retraction of the PM at death (Dauphinee et al. 2014). A protocol for the isolation of protoplasts from window stage leaves was also developed and utilized to compare developmentally regulated and environmentally induced PCD (Lord and Gunawardena 2010). Differences in pigmentation between NPCD and PCD cells can be used as a rough indicator of physiological status prior to exposure to harmful stimuli. Similarities found between the two modes of cellular death included the blebbing of the PM, increased numbers of transvacuolar strands and vesicles, Brownian motion in the vacuole, nuclear

condensation, TUNEL positive nuclei and tonoplast rupture. Additionally, just as in developmental PCD, mitochondria play a key role in death induced by heat-shock (Lord and Gunawardena 2010). Treatment of protoplasts with cyclosporine A, which inhibits pore formation in mitochondrial, increases protoplast viability when compared to the heat-shock treatment alone (Lord and Gunawardena 2010).

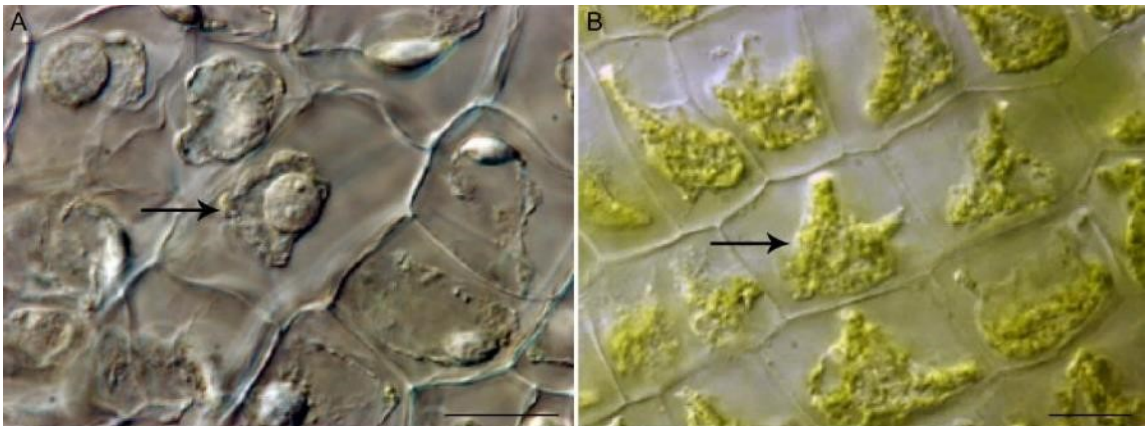

Figure 1.3. Inducing cell death in the lace plant. (A) Cells which have died via developmentally regulated PCD (~48 h process) showing a neatly package cell corpse (arrow). (B) 2 M NaCl wet mount cells turn green and die within ~4 h of initial exposure. The cells also have a condensed morphology (arrow) that is somewhat similar to that seen in developmental PCD, but there is less cytoplasmic clearing, and the process is considerably faster. Bars: 20 µm.

1.6. THESIS OUTLINE

The intracellular dynamics of PCD are well defined in the lace plant, however little is known about the key regulators and the signaling pathway controlling this process. In addition, biochemical and molecular techniques specific to the lace plant are limited and require development to advance this novel model system. Identifying the mechanisms regulating PCD is the next step towards understanding the PCD pathway and gaining the ability to induce or inhibit perforation formation. Therefore, the primary aim of this work

was the elucidation of key regulators in lace plant developmental PCD during perforation formation and the development of techniques to modulate the process. To achieve this goal, the following research projects were carried out:

1.6.1. Ethylene as a Hormonal Regulator of Lace Plant PCD

Ethylene is a fundamental gaseous phytohormone involved in various aspects of plant growth and development (Trobacher 2009). It has been implicated as a PCD-inducer in various developmental processes (Mattoo and Handa 2004) and therefore its potential involvement in lace plant PCD warranted investigation. Following ethylene biosynthesis modulation, gas chromatography and whole plant experiments were used to determine the effects of ethylene on lace plant development and perforation formation. If ethylene acts as a PCD induction signal, then fewer perforations are expected to develop following the inhibition of ethylene biosynthesis.

1.6.2. Antioxidants and ROS in Cell Death Signaling

The first visible sign that PCD has been initiated in lace plant cells is a loss of anthocyanins, which are potent antioxidants (Gunawardena et al. 2004; Wertman et al. 2012). Due to the conspicuous pattern of anthocyanins in the gradient of cell death found during the formation of perforations in the lace plant, the roles of antioxidants and ROS were determined. The effects of antioxidants and ROS were explored using pharmacological whole plant experimentation, long-term live cell imaging, the 2,2′-

azino-bis-3-ethylbenzothiazoline-6-sulfonic acid (ABTS) anti-radical activity assay, and western blot analysis. It is hypothesized that the balance, or relative proportion of antioxidants to ROS affects the fate of cells during perforation formation, with antioxidants providing resistance to PCD induction.

1.6.3. Functions of Autophagy in the Lace Plant

As discussed earlier, autolytic behavior plays a central role in cellular dismantling during lace plant developmental PCD and induced cell death (Wertman et al. 2012; Dauphinee et al. 2014). We hypothesize that autophagy is an essential component in the plant PCD signaling pathway. Techniques to describe lace plant autophagy included: a novel live cell imaging assay, transmission electron microscopy (TEM), immunolocalization, western blotting, and whole plant pharmacological experimentation.

1.6.4. Developing a Lace Plant Transformation Protocol

Genetic transformation biotechnology has changed the face of plant biology and agriculture (Stewart et al. 2011). The ability to alter the genome is a valuable tool for a model system. This particular aspect of the study of PCD in lace plant involved the development of plant transformation protocols, including those for the efficient induction of embryonic callus and regeneration of whole plants. Various explants were tested for stable transformation using an *Agrobacterium tumefaciens* vector containing the pJLU13 plasmid. The protocol for lace plant transformation developed here can be applied to

produce mutants overexpressing genes linked to key regulators of PCD and therefore increase abilities to manipulate and better understand the lace plant developmental signaling pathway.

CHAPTER 2

ETHYLENE IN LACE PLANT PCD SIGNALING

The work presented in Chapter 2 appears in:

Dauphinee AN, Wright H, Rantong G, and Gunawardena AHLAN (2012) The involvement of ethylene in programmed cell death and climacteric-like behaviour during the remodelling of lace plant (*Aponogeton madagascariensis*) leaves. Botany-Botanique 90(12): 1237-1244.

2.1. ABSTRACT

Programmed cell death (PCD) plays an important role in several plant developmental processes. The phytohormone ethylene has been implicated in PCD signalling in many plant systems, but it is also important in developmental processes such as seed germination, flowering, and climacteric fruit ripening. Lace plant (*Aponogeton madagascariensis* (Mirbel) H. Bruggen) is an aquatic monocot that develops perforated leaves via the deletion of cells through developmentally regulated PCD. The lace plant is ideal for studying PCD; however, little is known about the regulation of cellular death involved in this system. The current study examines ethylene as a potential signalling molecule in lace plant PCD and investigates climacteric-like behaviour during lace plant leaf development. Whole plants were treated with the ethylene biosynthesis inhibitor

aminoethoxyvinylglycine (AVG), the ethylene precursor 1-aminocyclopropane-1-carboxylic acid (ACC), or a combination of both. Subsequently, ethylene levels were monitored, and leaf development was analyzed. The results indicate that ethylene is involved in lace plant PCD signalling. AVG-treated plants had significantly lower ethylene outputs and a significant reduction in perforation formation. The inhibitory effect of AVG was recovered when AVG and ACC were applied simultaneously. To our knowledge, the data presented here show climacteric-like behaviour for the first time during the remodelling of leaves.

2.2. INTRODUCTION

Programmed cell death (PCD) plays an important role in the organization and maintenance of plants and can be divided into two broad categories: environmentally-induced and developmentally-regulated (Gunawardena 2008). Environmentally-induced PCD is caused by external factors, which include flooding, salt stress, heat shock, UV radiation, and pathogens (Kacprzyk et al. 2011). Developmentally-regulated PCD differs in that it has an endogenous induction signal, which include processes such as xylogenesis, petal senescence, and leaf morphogenesis (van Doorn and Woltering 2005; Reape and McCabe 2008; Gunawardena 2008). In the past few years, significant progress has been made in understanding the developmental signals and pathways regulating PCD in plants; however, no ubiquitous critical executor of plant PCD has been identified to date. A number of plant-specific hormones have been implicated in PCD signalling, including salicylic acid, jasmonic acid, abscisic acid, gibberellins, and ethylene

(Hoeberichts and Woltering 2003), although ethylene has most often been associated with the promotion of cellular death (Mattoo and Handa 2004; Noodén 2004). Specific examples of developmentally regulated PCD stimulated by ethylene include the degradation of the nucellus in squash (*Sechium edule*) after fertilization (Lombardi et al. 2012) and the senescence of floral organs in *Nicotiana mutabilis* (Macnish et al. 2010).

The ethylene biosynthetic pathway is initiated via the conversion of methionine to S-adenosyl methionine (AdoMet) by AdoMet synthetase. Following this, AdoMet is converted to 1-aminocyclopropane-1-carboxylic acid (ACC), which is the rate-limiting step of the pathway mediated by the enzyme ACC synthase. The final conversion is that of ACC to ethylene, carbon dioxide, and cyanide by ACC oxidase (Adams and Yang 1979; Trobacher 2009). Several studies in the past have employed inhibitors of ethylene biosynthesis such as aminoethoxyvinylglycine (AVG) and aminooxyacetic acid (AOA), which competitively inhibit ACC synthase (Yu and Yang 1979; Bae et al. 1996; Mattoo and Handa 2004). Gladish and Niki (2008) used several ethylene inhibitors, including AOA to suppress PCD during vascular cavity formation in submerged pea (*Pisum sativum*) roots, and were able to increase PCD with the application of exogenous ethylene in non-flooded conditions. Likewise, Chae and Lee (2001) used AOA and AVG to demonstrate the involvement of ethylene during PCD signalling in carrot (*Daucus carota*) suspension culture cells undergoing carbon starvation, and the application of AVG reduced cadmium-induced PCD in tomato suspension cells (Yakimova et al. 2006). Ethylene production can be stimulated by the application of exogenous ACC, which leads to an increase of PCD in epidermal cells of deepwater rice (*Oryza sativa*) at the site of

adventitious root emergence (Mergemann and Sauter 2000). Ethylene is also implicated in several other developmental and growth processes including, but not limited to, seed germination, flowering, abscission, and fruit ripening (Mattoo and Handa 2004; Noodén 2004).

The involvement of ethylene in the ripening of fruit has been well established (Hansen 1965; Dhillon and Mahajan 2011). Fruits are classified as climacteric or non-climacteric based on their level of ethylene production and respiratory behaviour during ripening (Rees 2012). In climacteric fruits, ethylene stimulates ripening (Oeticker 1995); respiration rates also increase during ripening and then decline as fruit senescence progresses. The initial burst of ethylene leads to sharp peaks of both ethylene and carbon dioxide production at the beginning of ripening (Biale; Tucker 1993). Climacteric-like behaviour has also been associated with other forms of PCD such as petal senescence (Serrano et al. 1991), leaf abscission (Morgan et al. 1992), and leaf senescence (Katz et al. 2005). Morgan et al. (1992) showed that in cotton leaves, a peak in ethylene production is observed 3–4 days before abscission. In citrus, detached leaves maintained constitutive amounts of ethylene production before peaking after 9 days, marking the beginning of leaf senescence (Katz et al. 2005).

Lace plant (*Aponogeton madagascariensis* (Mirbel) H. Bruggen) is an aquatic monocot that develops a unique perforated leaf morphology through developmentally regulated PCD. Lace plant provides an excellent system for studying PCD for several reasons, including the predictability of perforation formation, the ability to propagate plants via

sterile tissue culturing (Figure 2.1A, B), and the availability of thin, nearly transparent leaves that are ideal for live cell imaging (Gunawardena et al. 2006; Wertman et al. 2012). Newly cultured lace plants form three or four juvenile leaves that do not develop perforations; however, all leaves that emerge subsequently (referred to as adult leaves) develop perforations by the time they reach maturity (Figure 2.1C). Gunawardena et al. (2004) classified the development of perforations into five stages. Young leaves emerge from the corm having furled blades with a grid-like pattern of longitudinal and transverse veins; this point of development is known as the preperforation stage in which areoles (located between the vasculature) show no visible cytological indication that PCD will occur (Figure 2.1D). Next is the window stage (Figure 2.1E) in which cells at the center of the areole undergo PCD, evident by their loss of pigmentation. PCD continues to expand outwards towards the veins. Cells subsequently collapse and cell walls are degraded, giving rise to the perforation formation stage. Perforations enlarge during the perforation expansion stage. The deletion of cells via PCD halts four or five cell layers from the veins by the mature stage (Figure 2.1F).

Figure 2.1. Lace plant (*Aponogeton madagascariensis*) growth and development. Lace plants used for whole-plant experiments in this study were grown under axenic conditions in (A) Magenta boxes or (B) air-tight vials. (C) Adult lace plant leaves develop perforations (bottom arrow) by the time they reach maturity; please note that some areoles do not develop perforations (top arrow). (D) The initial stage of perforation formation is known as the preperforation stage in which there are no visible signs that programmed cell death (PCD) is occurring. During the window stage (E), PCD is initiated at the center of the areole and is readily observable due to a decrease in pigmentation. In the mature stage (F), PCD has stopped four–five cell layers from the vasculature. Scale bars: A–B, 1 cm; C, 5 mm; D, 40 µm; E, 125 µm; F, 200 µm.

The developmental cues involved in PCD signalling during lace plant leaf morphogenesis are yet to be understood. Because ethylene is involved in many plant developmental processes and has been implicated in PCD signalling, it warrants investigation within the

lace plant system. Initial work carried out by Gunawardena et al. (2006) provided some indirect evidence that ethylene may play a role in perforation formation in lace plant. The current study used AVG to inhibit and ACC to enhance ethylene biosynthesis in whole plants in which leaf development and ethylene production was monitored. Furthermore, this study examined ethylene and carbon dioxide evolution at various stages of leaf development in an attempt to elucidate whether or not lace plant leaves exhibit a climacteric pattern.

2.3. MATERIALS AND METHODS

2.3.1. Plant Material

The axenic lace plant cultures used during this study were propagated according to Gunawardena et al. (2006). Newly cultured corms were placed into autoclaved Magenta G47 boxes and embedded in 50 mL of solid Murashige and Skoog (MS) medium containing 1% agar onto which 200 mL of liquid MS medium (0% agar) was poured (Figure 2.1B). The plants were maintained at 24 °C and exposed to fluorescent light (F32T8/DX; Philips Electronics Ltd., Markham, Ontario) at an intensity of 125 $\mu mol \cdot m^{-2} \cdot s^{-1}$ on a 12 h light – 12 h dark cycle. All chemicals used during experimentation were purchased from Sigma Aldrich (St. Louis, Missouri), unless otherwise stated.

2.3.2. Whole-Plant Experimentation

Whole-plant experiments were carried out using 4- to 5-week-old lace plants, which had similar corm sizes and three–four perforated leaves, grown in Magenta boxes. The plants were transferred into 40 mL air-tight vials fitted with septum lids that contained 10 mL of solid and 20 mL of liquid MS medium (Figure 2.1B). Lace plants were then randomly assigned into four groups: AVG, ACC, a combination of both AVG and ACC, and control, which received an equal volume of distilled water. To determine optimal treatments, gradients of AVG and ACC concentrations were applied to whole plants and compared with controls in terms of ethylene production and leaf morphology. The AVG applications included 2, 4, 5, 10, and 25 μM, and the ACC concentrations tested were 1, 2, 5, 10, 25, 50, 100, 200, 500, and 1000 μM. At higher concentrations of AVG, there was a complete inhibition of perforation formation; however, the leaves that developed were short and narrow compared with controls (data not shown). At higher concentrations of ACC, leaves became elongated, had dark green and red pigmentation at maturity, and showed early signs of senescence compared with controls (data not shown). The optimal concentrations that significantly altered ethylene production but did not affect normal leaf development were 5 μM AVG, 2 μM ACC, and a combination of both 5 μM AVG and 2 μM ACC. Subsequent to treatment, the plants were maintained as mentioned above, and leaf development was monitored through photography and experimenter observations. One week after the beginning of the experiments, ethylene measurements were taken from the plants as described below, and two weeks after the initiation of the experiments, the leaves were harvested. Three independent experiments were carried out with six replicates per treatment (24 plants per experiment, 72 in total). Plants showing visible signs of infection were not considered during statistical analysis.

2.3.3. Detached-Leaf Experiments

Window-, mature-, and senescent-stage lace plant leaves were selected from aquarium-grown plants. Senescent leaves chosen for experiments had a varying proportion of tissues visibly undergoing senescence (observed as yellowing or browning areas). The leaves were carefully excised at the base of the petiole. Approximately 0.56 g of leaf tissues per stage were placed in 40 mL vials with septum-fitted lids. The leaves were then submerged in 30 mL of aquarium water that was supplemented weekly with 0.001g/L monopotassium phosphate, 0.01 g/L potassium nitrate, and 0.003 g/L CSM+B Plantex (Aquarium Fertilizers, Napa, California). Preliminary experiments showed that detached window- and mature-stage leaves continued to grow for up to a week under these conditions without showing any visible signs of senescence. However, preperforation leaves did not continue to grow and unfurl when detached; therefore, they were not used in this study. The vials were maintained as described for whole-plant experiments for three days prior to gas measurements. Five independent experiments were carried out under these conditions with four replicates per stage (12 vials per experiment, 60 in total).

2.3.4. Gas Measurements

Ethylene measurements were taken for whole-plant and detached-leaf experiments using a gas chromatograph (Carle Instruments, Anaheim, California) fitted with a 1.9 m × 3.2 mm (o.d.) activated alumina column with a hydrogen carrier flow of 1.17 mL/s and a

flame ionization detector. For all samples, 1 mL of the headspace was extracted using a syringe and then immediately injected into the gas chromatograph. For detached-leaf experiments, carbon dioxide measurements were taken following ethylene measurements. To achieve this, 3 mL of the headspace was extracted using a syringe and injected into a gas analyzer (GCS150; Gas Control Systems Inc., Sparta, Michigan). Ethylene and carbon dioxide output values for each replicate were divided by the mass of the sample to obtain the concentration of gas emitted per gram of tissue.

2.3.5. Morphological Data Collection

At the end of whole-plant experiments, leaves were excised from individual lace plant corms at the base of the petiole and arranged in chronological order. For each replicate, the last adult leaf that had developed perforations prior to treatment was chosen to be a control leaf as a qualitative comparison to all subsequent leaves that emerged following treatment. After the application of treatments, leaves were designated by a number in order of their emergence, with the control leaf (0) having the lowest designation. Representative leaf layouts, showing the progression of leaf development from left (control) to right (last leaf to develop) were photographed. The number of newly produced leaves (mature and window stage), the mature leaf lengths (base of petiole to leaf apex), and the number of perforate and imperforate areoles per mature leaf were recorded for individual plants. The percentage of perforations for individual leaves was calculated by dividing the number of perforate areoles by the total number of areoles (Figure 2.1C).

2.3.6. Microscopy, Photography and Image Preparation

Light micrographs of sections of the detached leaves were taken on a Nikon 90i research microscope (Nikon, Mississauga, Ontario), and the images were captured using a Nikon DXM 1200c digital camera. NIS Elements Advanced Research (3.1) software was used during micrograph acquisition. All photographs were taken with a Nikon L110 digital camera (Nikon, Mississauga, Ontario). Micrographs and photographs were edited and prepared for publication using Adobe Illustrator (13.0) and Adobe Photoshop (10.0) (Adobe Systems Inc., San Jose, California).

2.3.7. Statistical Analysis

A general linear model (GLM) analysis of variance (ANOVA) was used to determine statistical significance (Minitab release 15; Minitab Inc., State College, Pennsylvania). Individual treatment means were compared using a Waller–Duncan k ratio t test mean comparison (SAS release 8.0; SAS Institute Inc., Cary, North Carolina). A normal probability plot (NPP) of the residuals was used to test normality, while a fitted values versus residuals plot was used to examine constant variance. When the assumptions of the error term (ε_{ij}) were violated, transformations were used; in those instances, means shown in this paper were back-transformed. Only results significant at $P \leq 0.05$ are discussed, unless noted otherwise.

2.4. RESULTS

2.4.1. Whole-Plant Experimentation

For leaf morphology analysis, leaves were excised and representative leaf layouts were collected from control, 5 µM AVG, 2 µM ACC, and the combination of 5 µM AVG and 2 µM ACC treated plants (Figure 2.2). A PROC GLM ANOVA showed no significant difference in the number of new leaves formed ($P = 0.063$; Figure 2.3A) or the mean mature leaf lengths ($P = 0.997$); however, there was a significant difference in mean percentage of perforations ($P < 0.001$; Figure 2.3C). Mean comparison revealed that AVG-treated plants produced significantly fewer perforations compared with controls. There was no difference in the number of perforations formed among the leaves of control, ACC-treated and combination-treated plants. Additionally, at the time of harvest, the latest window-stage leaves to develop in AVG-treated plants appeared as though they would produce more perforations than the leaves that developed to maturity during the two-week experimental period (leaf 3 in Figure 2.2B).

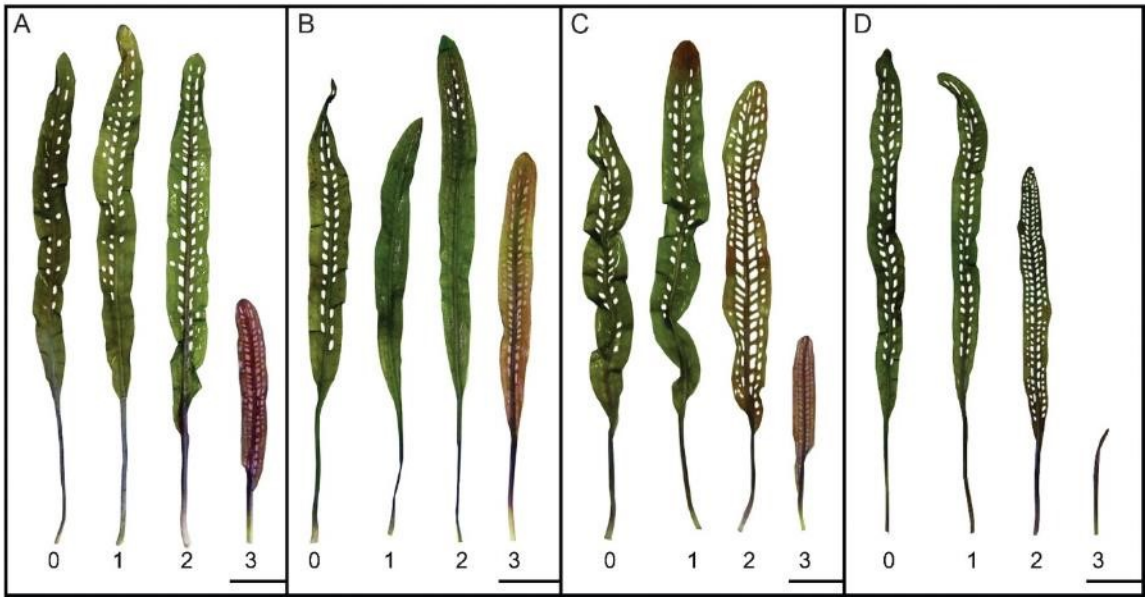

Figure 2.2. Leaf development of experimental lace plants. Leaf layouts for (A) control, (B) 5 µM aminoethoxyvinylglycine (AVG), (C) 2 µM 1-aminocyclopropane-1-carboxylic acid (ACC), and (D) the combination of 5 µM AVG and 2 µM ACC (COMB) treatments. In panels A–D, leaf 0 is a control leaf that had developed prior to the application of treatments. Leaves labeled 1–3 are those that developed subsequently. Scale bars: A–D, 15 mm.

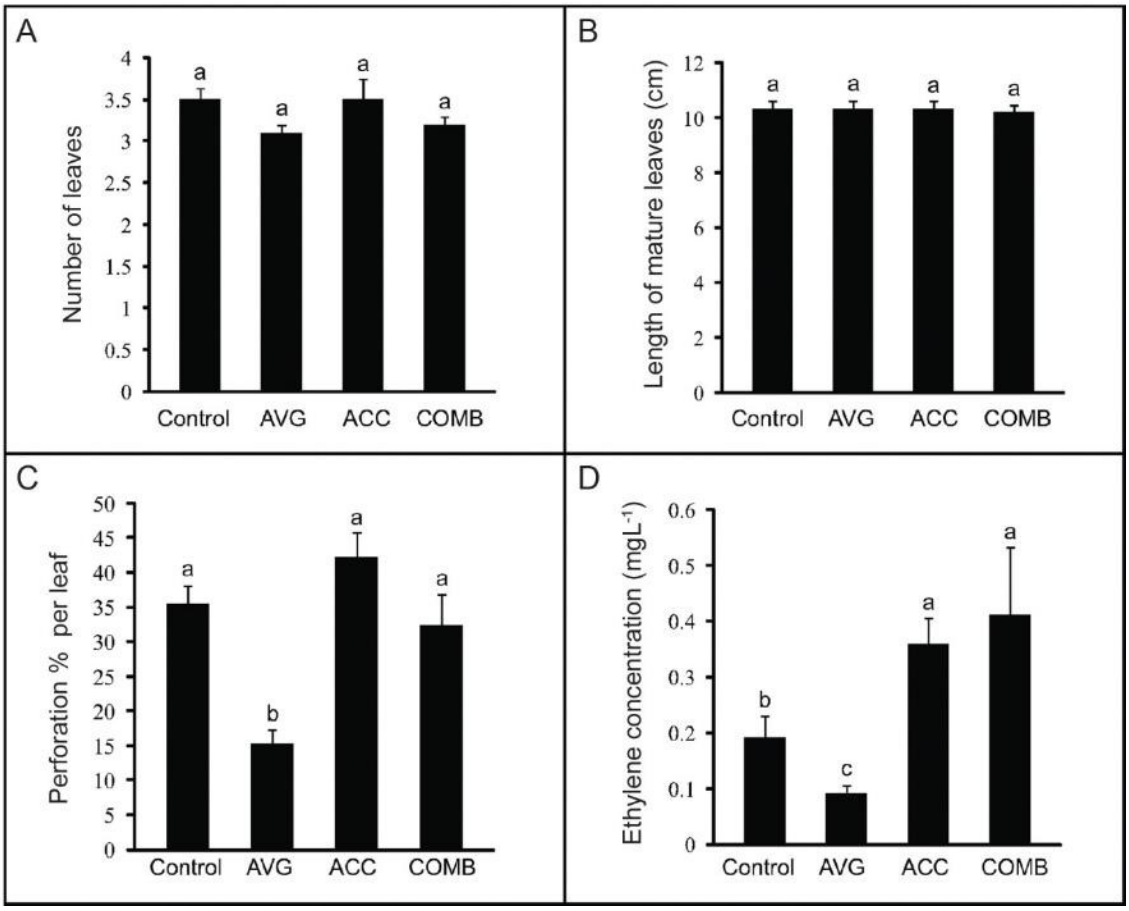

Figure 2.3. Summary of whole-plant experiments. Data for the control, 5 µM aminoethoxyvinylglycine (AVG), 2 µM 1-aminocyclopropane-1-carboxylic acid (ACC), and the combination of 5 µM AVG and 2 µM ACC (COMB) treatments. The parameters examined include (A) the number of leaves formed per plant, (B) the length of mature leaves, (C) the percentage of perforations per leaf, and (D) the ethylene concentration. Means represented by different letters are significantly different ($P \leq 0.05$). Error bars represent standard error of $n \geq 14$ plants per treatment.

2.4.2. Ethylene Levels

Ethylene production was determined from whole plants via gas chromatography (Figure 2.3D). The ethylene detected from AVG-treated plants was significantly lower compared with the control plants ($P < 0.001$). The ACC- and combination-treated plants

produced significantly higher amounts of ethylene than controls, but did not differ from each other.

2.4.3. Detached-Leaf Experiments

Detached lace plant leaves at the window, mature, and senescent stages of development were put in air-tight vials, and their ethylene and carbon dioxide emissions were measured (Figure 2.4). A PROC GLM ANOVA showed a significant difference in both ethylene and carbon dioxide emitted among lace plant leaves at different stages of development ($P < 0.05$). Mean comparison showed that window-stage leaves produced significantly more ethylene than mature- and senescent-stage leaves. Likewise, senescent-stage leaves emitted significantly higher ethylene levels than mature-stage leaves (Figure 2.4A). There was no difference in carbon dioxide produced in window- and senescence-stage leaves; however, both stages produced a significantly higher amount of carbon dioxide than mature leaves (Figure 2.4B).

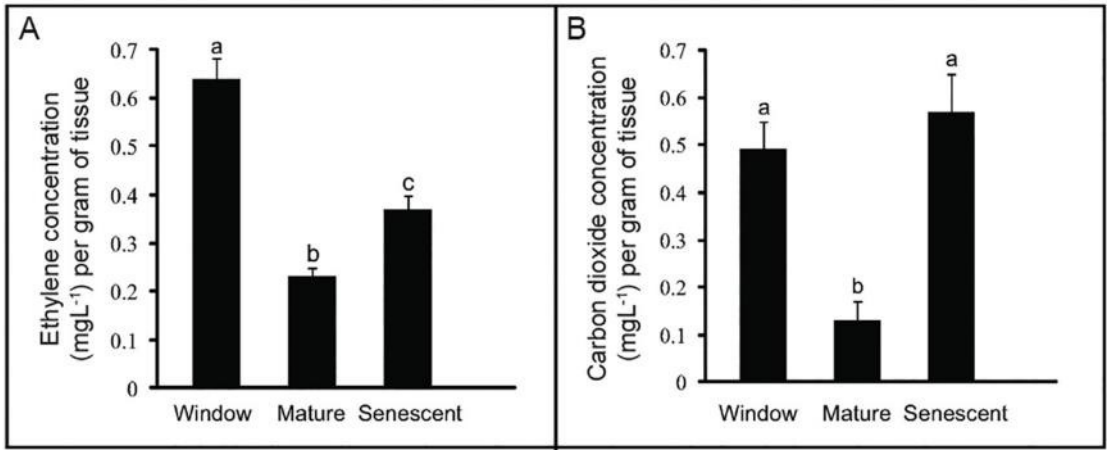

Figure 2.4. Gas concentrations detected from detached leaves. (A) Ethylene and (B) carbon dioxide produced per gram of leaf tissue in window-, mature-, or senescent-stage leaves. Means represented by different letters are significantly different ($P \leq 0.05$). Error bars represent standard error of $n \geq 14$ replicates per leaf stage.

2.5. DISCUSSION

The number of leaves formed per plant, as well as the leaf lengths were used to determine if chemical treatments had an impact on typical growth and development of the lace plants. Quantitative analysis showed that the number of new leaves formed and leaf lengths did not differ significantly among all four treatments, suggesting that typical lace plant leaf development, excluding perforation formation, had occurred. AVG-treated plants produced significantly fewer perforations compared with all other treatments, indicating that ethylene does play a role in lace plant PCD. It should be noted that the inhibitory effect on perforation formation from 5 µM AVG treatments appeared to subside, as observed in newly formed leaves at the end of the two-week period (leaf 3 in Figure 2.2B). The unabated presence of perforations in the combination treatment indicates that exogenous ACC, the precursor to ethylene, is able to overcome the inhibitory response of AVG. This was expected given that AVG reduces ethylene

production by limiting the amount of ACC produced. This observation suggests that reducing ethylene production limits PCD, whereas increasing ethylene output enhances PCD.

Detached leaf experiments revealed the presence of two ethylene peaks associated with PCD in lace plant leaves: one during the window stage and the other during senescence (Figure 2.4A). Ethylene levels are elevated during the window stage (when perforations are being formed), reduced during the mature stage (when perforations are fully formed), and then increase again during senescence of the mature leaves. This suggests the involvement of ethylene in climacteric-like behaviour during formation of perforations, as well as leaf senescence. Climacteric behaviour is characterized by low and constant amounts of ethylene (system I pathway) followed by a peak in ethylene production (system II pathway; Katz et al. 2005). It has been shown that ethylene is involved in leaf senescence in other species and that it is produced in a climacteric-like pattern (Aharoni and Lieberman 1979a; Aharoni and Lieberman 1979b; Jing et al. 2005). The two peaks in ethylene production during the two PCD processes (formation of perforations and leaf senescence) support the involvement of ethylene in lace plant PCD.

Several studies in climacteric behaviour during fruit ripening have shown that carbon dioxide peaks were the result of increased cellular respiration rates (McGlasson and Pratt 1964; Hadfield et al. 1995). High ethylene concentrations are thought to initiate an increase in respiration (Brady 1987; Hadfield et al. 1995), and our results in lace plant leaves appear to suggest a similar association. We speculate that fermentation in dying or

dead tissues may also be contributing to the increases in carbon dioxide observed. Our study suggests that ethylene and carbon dioxide may be involved in climacteric-like behaviour during lace plant leaf remodelling and senescence.

The data presented here provide evidence that endogenous ethylene plays a role in developmentally regulated PCD in the lace plant. Suppressed ethylene biosynthesis significantly reduces perforation formation without affecting normal leaf development and this effect can be reversed by stimulating endogenous ethylene production. Additionally, this is the first study to our knowledge to support the involvement of climacteric-like ethylene production in the remodelling of leaves. Future work will investigate the downstream interactions of ethylene with other phytohormones and apply molecular techniques to determine the regulation of genes associated with ethylene and lace plant PCD.

2.6. ACKNOWLEDGEMENTS

We thank Peter Harrison (Atlantic Food and Horticulture Research Centre, Kentville, Nova Scotia) for technical support with gas chromatography, Devin MacDonald (Dalhousie University) for assistance with morphological data collection, Christina Lord (Dalhousie University) for a revision of the final manuscript, and Anna Elliot (Dalhousie University) and Laura Voicu (University of Toronto) for preliminary work towards this study. Additionally, we thank Nancy Dengler (University of Toronto) for all of her guidance throughout this project.

CHAPTER 3

BALANCING ANTIOXIDANTS AND ROS

The work in this chapter appears in:

Dauphinee AN, Fletcher JI, Denbigh GL, Lacroix CR and Gunawardena AHLAN. Remodelling of lace plant leaves: Antioxidants and ROS are key regulators of programmed cell death. Planta. doi:10.1007/s00425-017-2683-y

3.1. ABSTRACT

The lace plant is an excellent model system for studying developmentally regulated programmed cell death (PCD). During early lace plant leaf development, PCD systematically deletes cells resulting in a perforated leaf morphology that is unique *in planta.* A distinct feature in young lace plant leaves is an abundance of anthocyanins, which have antioxidant properties. The first sign of PCD induction is the loss of anthocyanin pigmentation in cells that are targeted for destruction, which results in a visible gradient of cell death. The cellular dynamics and time course of lace plant PCD are well documented, however the signals involved in the pathway remain elusive. This study investigates the roles of antioxidants and ROS in developmental PCD signaling during lace plant perforation formation. The involvement of antioxidants and ROS in the

pathway was determined using a variety of techniques including pharmacological whole plant experimentation, long-term live cell imaging, the 2,2′-azino-bis-3-ethylbenzothiazoline-6-sulfonic acid (ABTS) anti-radical activity assay, and western blot analysis. Results indicate that antioxidants and ROS are key regulators of PCD during the remodelling of lace plant leaves.

3.2. INTRODUCTION

3.2.1. Programmed Cell Death

Programmed cell death (PCD) is a series of tightly controlled events leading to the demise of targeted cells (Kacprzyk et al. 2011; Bozhkov and Lam 2011). In multicellular eukaryotes it occurs as part of normal development or in the maintenance of tissue homeostasis and therefore, is a critical mechanism for survival (Coll et al. 2011). The signaling cascades of animal PCD are well understood in comparison to plants and have clearly defined molecular subroutines, as described by the nomenclature committee on cell death (Kroemer et al. 2005; Kroemer et al. 2009; Galluzzi et al. 2012). The identification of key regulators of plant PCD has been the focus of recent studies, which will contribute to our understanding of the process and the development of robust classification systems for the various forms of cell death observed in nature (van Doorn et al. 2011; Dauphinee and Gunawardena 2015).

3.2.2. Reactive Oxygen Species in PCD

Reactive oxygen species (ROS) are chemically unstable oxygen derivatives that act as signaling molecules in aerobic organisms for several biological processes in development, growth, and responses to environmental stimuli (Gechev et al. 2006; Baxter et al. 2014; Petrov et al. 2015). Elevated levels of ROS such as hydrogen peroxide (H_2O_2), superoxide (O_2^-) and reactive nitrogen species including nitric oxide (NO) are associated with PCD. ROS influence the production of phytohormones including ethylene, jasmonic acid, and salicylic acid, or cause posttranslational modifications that ultimately activate the genes, proteases and nucleases that carry out PCD (Van Breusegem and Dat 2006). In plants, major sources for ROS production are mitochondria, chloroplasts, peroxisomes, and cell walls through the activity of class III cell wall peroxidases and NADPH oxidases (Mignolet-Spruyt et al. 2016). The accumulation of ROS within cells can also trigger production of ROS-scavenging antioxidants, including but not limited to: anthocyanins, glutathione, ascorbic acid, superoxide dismutase-1 (SOD1), catalase (CAT), and glutathione peroxidase (Pandhair and Sekhon 2006; Ahmad et al. 2010). Although ROS have long been viewed as strictly detrimental compounds, they are now known to play important roles during normal cell signaling and homeostasis. The roles of redox homeostasis in the perception, signaling, and physiological responses in plants have been studied extensively (Pavet et al. 2005; Mignolet-Spruyt et al. 2016).

3.2.3. The Lace Plant Model System

The lace plant (*Aponogeton madagascariensis*) is an aquatic monocot that forms a unique perforated leaf morphology by the removal of specific cells via developmentally regulated PCD (Figure 3.1A; Gunawardena et al. 2004). The process of perforation formation has been characterized into five stages of leaf development by Gunawardena et al. (2004). Young leaves in the preperforation stage emerge from the corm with a complete vein pattern but are tightly furled and have a red pigmentation due to the presence of anthocyanins. Anthocyanins scavenge a wide array of reactive oxygen and nitrogen species, in fact purified anthocyanins can be up to four times more efficient than ascorbate and α-tocopherol (Wang et al. 1997; Gould 2004). The window stage is distinguishable in the unfurled leaves which have populations of central cells actively undergoing PCD within the areoles located between longitudinal and transverse veins (Figure 3.1B). Areoles of window stage leaves (Figure 3.1C) exhibit a distinct gradient of PCD, as described by Lord et al. (2011). Non-PCD, or NPCD stage cells (Figure 3.1D) contain anthocyanins and do not die during perforation formation. Early-PCD (EPCD; Figure 3.1E) cells have lost anthocyanin coloration and are fated to die. Late-PCD (LPCD; Figure 3.1F) cells are nearly transparent and on the brink of death. Following the window stage is perforation formation, where PCD advances and cells in the centermost portion of the areole are removed. The perforation increases in size during the expansion phase before halting 4-5 cell layers from the veins by the mature stage. Mesophyll cells at the perforation border then transdifferentiate into epidermal cells and deposit a protective layer of suberin (Gunawardena et al. 2007).

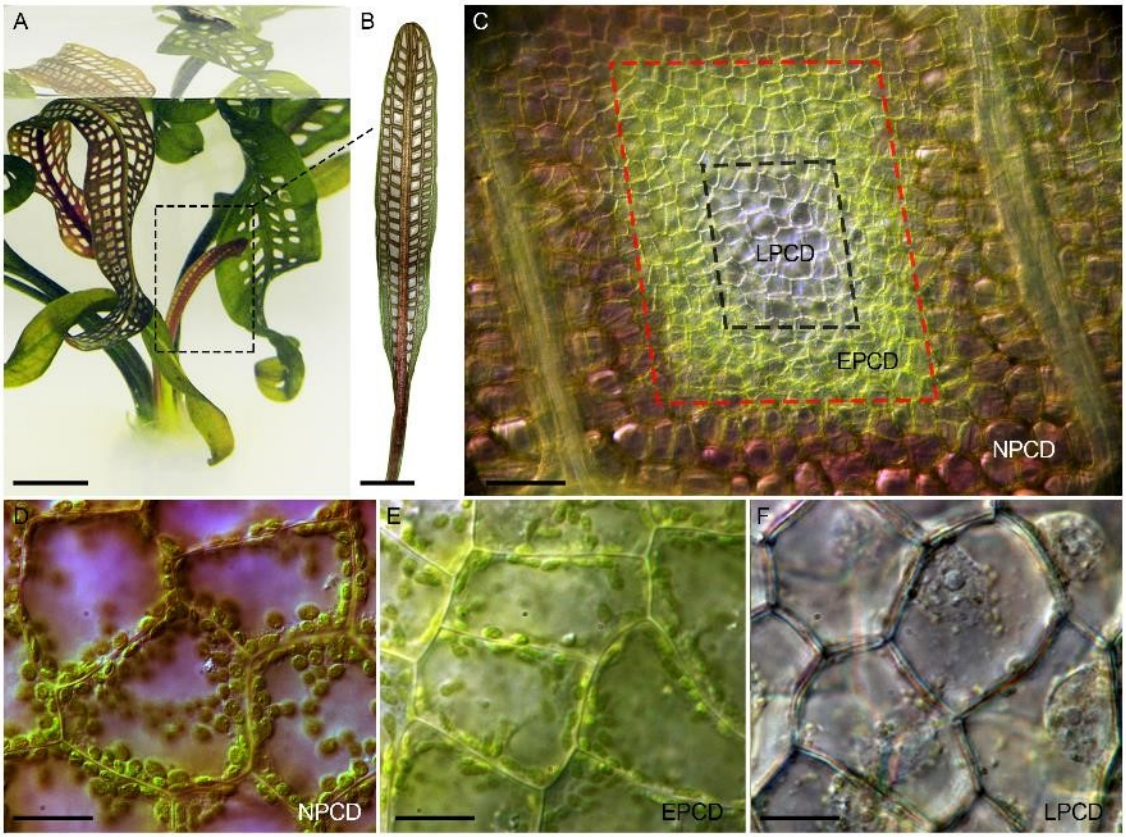

Figure 3.1. The lace plant (*Aponogeton madagascariensis*) model system. (A) Axenic lace plant cultures are maintained in Magenta GA-7 boxes. (B) Programmed cell death (PCD) is actively occurring in the window stage of leaf development (dashed line, panel A) between longitudinal and transverse veins (C) where a unique gradient of cell death exists as highlighted by the dashed lines. (D) Non-PCD (NPCD) cells are replete with anthocyanins and do not undergo PCD during leaf morphogenesis. (E) Early-PCD (EPCD) cells are fated to die and have lost their anthocyanin pigmentation. (F) Late-PCD (LPCD) cells are nearly transparent and are on the verge of death. Bars = 1 cm (A), 5 mm (B), 100 µm (C), 25 µm (D-F).

The lace plant has emerged as a model system for studying PCD due to the spatial and temporal predictability of PCD in leaves, which are thin and nearly transparent making them ideal for microscopy, as well as established axenic cultures suitable for pharmacological experiments (Gunawardena et al. 2006). The conspicuous pattern and disappearance of anthocyanins during the window stage in cells undergoing PCD during lace plant perforation formation suggests that antioxidant levels and ROS could be

involved in this signaling pathway. It is hypothesized that antioxidants and ROS play a significant role in the induction of lace plant PCD. This study employed whole plant experimentation, live cell imaging, spectrophotometric assays, and western blot analysis to elucidate the effects of antioxidants and ROS on lace plant PCD. Data indicate that antioxidants and ROS are key regulators of lace plant developmental PCD signaling.

3.3. MATERIALS AND METHODS

3.3.1. Tissue Culturing and Whole Plant Experiments

Aponogeton madagascariensis (Mirbel) H. Bruggen cultures were established and propagated according to Gunawardena et al. (2006). Plants were grown in Magenta GA-7 vessels containing 50 ml of solid MS medium consisting of 1.5% agar (Phytotechnology Laboratories) and 150 ml of liquid MS. Cultures were kept at 24°C under daylight deluxe fluorescent light bulbs (Philips) at an intensity of 125 μmol m^{-2} s^{-1} on 12 h light/dark cycles. Whole plant experiments were carried out using plants with a minimum of three perforated mature leaves. Optimized treatments included: (i) An antioxidant treatment of 400 μg/ml L-ascorbic acid and 200 μg/ml L-cysteine (Bioshop Canada), (ii) A ROS treatment of 1 mM H_2O_2 (Fisher Scientific) and (iii) The antioxidant + ROS treatment which consisted of a treatment with the antioxidant, followed by 1 mM H_2O_2 4-5 days later. Plants were allowed to grow for two weeks before their leaves were harvested and analyzed. Leaf measurements included length, width, and the number of perforations formed. A minimum of 12 plants were treated for each group.

3.3.2. Long-Term Live Cell Imaging

Time-lapse videos were captured using the audio video interleave (AVI) function of Nikon NIS AR software controlling a Nikon Eclipse 90*i* compound light microscope (Nikon Canada Inc). The live cell imaging technique described by Wertman et al. (2012) was employed, with some modifications. Whole window stage leaves were removed from plant cultures, rinsed with distilled water, and mounted in a custom grooved slide that matched the width and depth of the leaf midrib and allowed the blade to lie flat on the slide surface. Depending on the experimental conditions, either distilled water or a treatment was applied to the leaf before a glass coverslip was applied and sealed with melted VALAP (2:1:1 w/w mixture of paraffin wax, Vaseline and lanolin). Leaf observations were carried out for 12 h daily. The leaf was rinsed with distilled water and remounted every 6 h to reduce stress and contamination, and kept in the dark at 24°C in fresh treatment solution overnight until the next period of imaging. The time of death was determined at the point where all PCD area cells up to the NPCD boundary died. A minimum of three independent replicates were carried out for each treatment group.

3.3.3. Nitro Blue Tetrazolium (NBT) Staining

Histochemical detection of O_2^- in window stage leaves was performed using a modified protocol from Grellet-Bournonville and Díaz-Ricci (2011). Leaves from the various treatment groups were cut into 5 mm^2 sections and then immersed in stain solution

consisting of 50 mM potassium phosphate buffer (7.8 pH), 10 mM sodium azide, and 0.1% NBT (Sigma-Aldrich). The samples were then kept in the dark, vacuum infiltrated at 15 psi for 15 min and then incubated at room temperature for 15 min prior to microscopic observation. The negative control underwent the same procedure with the solution lacking NBT. After staining, specimens were mounted in distilled water and viewed using a Nikon Eclipse Ti microscope. In order to confirm the observed staining patterns in the various leaf stages without the interference of anthocyanin and chlorophyll pigmentation, samples were placed in 95% ethanol for 2-3 days. A minimum of three replicates were carried out for all groups.

3.3.4. Detection of Superoxide Dismutase 1 (SOD1) and Catalase (CAT)

Harvested leaves had their midrib removed, blot-dried, and frozen with liquid nitrogen. The tissues were homogenized on ice in a 1:1 ratio of Pipes buffer (6.8 pH) to protease inhibitor solution. The protease inhibitor solution was a 1:2 ratio of component A to component B, respectively. Component A was comprised of 10 mg/ml leupeptin and 10 mg/ml soybean trypsin inhibitor (Sigma-Aldrich) dissolved in Pipes buffer. Component B consisted of 10 mg/ml pepstatin and 20 mg/ml PMSF dissolved in 95% ethanol. The homogenized samples were then centrifuged at 16,000 *g* for 15 min. The supernatants were removed and quantified for total protein concentration via Bradford assay (Bradford 1976). Sample preparations for SDS polyacrylamide gel electrophoresis were made using a 1:1 ratio of sample to 2X Laemmli Sample Buffer (Bio-Rad) with 5% β-mercaptoethanol (v/v). The Precision Plus Protein Standards (Bio-Rad) and samples (10

μg protein weight) were loaded into 8-16% SDS polyacrylamide Mini-PROTEAN TGX precast gels (Bio-Rad) and resolved at 160 V for 1 h in ice cold running buffer (0.1% SDS (v/v), 25 mM Tris and 192 mM glycine, 8.3 pH). Proteins were transferred overnight at 120 mA to a 0.2 μm nitrocellulose membrane (Bio-Rad) in transfer buffer (20% methanol (v/v), 25 mM Tris and 192 mM glycine, 8.3 pH) at room temperature.

Ponceau staining of the nitrocellulose membrane was done for 5 min with mild shaking at room temperature, followed by a 2 min rinse with TBS-T and then photographed. Nitrocellulose membranes were then blocked for 1 h at room temperature with mild shaking using 3% (w/v) low fat milk powder in TBS-T (Tris buffered saline with Tween 20; 10 mM Tris, 140 mM NaCl, 0.1% Tween-20, 7.4 pH). The membrane was then incubated at room temperature for 30 min in a 1:1,000 dilution of the SOD-1 rabbit polyclonal antibody (Santa Cruz Biotechnology, #sc-11407) in TBS-T, then rinsed four times for 1, 1, 2, and 3 min respectively. The membrane was then transferred to TBS-T with a 1:10,000 dilution of goat anti-rabbit IgG HRP-conjugated antibody (Santa Cruz Biotechnology, #sc-2004) for 30 min, then rinsed as mentioned above with the addition of a final 2 min rinse in TBS. Secondary antibody localization was achieved using a Pierce ECL Western Blotting Substrate (Thermo Fisher Scientific) according to the manufacturer's instructions and imaged using a MF-ChemiBIS 3.2 gel documentation system (DNR Bio-Imaging). Following imaging, the membrane was rinsed for 5 min in TBS-T and then incubated overnight at 2°C in a 1:5,000 dilution of CAT rabbit polyclonal antibody (Agrisera, #AS09 501) in 5% (w/v) low fat milk in TBS-T. The next day the secondary antibody incubation and imaging was performed as mentioned above.

A minimum of four independent replicates were carried out for all treatment groups. An image of the Ponceau-stained membrane was converted to greyscale, imported into Image Studio Lite and quantified to confirm equal loading and protein transfer (LI-COR Biosciences). Image Studio Lite was also used to determine individual band intensities.

3.3.5. Anthocyanin and ABTS Spectrophotometric Assays

Tissue samples (20 mg) were excised from mature and window stage leaves taken from sterile cultures. The anthocyanin extraction protocol was adapted from Li *et al.* (2010). Tissue samples were ground and macerated in 200 µl of formic acid/methanol (5/95, v/v) and placed at room temperature in the dark for 50 min, followed by 10 min centrifugation at 10,000 g. The supernatant was collected and absorbance immediately read at 520 nm using a SmartSpec Plus Spectrophotometer (Bio-Rad). The ABTS (2,2′-azino-bis-3-ethylbenzothiazoline-6-sulfonic acid) assay kit was used according to the manufacturer's instructions (Zen-Bio). Absorbance was determined using a SpectraMax Plus 384 Microplate Reader and Softmax Pro 5 software (Molecular Devices). Standard curves of ascorbic acid (ABTS) and cyanidin-3-rutinoside (anthocyanin) were generated, and results were expressed as vitamin C equivalents and cyanidin-3-rutinoside equivalents (C3RE), respectively. A minimum of 4 replicates were analyzed for each group.

3.3.6. Image and Video Processing

Photographs were acquired using a Nikon L110 digital camera. All images and videos were prepared for publication using Photoshop and Premiere Pro, respectively (Adobe

Creative Cloud; Adobe Systems Inc.). When necessary to improve image quality, alterations to brightness, contrast, and color were made evenly. In the whole plant layouts and detached window stage leaf images, backgrounds and or shadows were removed using Photoshop. Window stage leaf micrographs were acquired by a Nikon AZ100 microscope and multiple images were merged together using the layer mask tool in Photoshop.

3.3.7. Statistical Analysis and Data Representation

A one-way ANOVA followed by a Tukey or Dunnett's test was carried out in order to detect significant differences among means. All data are expressed as mean ± SE unless otherwise stated. Analyses were carried out using GraphPad Prism 5 software (GraphPad Software Inc.).

3.4. RESULTS

3.4.1. Whole Plant Experiments

Lace plants grown in axenic cultures were utilized to determine the effects of antioxidants and ROS on developmental PCD and perforation formation. Control plants (Figure 3.2A) had mature leaves with a length of 13.51 ± 0.49 cm (Figure 3.2E) and 122.60 ± 10.26 perforations (Figure 3.2F). An optimized antioxidant combination treatment of 400 µg/ml ascorbic acid (AA) and 200 µg/ml L-cysteine (Cys; Figure 3.2B) resulted in leaves with a length of 13.09 ± 0.49 cm (Figure 3.2e) and 13.67 ± 4.92 perforations (Figure 3.2F), which was significantly fewer perforations than controls. A 1

mM H_2O_2 (Figure 3.2C) ROS treatment showed no differences from the control in terms of leaf length (13.09 ± 0.49 cm; Figure 3.2E) and perforations (120.70 ± 9.11; Figure 3.2F). Higher concentrations of H_2O_2 (≥ 5mM) were too extreme and killed the plants' leaves (data not shown). The antioxidant + ROS treatment (Figure 3.2D) resulted in significantly fewer perforations (62.69 ± 11.83; Figure 3.2F) than the control, but more than the antioxidant (AA + Cys) treatment alone. The antioxidant + ROS treatment group leaf lengths of 13.74 ± 0.6254 cm (Figure 3.2E) did not differ significantly from the control.

The number of perforations by leaf were analyzed for the control, antioxidant, ROS and antioxidants + ROS groups (Figure 3.2G). Control and 1 mM H_2O_2 treated plants showed very similar trends with a steady increase in the number of perforations in each subsequent leaf (Figure 3.2G). The antioxidant and the antioxidant + ROS treatment groups both had strong PCD inhibition by leaf 1, however perforation formation sharply increased in the antioxidant + ROS treatment by leaves 2 and 3 (Figure 3.2G). Micrographs of window stage leaves (Figure 3.2H-K), one week following the onset of experimentation showed a visible difference in anthocyanin pigmentation in the AA + Cys treatment group (Figure 3.2I), which did not have the typical window stage gradient of cell death as seen in the control (Figure 3.2H) and H_2O_2 specimens (Figure 3.2J). The window stage leaves of the antioxidant + ROS treatment (Figure 3.2K) had anthocyanin pigmentation, but it was not as prominent as the control and H_2O_2 leaves.

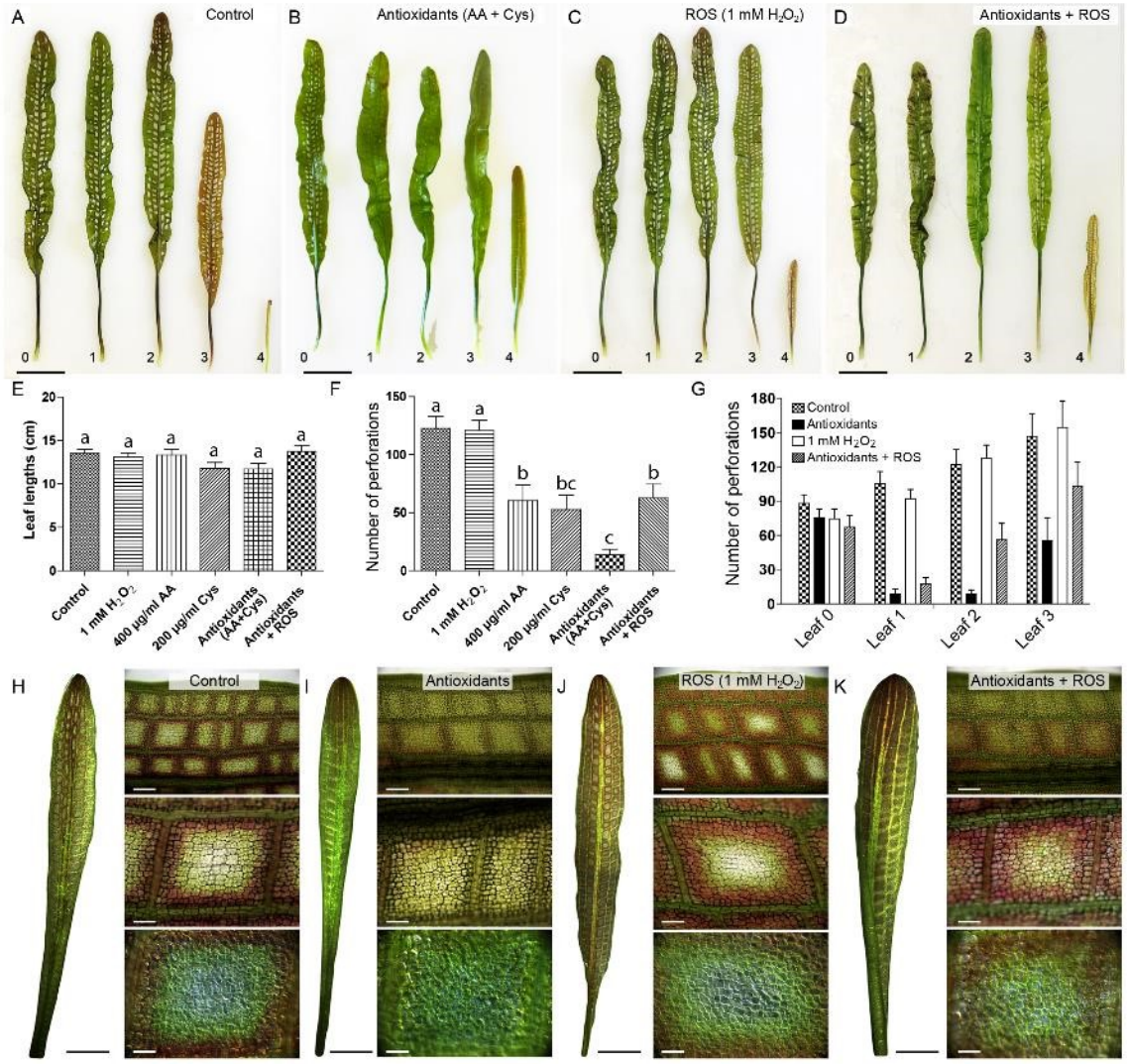

Figure 3.2. Whole plant effects of antioxidant and ROS treatments. Representative leaf layouts showing the control (A), the antioxidant combination of 400 µg/ml ascorbic acid (AA) and 200 µg/ml cysteine (Cyst) (B), 1 mM H_2O_2 and an antioxidant + ROS treatment receiving 400 µg/ml AA (C) and 200 µg/ml Cyst followed by 1 mM H_2O_2 4-5 days later (D). Leaves were arranged chronologically – leaf 0 represents a control leaf, which developed prior to treatment, while leaves 1-4 developed afterwards (4 being the youngest). The length (E) and the mean number of perforations (F) were quantified for post-treatment mature leaves along with the mean number of perforations by leaf (G). Representative window stage images (1 week after the beginning of the experiment) were taken for control (H), the AA and Cyst combination (I), 1 mM H_2O_2 (j) and antioxidant + ROS (K) treatments. Bars = 2 cm (A-D), 5 µm (leaves, H-K), 250, 100 and 50 µm (micrographs, top to bottom, H-K). Means with different letters differ significantly and error bars represent standard error. One-way ANOVA, Tukey test ($P < 0.05$; $n \geq 12$).

3.4.2. ROS Detection in Lace Plant PCD

The stages of lace plant perforation formation were investigated in terms of ROS production, specifically O_2^- using nitro blue tetrazolium (NBT) staining (Figure 3.3A). Preperforation stage leaves showed little to no NBT staining. Window stage leaves had NBT staining predominantly in PCD cells. As the perforation formed centrally, the most abundant staining was in LPCD stage cells. Dark staining in PCD cells bordering the degraded cells was also observed during the expansion phase of the perforation. In mature leaves, light NBT staining was visible but ubiquitous throughout the cells (Figure 3.3A). Specimens fixed and cleared in 95% ethanol were also subjected to NBT to confirm the staining patterns without obfuscation from the naturally occurring leaf pigments. Likewise, NBT staining was observed in all stages, most importantly there was little to no staining in preperforation leaves (Figure 3.3B), or the NPCD region of the window stage (Figure 3.3C). PCD cells of the window stage (Figure 3.3c) were prominently stained and there was ubiquitous staining in the mature stage (Figure 3.3D). NBT staining of antioxidant treated window stage leaves had little to no formazan precipitation, while the mature leaves had some staining throughout the tissue. (Figure 3.3E). Leaves treated with ROS (1 mM H_2O_2, Figure 3.3F) had similar staining to the controls.

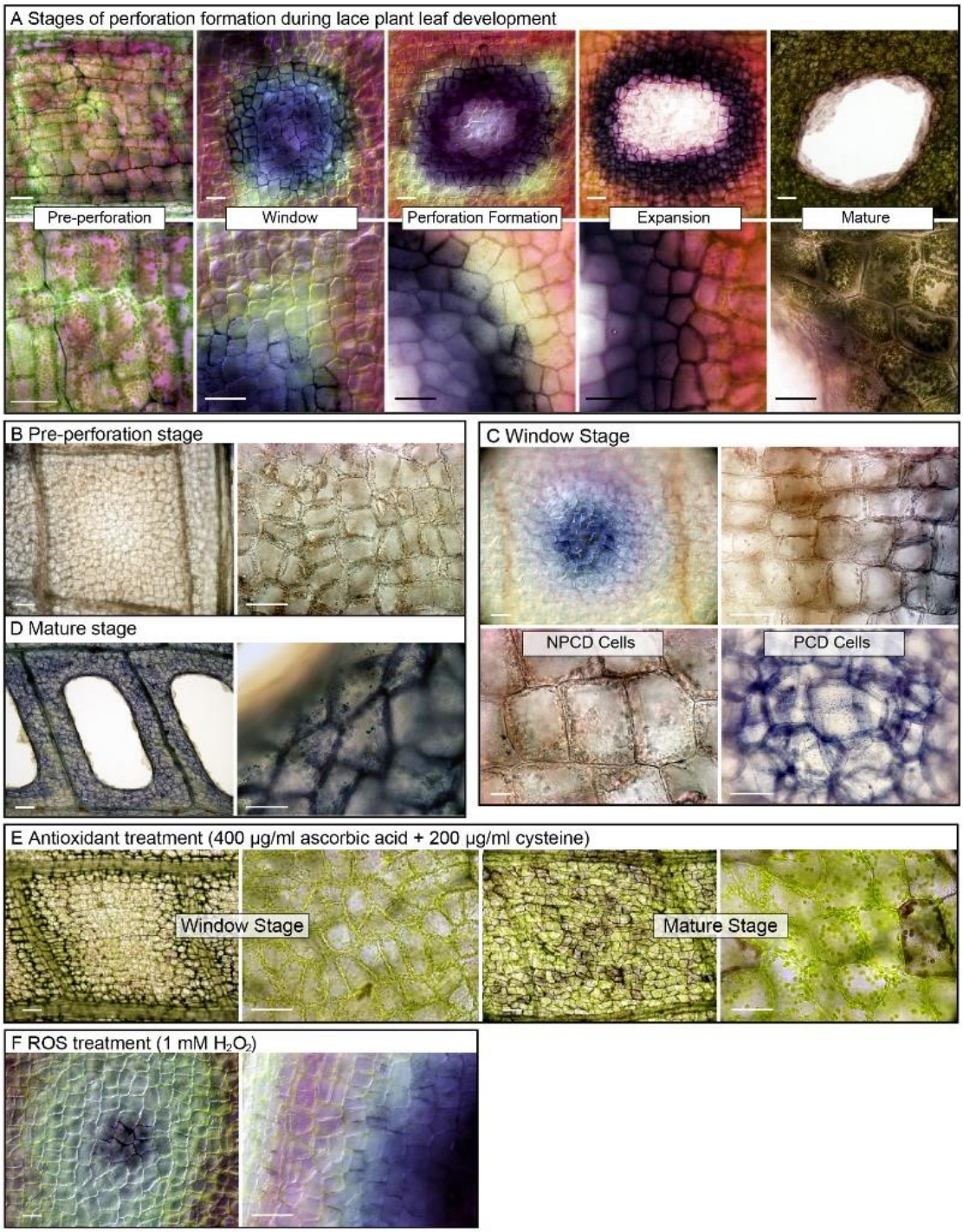

Figure 3.3. Nitro blue tetrazolium (NBT) staining in lace plant leaves. Preperforation stage leaves in which programmed cell death (PCD) has not yet initiated (A). Window stage leaves, where PCD is actively occurring in the center of areoles. PCD radiates outward and a hole forms centrally in the perforation formation stage. The perforation expansion is demarcated by a drastic increase of dead cells and enlargement of the hole and precedes the mature stage where PCD halts 4-5 cell layers from the veins. Cleared and fixed stained specimens for the preperforation (B), window (C) and mature (D)

stages. Antioxidant (400 µg/ml ascorbic acid + 200 µg/ml cysteine) treated window and mature stage leaves (E). Early window stage leaf treated with ROS (1 mM H_2O_2) (F). Bars = 40 µm.

3.4.3. Long-Term Live Cell Imaging

The treatments optimized in whole plant experiments were utilized for detached, early-window stage leaves. The detached leaves were observed using a modified long-term live cell imaging technique developed by Wertman et al. (2012) (Figure 3.4; Appendix A: Online Resource 3.1 and 3.2). In the control treatment (Figure 3.4A), the time for all PCD stage cells to die was 62.08 ± 4.89 h (Figure 3.5). The antioxidant treatment (Figure 3.4B) slowed the progression of PCD significantly compared to the control, as the time for PCD stage cells to die was 111.43 ± 8.80 h (Figure 3.5). There was also a strong phenolic ring that formed centrally, approximately 36-48 h into the observation (T48; Figure 3.4B), which was more pronounced than that observed in control samples (T36; Figure 3.4A). The 1mM H_2O_2 ROS treatment (Figure 3.4c) had a time of death of 54.85 ± 1.75 h (Figure 3.5), which did not differ significantly from the control. The 5 mM H_2O_2 ROS treatment increased the rate of cell death significantly (Figure 3.4D), as the time of death was 29.88 ± 2.21 h (Figure 3.5). After death of the PCD area, even NPCD cells lost their pigmentation and died approximately 36-48 h into the experiment (T48, Figure 3.4D).

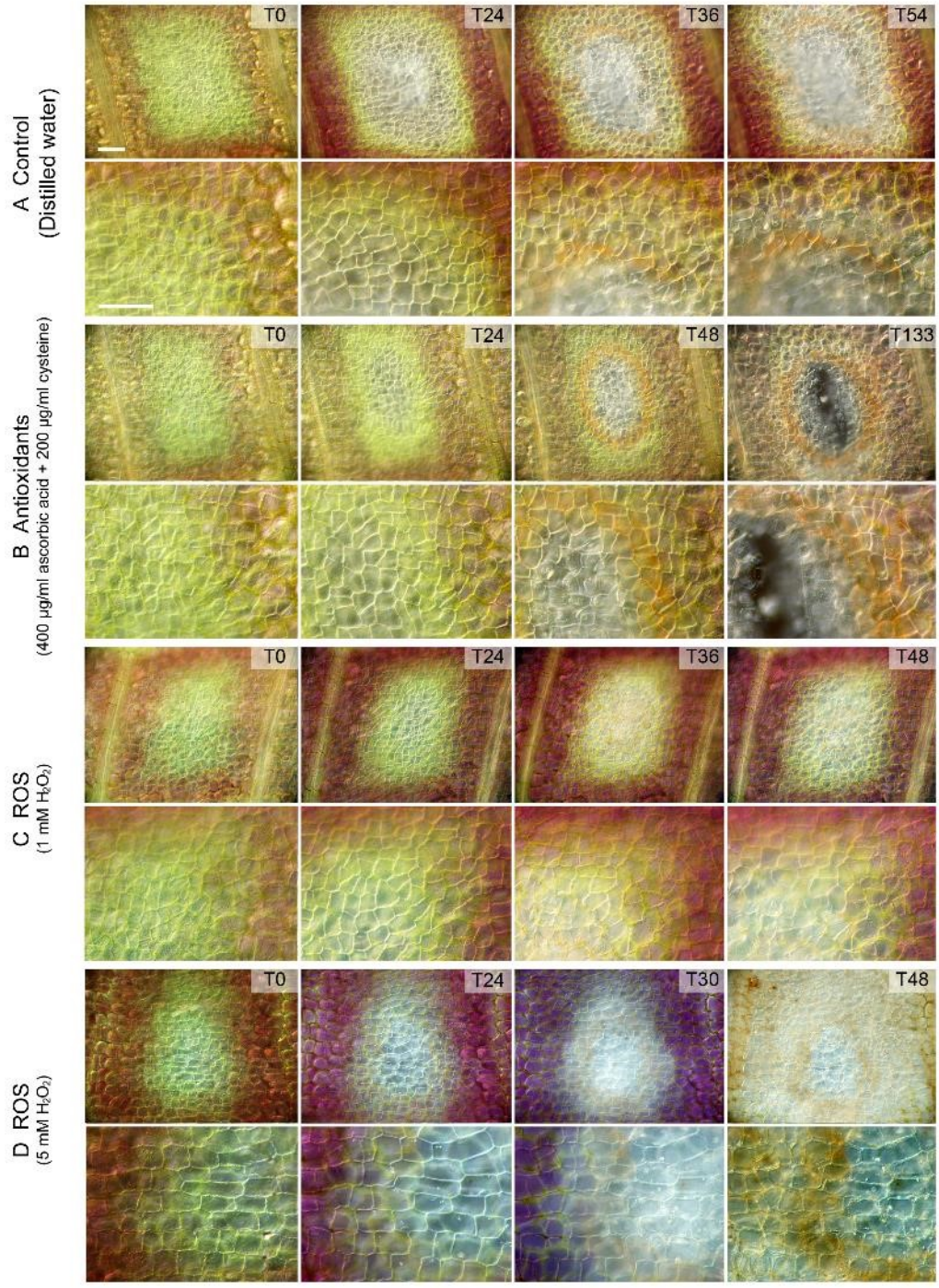

Figure 3.4. Long-term live cell imaging of window stage leaves. Control leaves at T0, 24, 36 and 54 h, just prior to the death of the leaf (A). Antioxidant-treated leaves [400 µg/ml ascorbic acid (AA) and 200 µg/ml L-Cysteine (Cys)] at T0, 24, 48 and 133 h (B). The 1 mM H_2O_2 ROS treatment at T0, 24, 36 and 48 h (C). The 5 mM H_2O_2 treatment at T0, 24, 30 and 48 h (D). The top row shows a generalized view of the areole, the bottom focuses on the PCD gradient at a higher magnification. Please see Appendix A: Online Resource 3.1 and 3.2 for more detail. Bars = 50 µm.

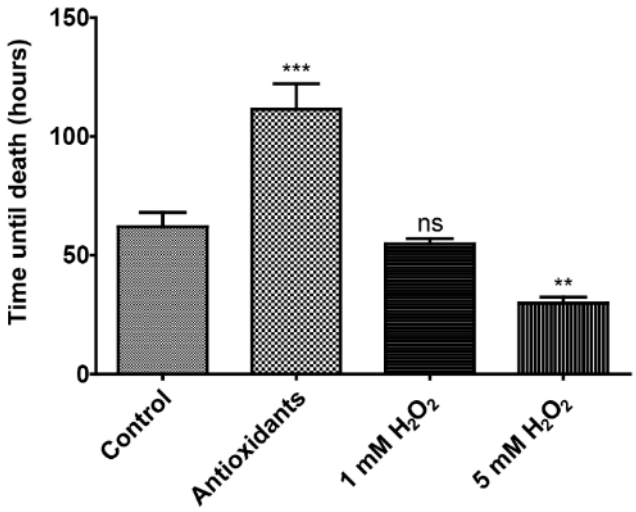

Figure 3.5. Long-term live cell imaging, mean times for death of PCD areas. Window stage leaves were observed under the control, antioxidant (400 µg/ml ascorbic acid + 200 µg/ml cysteine), 1 mM H_2O_2 and 5 mM H_2O_2 treatment groups. Antioxidant treatment significantly increased the mean time for death compared to the control, while the 1 mM H_2O_2 treatment had no effect, however 5 mM H_2O_2 exposure increased the rate of death. (One-way ANOVA, Dunnett's multiple comparison test, ***, $P < 0.001$; **, $P < 0.01$; ns, non-significant; $n = 3$). Error bars represent standard error.

3.4.4. SOD1 and CAT Detection

The levels of two antioxidant enzymes (SOD1 and CAT) were investigated for window stage and mature leaf extracts via western blotting for the control and each of the treatments (Figure 3.6). Among the window stage samples, the relative SOD1 band intensities were significantly lower in antioxidant, as well as the antioxidant + ROS treated leaves compared to controls, but there were no differences observed from the ROS (1 mM H_2O_2) treatment (Figure 3.6A, B). No significant differences in SOD1 were detected among the treatment groups for mature stage leaves (Figure 3.6A, C). The relative CAT band intensities showed no significant difference in window stage leaves among the control and other treatment groups (Figure 3.6A, D). In mature leaves, the

antioxidant treated leaves had significantly higher CAT proteins than the control, but there were no differences between the control and either the H_2O_2 (ROS) or antioxidant + ROS treatment groups (Figure 3.6A, E).

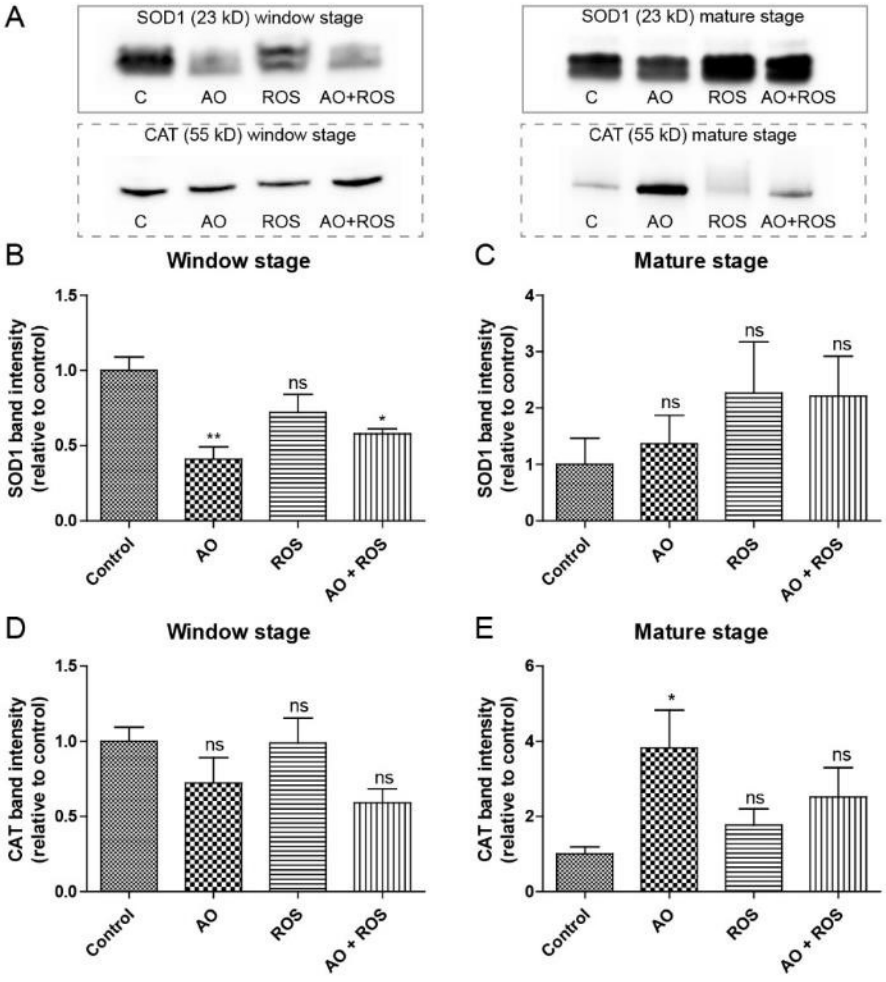

Figure 3.6. Detection of superoxide dismutase 1 (SOD1) and catalase (CAT). Western-blotting for the control (C), antioxidant (AO; 400 µg/ml ascorbic acid and 200 µg/ml Cys), 1 mM H_2O_2 reactive oxygen species (ROS) and AO + ROS treatment groups. Immunoprobing for SOD1 and CAT (A). SOD1 mean protein band intensities for window stage (B) and mature leaves (C). CAT mean protein band intensities for window stage (D) and mature leaves (E). (One-way ANOVA, Dunnett's multiple comparison test, **, $P < 0.01$; *, $P < 0.05$ ns, non-significant; $n \geq 4$). Error bars represent standard error.

3.4.5. Anthocyanin and ABTS Spectrophotometric Assays

Spectrophotometric assays were used to determine anthocyanin and antioxidant scavenging levels in window stage and mature lace plant leaves (Table 3.1). Total anthocyanin content (C3RE) ranged from 0.34-3.29 mg/g. In both window and mature leaves, plants exposed to the antioxidant combination treatment had the lowest anthocyanin levels. Among the window stage, the antioxidant treatment was significantly different compared to all other groups. Mature leaves had significantly lower anthocyanins levels compared to window stage leaves with the exception of the window stage antioxidant treatment group. The ABTS assay showed higher radical scavenging activity in window stage leaf extracts compared to mature leaves across all treatment groups, however no significant differences were observed among treatment groups within each developmental stage. Antiradical scavenging capacity from the ABTS assay ranged from 1.69-1.88 mg vitamin C equivalents per gram.

Table 3.1. Anthocyanin and 2,2'azino-bis(3-ethylbenzothiazoline-6-sulfonic acid) (ABTS) spectrophotometric assays. Anthocyanin content was measured for window stage and mature leaves for the control, antioxidant (400 µg/ml AA + 200 µg/ml Cys), ROS (1 mM H_2O_2), and the antioxidant + ROS treatment groups. Antiradical scavenging activity was determined using the ABTS assay. Anthocyanin levels were expressed in cyanidin-3-rutinoside equivalents and ABTS in vitamin C equivalents. Means with different letters differ significantly. One-way ANOVA, Tukey test ($P < 0.05$; $n \geq 4$).

	Anthocyanin		**ABTS**	
	mg C3RE/g	Grouping	mg VCE/g	Grouping
Window Stage				
Control	2.58 ± 0.10	AB	1.87 ± 0.04	A
Antioxidants	0.34 ± 0.17	C	1.88 ± 0.05	A
ROS (H_2O_2)	3.29 ± 0.29	A	1.87 ± 0.01	A
Antioxidants + ROS	2.27 ± 0.32	B	1.86 ± 0.03	A
Mature Stage				
Control	0.95 ± 0.11	C	1.70 ± 0.03	B
Antioxidants	0.70 ± 0.14	C	1.73 ± 0.03	B
ROS (H_2O_2)	1.22 ± 0.23	C	1.75 ± 0.05	B
Antioxidants + ROS	0.71 ± 0.11	C	1.69 ± 0.04	B

3.5. DISCUSSION

PCD is integral for the development and defense of plants and critical for their sessile lifestyle (Bozhkov and Lam 2011; van Doorn et al. 2011). Although there have been great advances in our understanding of plant PCD, the underlying mechanisms regulating the process are still being unraveled (van Doorn et al. 2011; Olvera-Carrillo et al. 2015; Van Durme and Nowack 2016). The lace plant has emerged as an excellent model for studying developmental PCD during leaf morphogenesis (Dauphinee and Gunawardena 2015). A striking feature of the lace plant is the presence of anthocyanins during PCD in early development and their distribution pattern in the cell death gradient. This study investigated the role of antioxidants and ROS during developmental PCD in the novel lace plant model system.

Whole plant experimentation was used to evaluate the effects of antioxidants and ROS on perforation formation. A gradient of concentrations was tested for either ascorbic acid or cysteine, along with a combination of the two, to determine which was most effective at reducing the number of perforations. Ascorbic acid (also vitamin C, or ascorbate) has long been known for its antioxidant properties and exogenous applications have been shown to reduce oxidative damage (Smirnoff and Wheeler 2000; Arrigoni and De Tullio 2002). Examples include the ability to reduce insult from salt stress in tomato seedlings (Shalata and Neumann 2001), and the hypersensitivity of vitamin C deficient mutants to ozone and UVB stress (Smirnoff and Wheeler 2000). Similar to ascorbic acid, cysteine is an antioxidant and it is the rate-limiting precursor for glutathione production (Lu 2013). Glutathione is critical for redox homeostasis as it is a component of the ascorbate-glutathione pathway that deals with the degradation of H_2O_2 (Szalai et al. 2009). Whole plant treatments revealed that the optimized combination antioxidant treatment (400 µg/ml ascorbic acid and 200 µg/ml cysteine) significantly decreases the formation of perforations and does not have a significant effect on leaf lengths, suggesting that growth was not adversely affected. The combination of ascorbic acid and cysteine was more effective at inhibiting perforations than either of the compounds alone (Figure 3.2f). This may be due to the increased quantity of antioxidants in this combination group, or the additional cysteine that can increase glutathione levels (Lu 2013) and may have stabilized the ascorbic acid, which is a known effect of glutathione in aqueous solutions (Touitou et al. 1996). The ability of H_2O_2 to induce PCD and its implication within the signaling cascade has been established (Gechev and Hille 2005; Gechev et al. 2006; Gadjev et al. 2008a). The 1 mM H_2O_2 treatment did not affect the number of perforations compared to

the control group (Figure 3.2). However, its application did increase lace plant PCD in the antioxidant + ROS treatment group, as evidenced by the increased number of perforations in leaves 2 and 3 (Figure 3.2). Therefore, the application of 1 mM H_2O_2 was able to negate the inhibitory effect of the antioxidant treatment, which is consistent with the literature.

NBT staining of leaves from each stage of perforation development indicated that O_2^- anions accumulate in PCD cells suggesting that dying cells are under oxidative stress. Oxidative stress occurs when there is an imbalance between antioxidants and oxidants in favor of the oxidants that leads to intracellular damage and can trigger cell death if the insult is severe enough (Sies 1997; Kacprzyk et al. 2011). Strong NBT staining was not observed in NPCD cells, indicating they have lower stress levels than neighboring PCD cells. Furthermore, it suggests that NPCD cells, which have abundant anthocyanins have greater antioxidant levels and may be able to neutralize ROS effectively compared to PCD stage cells. Superoxide radicals are primarily generated by the electron transport chain of mitochondria and the membrane-bound PSI electron acceptor found in chloroplast thylakoids (Bowler et al. 1992; Gill and Tuteja 2010). Previous studies in the lace plant have shown that chloroplast degradation occurs as cells transition to the later phases of PCD (Wright et al. 2009), and mitochondrial dysfunction and loss of membrane potential occurs during these later stages as well (Lord et al. 2011). It is well established that as ROS accumulate, there is further damage to mitochondria and a reduction in antioxidant defense (Lin and Beal 2006). The positive feedback loop of ROS production and intracellular damage may be responsible for the sharp contrast observed in NBT

staining between the NPCD and PCD regions. The fact that antioxidant treated leaves also had less NBT staining, specifically in the window stage (Figure 3.2e) further supports this notion.

Long-term live cell imaging experiments showed a similar trend to the whole plant results. The antioxidant treatment reduced the rate of death in PCD cells and increased the lifespan of the detached leaf significantly compared to the control. In contrast, the 5 mM H_2O_2 treatment increased cell death rates and leaves expired faster than the control. In addition to the increased lifespan, the antioxidant treatment appeared to promote the formation of a phenolic ring within the center of the areole, which was faint or incomplete in the other treatment groups by comparison. Histochemical tests with Fluorol Yellow 088 suggest that the phenolic rings (Figure 3.4B) contain suberin (data not shown). Mature lace plant leaves develop brown-colored rings of suberin at the edge of the perforation boundaries to protect against pathogens and nutrient loss (Gunawardena et al. 2007). Similarly, in wounded Arabidopsis leaves, PCD and the deposition of phenolic compounds serves to prevent the entry of pathogens (Cui et al. 2013). In Arabidopsis *bos1* mutants lacking the wound response, there is a ROS-associated runaway cell death process throughout the plant. The phenolic rings observed here in antioxidant treated window stage leaves appear to form a protective barrier to isolate dying cells and are believed to serve the same purpose as in mature lace plant leaves.

Western-blot analysis was performed in order to determine how the levels of two critical antioxidant enzymes (SOD1 and CAT) differed between window stage leaves actively

undergoing PCD, and mature stage leaves where developmental PCD has halted in all experimental plants. In general, there were higher levels of SOD1 in mature leaves compared to the window stage. Cells within mature stage leaves are advanced in age which may factor in to differential ROS production compared to the window stage. Mature leaves also have fully mature chloroplasts that are known to produce O_2^- (Mignolet-Spruyt et al. 2016). Further support comes from the NBT staining, which revealed O_2^- throughout the mature leaves. There was a significant decrease in SOD1 levels in the antioxidant, as well as the antioxidant + ROS treated window stage leaves compared to the control, which suggests that these cells were less stressed from O_2^- and therefore required lower levels of the protein to maintain homeostasis. A significant increase in CAT levels were observed following antioxidant treatment in mature leaves. Previous studies have shown that ascorbic acid, cysteine, and glutathione inhibit CAT activity (Foulkes and Lemberg 1948; Davisons et al. 1986) and in response to ascorbic acid treatment, there is increased expression of ascorbate peroxidase and *CAT* in cucumber protoplasts (Ondrej et al. 2010), which may account for the strong effect observed in the mature stage antioxidant treatment group.

The spectrophotometric assays revealed that anthocyanin levels were generally lower in mature leaves compared to the window stage. In window stage samples, there was significantly lower anthocyanin in the antioxidant treatment compared to the control and the highest levels observed were in the H_2O_2 samples. These results matched observations in window stage leaves from whole plant experiments and further support the notion that anthocyanins are also produced by plants in response to stress (Chalker-

Scott 1999). Anthocyanins are naturally present in young lace plant leaves. The ABTS assay indicated that mature leaves have significantly lower antiradical activity compared to window stage leaves, which coincides with lower anthocyanin levels.

Anthocyanins are water-soluble phenolic pigments with antioxidant properties that are involved in various stress responses and can be found in nearly all plant tissues (Chalker-Scott 1999; Liakopoulos et al. 2006; Tanaka et al. 2008). They are often located in epidermal cell layers in leaf tissues, however in the lace plant they are found in the mesophyll, which is also known to occur in genera including: *Syzygium*, *Rhododendron*, *Viburnum*, and *Mahonia* (Chalker-Scott 1999). Anthocyanins are also known to accumulate in young tissues in a process known as juvenile reddening and increase in aging tissues prior to senescence, which is a form of PCD (Chalker-Scott 1999; Lee 2002; Thomas et al. 2003). In addition, anthocyanins provide tolerance to environmental stress induced by drought, wounding, chilling or freezing, UVB and heavy metals, and they offer resistance to herbivory and pathogens (Gould 2004). To the best of our knowledge however, the lace plant represents the only known association of anthocyanins with PCD in early leaf development. Further research is underway to understand the specific forms of anthocyanins present and their potential roles relative to development and stress in lace plant leaves.

Preperforation stage leaves emerge from the corm with a complete vein pattern and an abundance of anthocyanins (Gunawardena et al. 2004). As leaves reach the window stage of development, the PCD gradient is established, but it is not currently known how this gradient is formed or what developmental cue triggers anthocyanin biosynthesis in these

young leaves. Anthocyanins are typically synthesized within individual cells and are not known to travel long distances throughout the plant body (Landi et al. 2015). However, the anthocyanin precursors naringenin, dihydrokaempferol, and dihydroquercetin can move from shoots to roots via cell-to-cell in Arabidopsis (Buer et al. 2007). Moreover, flavonoids can travel from cotyledons to the root tip through the vascular tissue (Buer et al. 2007). It may be possible that the veins transport the signals for anthocyanin biosynthesis, or its precursors to the areoles or cells, but there is no supporting evidence in the lace plant except for the loss of anthocyanins centrally within areoles at the onset of PCD. Catalase is a sink for H_2O_2 in plants, which is produced in various stress responses including high light exposure. Vanderauwera et al. (2005) found that catalase deficient Arabidopsis plants, following exposure to intense light, upregulate a transcriptional cluster responsible for anthocyanin regulation and biosynthesis. It may be possible that an initial increase in ROS, specifically H_2O_2, contributes to the establishment of the antioxidant gradient observed in window stage leaves. Our results indicated that PCD-inhibited mature leaves following antioxidant exposure also have high catalase protein levels compared to control condition. The signal responsible for the establishment, and subsequent disappearance of anthocyanins during PCD remains unknown in the lace plant. We hypothesize that a gradient of anthocyanins, which is highest in the NPCD cells, offers resistance to PCD induction.

Future work will include the identification of the molecular and biochemical mechanisms controlling PCD, as well as the initial developmental stimuli leading to the observed decrease of anthocyanins and increase in ROS levels described here. Candidates include

phytohormones such as ethylene, salicylic acid, and jasmonates, or even ROS themselves. Ethylene has been implicated in lace plant PCD signaling during perforation formation and senescence (Dauphinee et al. 2012; Rantong et al. 2015), however the relationship between ethylene, antioxidants and ROS remains unknown. Positive feedback loops are known to exist between various hormones, reactive nitrogen species, and ROS, which ultimately trigger downstream effectors such as nucleases and proteases that carry out PCD (Van Breusegem and Dat 2006). The links between anthocyanins and vein patterning also warrants investigation. Disrupting vein development with auxin inhibitors such as N-1-naphthylphthalamidic acid or auxinole is hypothesized to alter the pattern of anthocyanin deposition and perforation formation.

A model and summary for the involvement of antioxidants and ROS in lace plant PCD is illustrated below (Figure 3.7). Our results indicate that antioxidants are important for redox homeostasis and that the loss of antioxidants or increased ROS plays a significant role in the lace plant PCD pathway. Due to the rarity of this natural phenomenon and the conspicuous pattern of anthocyanins during PCD, we believe that investigation into the species of anthocyanins and antioxidants involved is a priority moving forward, as there may be potential industrial or medicinal applications for lace plant extracts.

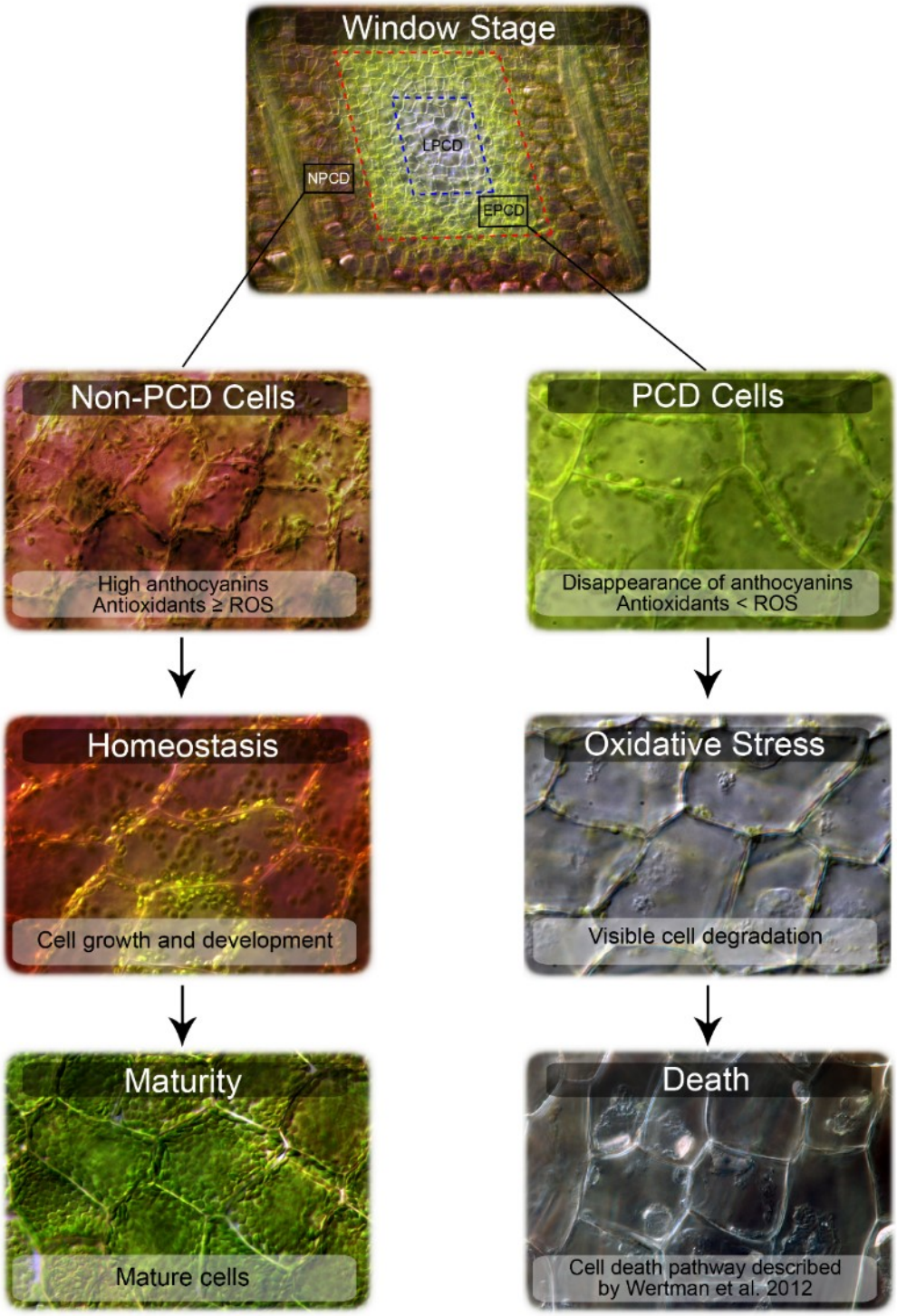

Figure 3.7. Antioxidants and ROS in lace plant developmental PCD signaling. The window stage of leaf development has a unique gradient of PCD. NPCD (non-PCD) cells within the gradient are found 4-5 cell layers from the veins and contain anthocyanins. Cells undergoing PCD are found centrally and have lost their anthocyanin pigmentation.

3.6. AUTHORS' CONTRIBUTIONS

AND carried out all experimentation with the exception of the spectrophotometric assays. JIF ran the spectrophotometric assays and contributed to the whole plant experiments, plant culturing, and assisted with long-term live cell imaging. GD contributed to the NBT staining and long-term live cell imaging. AND drafted the first MS including figure preparation and revised the final manuscript. AHLAN and CRL contributed to MS revisions and final MS preparation. AHLAN designed and supervised the experiments while CRL co-supervised this study.

3.7. ACKNOWLEDGEMENTS

We thank Jaime Wertman (Dalhousie University) for a critical review of the manuscript. We also thank Stephen Chew (Dalhousie University) for his assistance with long-term live cell imaging and western blot experiments, which was supported by a Sarah Lawson Research Scholarship. Funding was provided by the Natural Sciences and Engineering Research Council of Canada (NSERC) through the Discovery Grants Program for both CRL (grant #121550) and AHLANG (grant #45162). AHLANG also received funding from the Canadian Foundation for Innovation (CFI) Leaders Opportunity Fund (grant #14831). PhD support for AND was provided by NSERC and The Killam Trust.

CHAPTER 4

THE ROLES OF AUTOPHAGY IN THE LACE PLANT

4.1. ABSTRACT

The lace plant is an aquatic monocot that utilizes programmed cell death (PCD) to form perforations throughout its leaves as part of normal development. The lace plant is a novel model system representing a unique form of developmental PCD. The role of autophagy in lace plant PCD was determined using a novel live cell imaging assay, transmission electron microscopy (TEM), immunolocalization, western blotting, and whole plant pharmacological experimentation. Live cell imaging revealed that the promotion (or enhancement) of autophagy significantly decreased cell death rates compared to the control whereas inhibition had the opposite effect. Ultrastructural analysis using TEM linked autophagy to cellular dismantling, and autophagosomes were found near endoplasmic reticulum-like membranes. Chloroplast degradation and evidence for chlorophagy was observed during normal development and following exposure to stress. The involvement of autophagy in lace plant PCD was further supported using immunolocalization of Atg8 (integral protein for autophagosome formation), where a significant increase in fluorescent puncta were observed in dying cells compared to healthy control cells. The promotion of autophagy in whole plants led to the production of fewer perforations compared to the control and its inhibition increased the number of perforations. Our data indicate that autophagy predominantly

contributes to cell survival, however it also plays a role in cellular degradation during developmental PCD.

4.2. INTRODUCTION

4.2.1. Programmed Cell Death Classifications

Programmed cell death (PCD) is an essential mechanism in the development and defense of multicellular organisms as it allows for the precise deletion of unwanted or compromised cells while facilitating nutrient recycling (Greenberg 1996; Green 2011; Kacprzyk et al. 2011). In animals, there are two classic forms of PCD based on morphological characteristics: apoptosis (Type I cell death) and autophagic cell death (Type II cell death) (Kroemer 2009; Green 2011; Galluzzi et al. 2012). The morphological types of PCD were long viewed as active processes requiring energy in the form of ATP and contrasted with necrosis (Type III cell death), which was characterized as a passive death brought on by severe damage and evident as an early rupture of the plasma membrane (Green 2011). The defining morphological feature of apoptosis is the packaging of degraded cellular contents into discrete apoptotic bodies for subsequent digestion, whereas autophagic cell death is identifiable by a high degree of vacuolization and double-membrane bound lytic vesicles called autophagosomes (Edinger and Thompson 2004).

The mechanisms controlling plant PCD are not as well understood compared to animal systems that have clearly defined biochemical subroutines (Galluzzi et al. 2012). The

signaling pathways of plant PCD are being unraveled in a variety of systems and there have been significant advancements in the field (Bozhkov and Lam 2011; Daneva et al. 2016). Recent attempts to classify plant PCD based on morphology have distinguished at least two forms: i) vacuolar cell death which occurs during tissue patterning and involves autophagy-like processes and the release of hydrolases from lytic vacuoles and ii) necrosis, which is typically associated with abiotic stress and features early plasma membrane (PM) rupture, protoplast shrinkage, and a lack of autolytic behavior (van Doorn et al. 2011). Although there has been some debate over the morphological classification of plant PCD (Dauphinee and Gunawardena 2015) it is evident that autophagy, or "self-eating" plays a significant role in the majority of developmental systems described to date.

4.2.1. Forms of Autophagy in Plants

Autophagy, not to be confused with autophagic/type II cell death, involves the breakdown of cellular constituents for remobilization (Green 2011; Liu and Bassham 2012). Autophagy is a survival mechanism that is important for cellular division and helps to maintain cellular homeostasis under stressful conditions such as nutrient deprivation or starvation (Bassham 2007). Autophagy has also been implicated in PCD signaling (Bozhkov and Jansson 2007), suggesting it has a dual role in the life and death of cells (Baehrecke 2003). Previous classifications of plant autophagy based on ultrastructure suggested there are at least three major forms: i) microautophagy, which involves the direct passing of contents into the vacuole; ii) macroautophagy, where

double-membrane bound structures known as autophagosomes surround cytoplasmic contents and then fuse with the tonoplast – the result is a single membrane autophagic body with the contents slated for degradation in the vacuole (Liu and Bassham 2012; Yang et al. 2016), and iii) mega-autophagy, which is characterized by cellular degradation following the release of hydrolases from the vacuole after tonoplast rupture (Van Doorn and Papini 2013). However, more recently mega-autophagy has been called into question; even though it is an autolytic process, there is no evidence indicating it is dependent on Atg proteins (van Doorn 2011). Macro-autophagy, hereafter referred to as autophagy is the most studied form and the focus of the current study.

4.2.2. Autophagy Signaling Pathway and Modulation

In humans, autophagy is known to play a significant role in ageing and the progression of several disorders including, but not limited to: neurodegenerative disease, liver disease, heart disease and cancer (Jiang and Mizushima 2014). Due to the significant involvement of autophagy in a wide range of developmental processes and diseases, there has been substantial effort to develop drugs that modulate autophagic flux (e.g. Figure 4.1). Autophagy is an evolutionary conserved process in fungi, plants, and animals. In fact, a great deal of our understanding of the regulatory genes involved in autophagy originated from yeast (*Saccharomyces cerevisiae*) mutagenic studies (Liu and Bassham 2012). There are 34 autophagy-related (*ATG*) genes identified in yeast to date and among them is the key *ATG*8 gene family encoding ubiquitin-like proteins that are integral for autophagosome membrane formation (Shpilka et al. 2011). The central regulator of

autophagy is the mammalian target rapamycin (mTOR) kinase, which is a component of two complexes: mTORC1 and mTORC2. Autophagy is inhibited by mTORC1 and therefore compounds such as rapamycin (Ballou and Lin 2008) and aspirin (acetylsalicylic acid; Din et al. 2012) which block mTOR, promotes autophagosome formation (Heras-Sandoval et al. 2014). Autophagy is also upregulated in response to starvation or nutrient deprivation and osmotic stress through the inhibition of mTOR (Kwak et al. 2012; Liu and Bassham 2012; Heras-Sandoval et al. 2014). Upstream of mTOR is the phosphoinositide 3-kinase (PI3K) / Akt (protein kinase B) signaling pathway (Heras-Sandoval et al. 2014). Inhibition of PI3K with compounds such as wortmannin or 3-methyladenine (3MA) interferes with autophagosome formation (Yang et al. 2013). Autophagy can be inhibited by halting the breakdown of autophagic bodies by indirectly raising the vacuolar pH through the specific inhibition of vacuolar ATPases (Huss et al. 2002). Mishra et al. (2017) recently developed a firefly-luciferase yeast pexophagy assay to rapidly analyze the effects of FDA approved small molecules from the library of pharmacologically active compounds. Bay 11 and ZPCK (Z-L Phe chromethyl ketone) were the most promising inhibitors identified by high throughput screening (HTS) yeast assay and also had the ability to effectively suppress autophagy in mammalian cells and the lace plant (*Aponogeton madagascariensis*) model system. The lace plant was shown to be a tractable system for studying autophagy *in planta*.

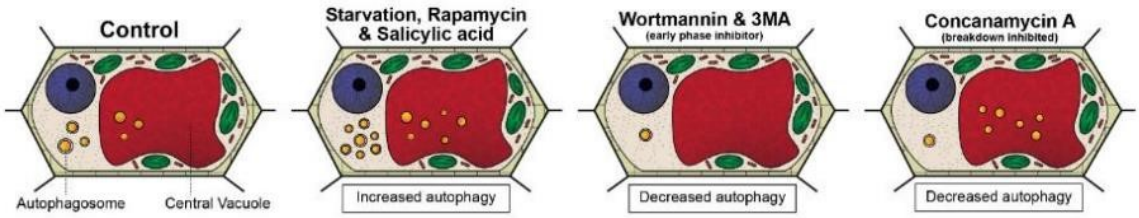

Figure 4.1. Modulation of autophagy. Compared to the control, starvation, rapamycin, and acetylsalicylic acid increase the number of autophagosomes within the cell. Wortmannin and 3-methyladenine (3MA) are early phase inhibitors of autophagy. Concanamycin A inhibits the breakdown of autophagic bodies in the vacuole (Mishra et al. 2017).

4.2.3. The Lace Plant Model System

The lace plant is an aquatic monocot with a unique perforated morphology created by developmentally regulated PCD (Figure 4.2A; Gunawardena et al. 2004). The lace plant is an excellent model for studying PCD due to the predictability of perforation formation, its nearly transparent leaves that facilitate live cell imaging and established sterile cultures for pharmacological experimentation (Gunawardena 2008). The first visible sign that PCD is underway is the disappearance of anthocyanins between longitudinal and transverse veins in spaces known as areoles (Gunawardena et al. 2004). The disappearance of anthocyanins provides a visual gradient of PCD within each areole (Figure 4.2B-C): Non-PCD (NPCD; Figure 4.2D) cells retain anthocyanins throughout perforation formation, early-PCD (EPCD; Figure 4.2E) cells have lost anthocyanin and are fated to die but still have an abundance of chlorophyll pigmentation, and cells that are in the late-PCD (LPCD; Figure 4.2F) stage are nearly devoid of pigmentation and near death (Lord et al. 2011). The dynamics and time-course analysis of lace plant PCD has

been described in detail (Wertman et al. 2012), however the regulators of the process remain elusive.

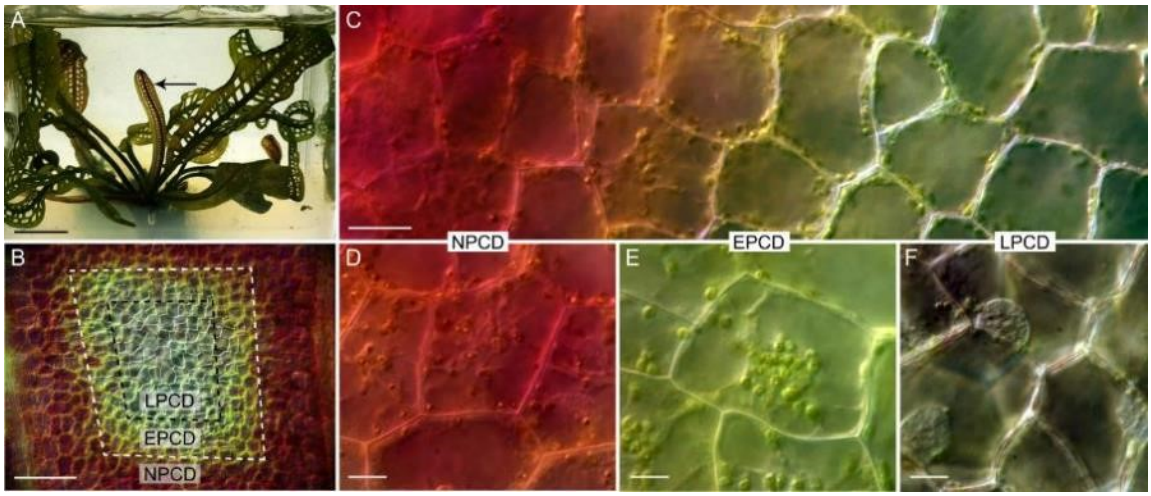

Figure 4.2. The lace plant developmental PCD model system. (A) Lace plant grown in axenic magenta box culture producing a window stage leaf (arrow) where PCD is actively occurring. Between the longitudinal and transverse veins is the areole (B), and in the window stage of leaf development there is a gradient of cell death (C).(Lord et al. 2011) D-F higher magnification of representative cells along the gradient of cell death. (D) Non-PCD (NPCD) do not die during perforation formation. (E) Early-PCD (EPCD) cells have lost anthocyanin pigmentation and are undergoing PCD. (F) Late-PCD (LPCD) cells are nearly devoid of pigmentation and are near death.(Lord et al. 2011) Scale bars: A = 1 cm; B = 80 µm; C = 20 µm; D-F = 10 µm.

Lace plant PCD results in cell auto-lysis, characterized as a rupture of the tonoplast in the final phases of cell death (Wertman et al. 2012; Dauphinee et al. 2014). Preliminary evidence suggests that autophagy may have a role in PCD (Wertman et al. 2012). Dauphinee et al. (2014) showed that cell death induced by abiotic stressors at various degrees of insult all result in tonoplast collapse in the lace plant. Additionally, leaf cells treated with 30 mM NaOH had abundant vesicle formation and chloroplasts were seen within vesicles that fused to the central vacuole moments before death. Furthermore, Mishra et al. (2017) showed that MDC staining and Atg8 immunolocalization can be

used to detect autophagosomes in the lace plant and that autophagic flux can be modulated pharmacologically. Despite the aforementioned evidence surrounding autophagic processes in the lace plant, its function in lace plant developmental PCD remains unexplored. Therefore this work aims to determine the role of autophagy in PCD signaling during perforation formation.

4.3. MATERIALS AND METHODS

4.3.1. Plant Material, Pharmacological Experimentation and Autophagy Modulation

Lace plants were propagated according to Gunawardena et al. (2006) and grown in magenta Murashige and Skoog (MS) liquid and solid (1% agar) media. To test the effects of various modulators on PCD during perforation formation, 40 mL septum-lidded vials were used (Sigma Aldrich). Plants were grown in magenta boxes under daylight deluxe fluorescent lightning (Phillips) on 12 hour dark/light cycles at an intensity of 125 $\mu mol\ m^{-2}\ s^{-1}$ for approximately 6 weeks and then transferred to the vials and allowed to acclimate for 2-3 weeks. Once plants produced 2-3 perforated leaves they were selected for experimentation and assigned randomly to a treatment group. Treatments were optimized using detached window stage leaves according to Mishra et al. (2017) Autophagy modulation was achieved using the following treatments: 5 µM rapamycin (Enzo Scientific, BML-275), 5 µM wortmannin (Cayman Chemical, 10010591), and 1 µM concamaycin A (Santa Cruz Biotechnology, sc-202111). Additionally, a control group received an equal volume of DMSO (BioShop Canada, DMS666).

4.3.2. Live Cell Imaging Assay

The live cell imaging assay was modified from Wertman et al. (2012). Window stage leaves were detached from the plant to acclimate in distilled water overnight under the conditions described above. The following morning, the leaves were mounted in the designated treatment solution and placed on a custom grooved slide. The slide was then sealed with VALAP (a mixture of Vaseline, lanolin and paraffin wax) according to Kacpryzk et al. (2015) Videos of cells in whole leaf mounts subjected to the various treatments were captured on a Nikon Eclipse 90i microscope fitted with a DXM1200C digital camera using the audio video interleave recording function of NIS Elements AR 3.1 software (Nikon Instruments). Experiments ran for a maximum of 6 h, or until all LPCD stage cells expired. The number of dead cells (collapsed PMs visible) were counted prior to the beginning of the experiment and at the end of the observation period to determine the death rate per hour. Evans Blue (Sigma-Aldrich, 46160) staining was used to facilitate the counting of dead cells at the end of the experiments and carried out according to Wertman et al. (2012).

4.3.3. Atg8 Immunolocalization

Intracellular detection of Atg8 was achieved using an immunolocalization protocol adapted from Pasternak et al. (2015). Window stage leaves from axenic cultures were treated for 2 h with autophagy modulators or with an equal volume of DMSO for the

control group. The leaves were then fixed in 100% methanol at 37°C for 30 min. The tissues were then transferred to 800 µl of fresh 100% methanol and hydrophilized to a concentration of 20% methanol at 60°C through the addition of 200 µl of distilled water every two min for 32 min. Leaves were then cut into 2 mm^2 pieces and rinsed in distilled water before being placed onto a multi-well slide. The leaf pieces were then allowed to dry on the slide for approximately 5 min until all excess liquid evaporated. Blocking was done for 30 min at 37°C with 4% (w/v) low fat milk in 1X MTSB (microtubule stabilization buffer: 7.5 g Pipes, 0.85 g EDTA, 0.61 g $MgSO_4*7H_2O$ and 1.25 g KOH, pH 7). Incubation with the Atg8 rabbit polyclonal primary antibody (Agrisera, AS14 2769) was done at 37°C for 30 min at a 1:1,000 dilution in MTSB. Samples where then rinsed for five min three times with MTSB. Secondary incubation was done with a 1:2000 dilution of Goat anti-rabbit Dylight® 488 polyclonal antibody (Agrisera, AS09 633) in MTSB. The samples were then rinsed as above and mounted in MOWIOL (Sigma) prior to viewing with a Nikon Eclipse *Ti* C1 confocal system (Nikon). Z-stack images were analyzed and converted to maximum intensity projections (MIPs) using NIS Elements AR 3.1 software and fluorescent punctate structures (puncta) were counted automatically using Image J (particle analysis set to a lower brightness threshold of 75).

4.3.4. Immunoblotting for Atg8

Mature stage leaves from pharmacological experiments were blot dried, and had their midribs removed prior to freezing in liquid nitrogen. Tissues were macerated on ice in equal volumes of Pipes buffer (pH 6.8) and a protease inhibitor solution. The protease

inhibitor solution consisted of a 1:2 ratio of two components (Component A: 10 mg/ml leupeptin and 10 mg/ml soybean trypsin inhibitor dissolved in Pipes buffer; Component B: 10 mg/ml pepstatin and 20 mg/ml PMSF dissolved in 95% ethanol). Following maceration, the samples were centrifuged for 15 min at 16,000 g. Total protein concentration of the supernatant was determined by Bradford assay. A 1:1 mixture of sample to 2X Laemmli Buffer (Bio-Rad, 1610737) with 5% β-mercaptoethanol (v/v) was prepared prior to gel electrophoresis. A total of 10 µg of protein was loaded for each sample lane, along with 5 µl of the Precision Plus Protein Standards solution (Bio-Rad, 1610374) in a 8-16% SDS polyacrylamide Mini-PROTEAN TGX precast gel (Bio-Rad, 456-1103). The gel was resolved at 100 V for 2 h in ice-cold running buffer (0.1% SDS (v/v), 25 mM Tris and 192 mM glycine, 8.3pH). Protein transfer to a 0.2 µm nitrocellulose membrane (Bio-Rad, 1610112) occurred overnight at 120 mA in a transfer buffer (20% methanol (v/v), 25 mM Tris and 192 mM glycine, 8.3 pH) at room temperature.

Ponceau staining on the membrane was done for 5 min to visualize protein transfer and then rinsed for 2 min in TBS-T (10 mM Tris, 140 mM NaCl, Tween-20, pH 7.4) prior to being photographed in a light box to reduce glare. The membrane was blocked in a 5% (w/v) low fat milk powder TBS-T solution with mild shaking. The membrane was then incubated overnight with the Atg8 primary antibody (detailed above) at a 1:10,000 dilution in TBS-T with 3% low fat milk powder (w/v) at 2°C. The following day, the membrane was rinsed with mild shaking in 1, 2, and 3 minute intervals in TBS-T. The secondary antibody (HRP conjugated Goat-anti rabbit polyconal; AS609 602, Agrisera)

was applied at a 1:20,000 dilution in TBS-T for 30 min and then the membrane was rinsed as above with an additional 2 min rinse in TBS (10 mM Tris, 140 mM NaCl, 0.1%, pH 7.4). Clarity Western ECL Substrate (Bio-Rad) was used according to the manufacturer's instructions. Protein bands were resolved using an MF-ChemiBIS 3.2 gel documentation system (DNR Bio-Imaging). Normalization of the protein lanes (image of ponceau staining) and the individual bands (immunoprobing results) were achieved using Image Studio Lite (Li-COR Bioscience). The signal intensities for individual protein bands were normalized using the mean of the control group prior to statistical analysis (see section 4.3.6 for details).

4.3.5. Transmission Electron Microscopy

Window stage leaves were treated for 2 h (30 min under vacuum at 15 psi) with autophagy modulators in distilled water in the dark prior to being cut into 2 mm^2 pieces. Additionally, leaf tissues were exposed to 30 mM NaOH according to Dauphinee et al. (2014). The leaf pieces were then fixed for a minimum of 2 h with 2.5% glutaraldehyde diluted in a 0.1 M sodium cacodylate buffer. The samples were then washed three times for 10 min each time, with the 0.1 M sodium cacodylate buffer. Secondary fixation with 1% osmium tetroxide was done for 48 h under vacuum (20 psi). The samples were then rinsed with distilled water briefly before being placed in 0.25% uranyl acetate at 4°C overnight. The samples were then dehydrated through a graduated series of acetone at 50, 70, 70, 95, 95, 100 and 100% for 10 min at each step of the process. Epon-Araldite resin was used to infiltrate the samples, initially in a 3:1 ratio of 100% acetone to resin for 3 h.

This step was followed by transferring the samples to a 1:3 ratio of 100% acetone and resin overnight. The samples were then placed in 100% Epon-Araldite resin for 3 h, two times. The samples were embedded in 100% Epon-Araldite resin and cured for 48 h at 60°C. Thin sections were cut using an Ultracut E Ultramicrotome (Reicher-Jung) with a diamond knife (100 nm thickness) and placed on formvar/carbon support film copper grids (Cedarlane, FCF205-CU-25). Staining was done using 2% aquous uranyl acetate for 10 min, followed by two 5 minute rinses with distilled water, 4 min in lead citrate counterstain and then a final quick rinse with distilled water. The samples were viewed with a JEM 1230 Transmission Electron Microscope (JEOL) at 80 kV and images were captured using a Hamamatsu ORCA-HR digital camera.

4.3.6. Statistical Analysis and Data Representation

Data analysis and graphical representations used GraphPad Prism 5 software (GraphPad Software Inc.). Data are represented as mean ± standard error. A one-way ANOVA was used for multiple comparisons. Maximum intensity projections of confocal z-stacks were made using NIS Elements AR 3.1 software. Figures were prepared using Adobe Illustrator and Adobe Photoshop, whereas videos were made with Premiere Pro (CC; Adobe Systems Inc). When necessary to improve clarity, adjustments to brightness, contrast, and exposure were made evenly within an individual image. Error bars represent standard error unless otherwise stated.

4.4. RESULTS

4.4.1. Live Cell Imaging Assay

In order to determine the effect of autophagy on cell death in the lace plant, a live cell imaging assay was developed, taking advantage of the unique characteristics of the lace plant gradient of cell death (Figure 4.3; Appendix A: Online Resource 4.1 and 4.2). Window stage areoles with 1-3 dead cells (asterisks, Figure 4.3A and dashed box, Figure 4.3C) were selected and continuous videos were captured for the control, 5 μM rapamycin, 1 μM concanamycin A and 5 μM wortmannin treatment groups (Figure 4.3A). At the end of experiments, DIC micrographs were taken (Final, Figure 4.3A) prior to Evans Blue staining (Final + Evans Blue, Figure 4.3A and 4.3D) was done to facilitate scoring of dead cells. The rate of cell death (% of LPCD cells per hour) was determined for each treatment group (Figure 4.3B). Leaves of the control group had a mean cell death rate of 6.79 ± 0.38 (% LPCD cells per hour). The 5 μM rapamycin treatment significantly reduced cell death to 1.74 ± 0.18 (% LPCD cells per hour). Conversely, the 1 μM concanamycin A and 5 μM wortmannin treatments significantly increased cell death rates in relation to the control to 15.00 ± 1.89 and 16.24 ± 1.72 (% LPCD cells per hour), respectively.

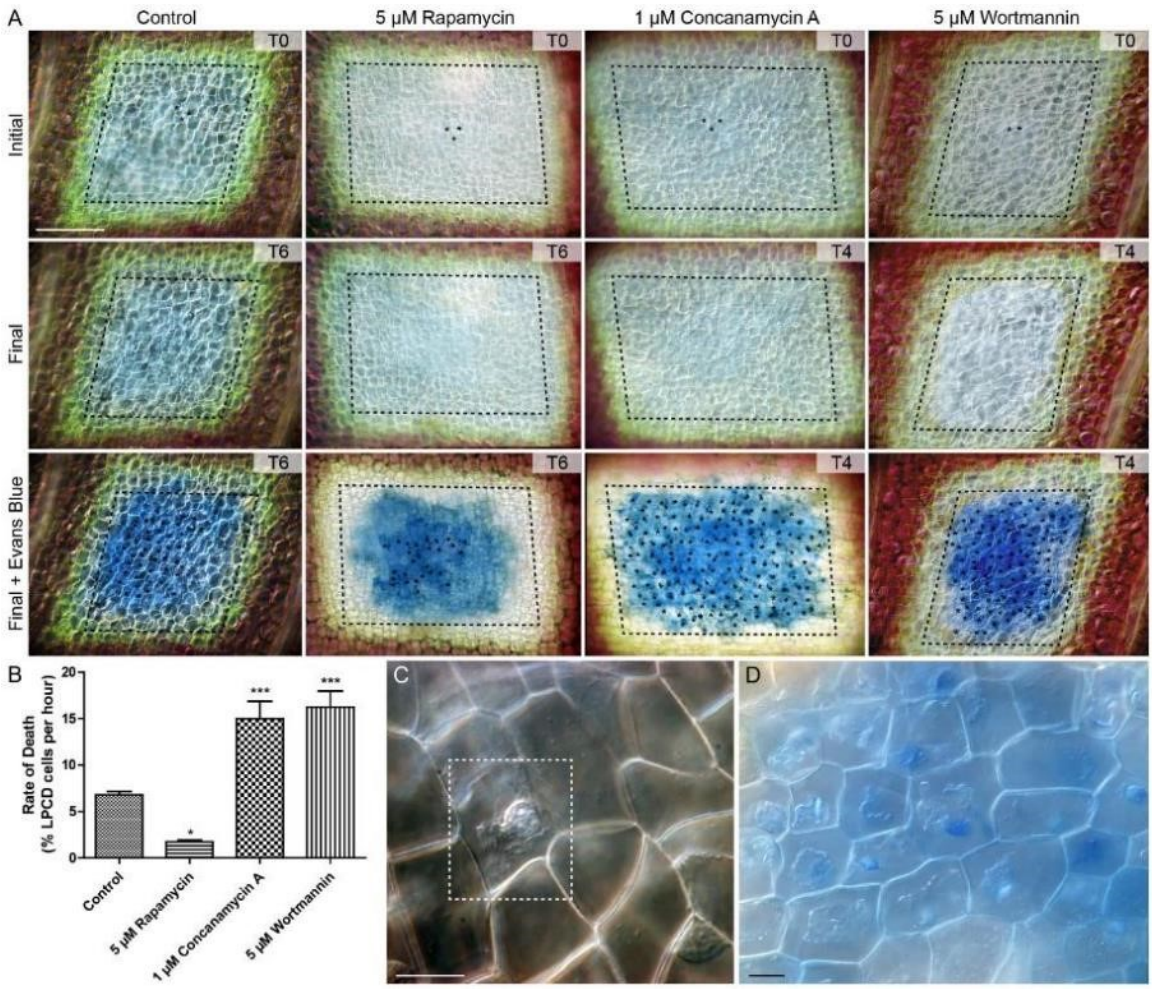

Figure 4.3. Live cell imaging assay. (A) Initial and final micrographs of window stage leaves. Evans blue staining was performed at the end of the experiments to facilitate the final scoring of cell death (asterisks). Treatments included: control, 5 µM rapamycin, 1 µM concanamycin A and 5 µM wortmannin. T = time, rounded up to the nearest hour. (B) The rate of death was calculated as the % of late programmed cell death (LPCD) cells per hour. (C) High magnification view of unstained dead cells (dashed box) in a window stage leaf. Evans Blue staining (D) was used to facilitate quantification of dead epidermal cells at the end of experiments. (One-way ANOVA, Dunnett's multiple comparison test ($n \geq 4$; ***, $P < 0.001$; *, $P < 0.05$). Error bars represent standard error. Scale bars: A = 150 µm; C-D = 5 µm.

4.4.2. Ultrastructure of the Lace Plant PCD Gradient

The lace plant PCD gradient was analyzed using transmission electron microscopy (TEM; Figure 4.4A). NPCD cells (Figure 4.4B) generally contain more cytoplasm

compared to EPCD (Figure 4.4C) and LPCD cells (Figure 4.4D). Vesicles, or pro-vacuoles were most abundant in NPCD and EPCD cells. Other noticeable features included increased vacuolization of the cells as PCD advanced (Figure 4.4D). The LPCD cells had the largest central vacuoles (cv, Figure 4.4B-D) in proportion to cytoplasm, and exhibited larger vacuolar aggregates (black arrows, Figure 4.4B-D) compared to the EPCD and NPCD stages. In all cell stages, there was an abundance of electron-dense granular bodies within the vacuole (white arrows), as initially observed by Gunawardena et al (2004).

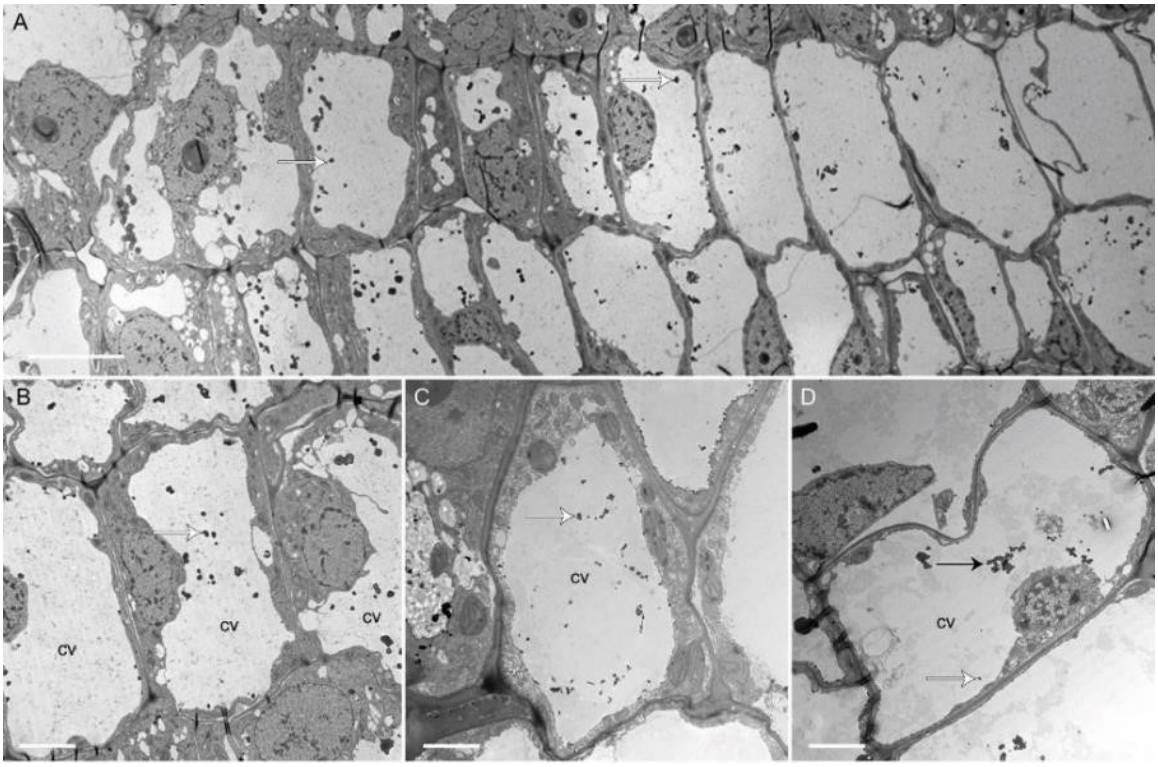

Figure 4.4. (A) Transmission electron microscopy (TEM) of the PCD gradient. (B) TEM of cells in the non-programmed cell death (NPCD), (C) early-programmed cell death (EPCD), and (D) late-programmed cell death (LPCD) zones where aggregates are frequently observed (black arrow). Please note that in all stages there is an abundance of electron-dense granular bodies (white arrows) in the vacuoles, as initially described by Gunawardena et al.(Gunawardena et al. 2004) cv = central vacuole. Scale bars: A = 20 µm; B-D = 5 µm

4.4.3. Autophagy in NPCD Cells

The ultrastructure of NPCD cells was analyzed for the control, 5 μM rapamycin, and 1 μM concanamycin A groups (Cells, Figure 4.5). Double-membrane bound autophagosomes were observed in the cytoplasm of the control (Cytoplasm, Figure 4.5) and in a great number of cells in the 5 μM rapamycin group. They were not observed as regularly in concanamycin A-treated samples, however they were visible/present in the cytoplasm (Cytoplasm, Figure 4.5). Aggregates, or autophagic bodies were found in the vacuoles of all treatment groups. However in general, the rapamycin and concanamycin A treatments appeared to have more contents in the vacuole compared to the control (Vacuole, Figure 4.5).

4.4.4. Autophagy in EPCD Cells

In EPCD cells, the general ultrastructure was similar to the NPCD cells, but there was a general increase in the vacuole to cytoplasm ratio. The highest number of double-membrane bound autophagosomes was observed in the cytoplasm of 5 μM rapamycin treated leaves (Cytoplasm, Figure 4.6). EPCD stage cells from the concanamycin A treatment group also had autophagosomes and resembled the control group (Cytoplasm, Figure 4.6). All treatment groups had autophagic bodies within their vacuoles, however the concanamycin A-treated samples had larger aggregates compared to the other groups (Vacuole, Figure 4.6).

4.4.5. Autophagy in LPCD Cells

Cells in the LPCD stage appeared to be greatly degraded and had a large vacuole with little cytoplasm remaining (Cell, Figure 4.7). All treatment groups had cytosolic autophagosomes (Cytoplasm, Figure 4.7) and autophagic bodies within the vacuole (Vacuole, Figure 4.7). The rapamycin and concanamycin A groups both had large vacuolar aggregates containing membranous bodies (Vacuole, Figure 4.7).

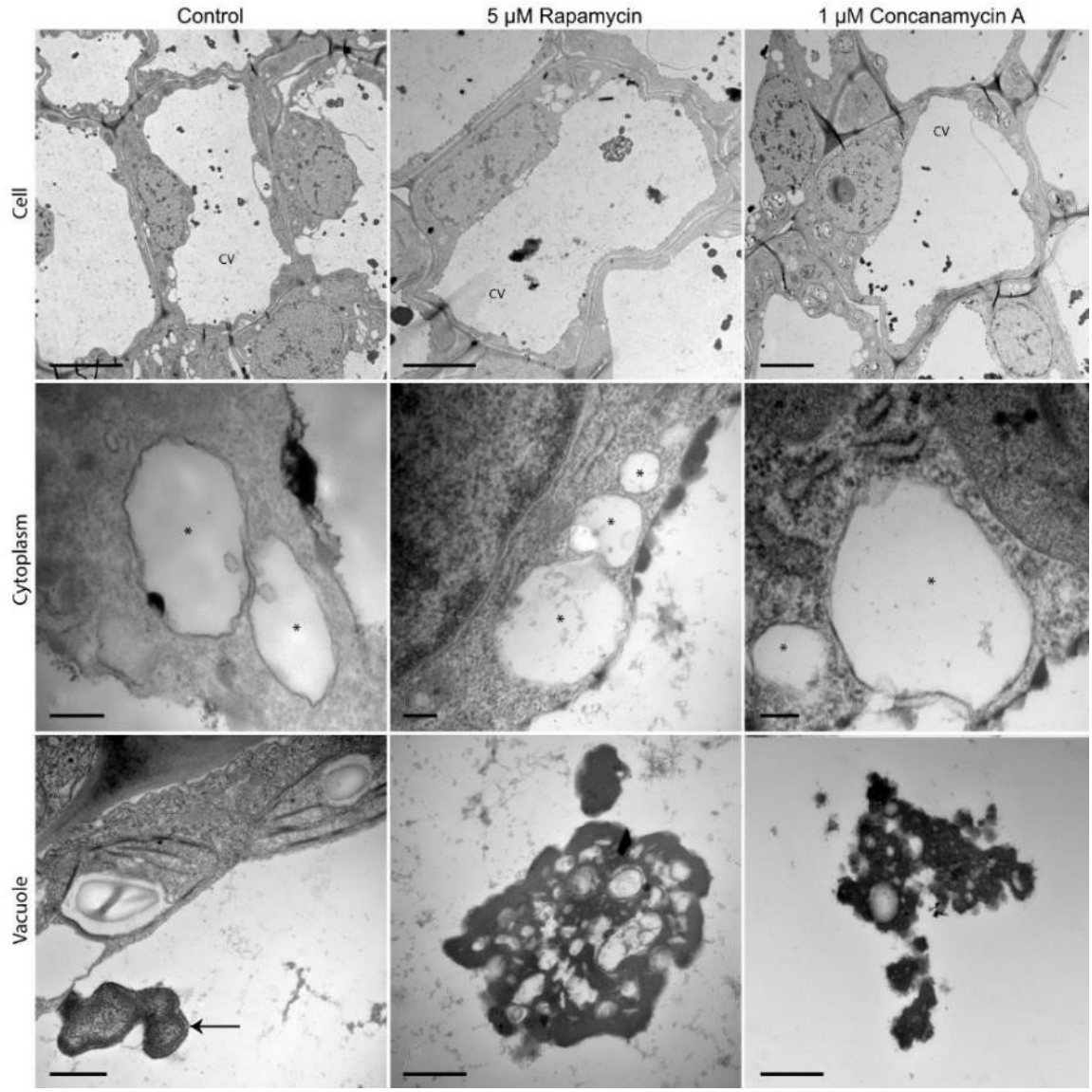

Figure 4.5. Autophagy modulation in non-programmed cell death (NPCD) cells. Transmission electron microscopy (TEM) of control, 5 µM rapamycin, and 1 µM concanamycin A-treated NPCD cells from window stage leaves. Representative micrographs include cells, cytoplasm containing autophagosomes (*), and autophagic bodies within the central vacuole (cv). The control group had small electron dense granular bodies (black arrow, vacuole). Scale bars: Cell row = 5 µm; cytoplasm row = 200 nm; vacuole row = 500 nm.

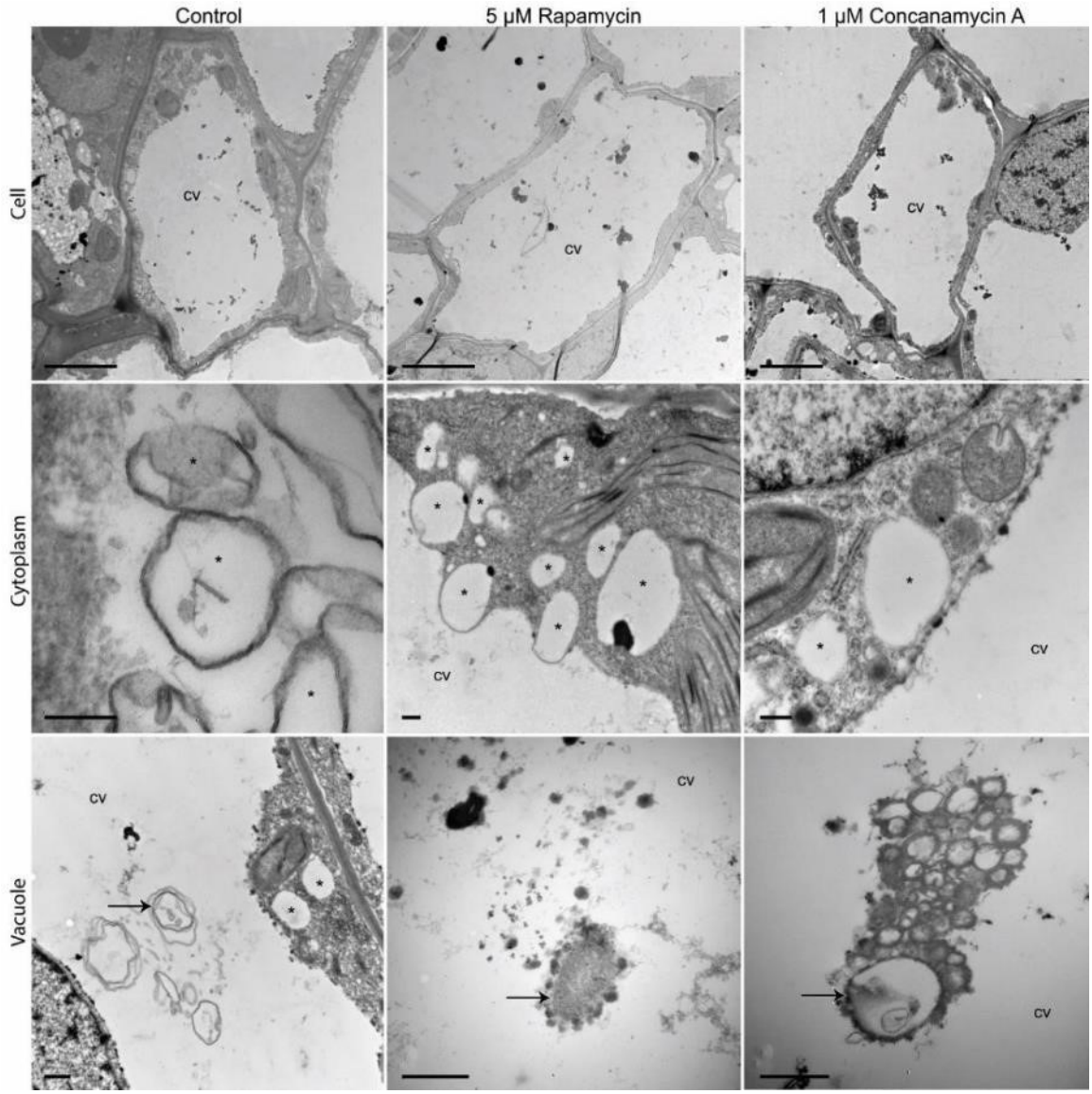

Figure 4.6. Autophagy modulation in early-programmed cell death (EPCD) cells. Transmission electron microscopy (TEM) of control, 5 µM rapamycin, and 1 µM concanamycin A-treated EPCD cells from window stage leaves. Representative micrographs include whole cells, cytoplasm containing autophagosomes (*), and vacuolar autophagic bodies (arrows). Scale bars: Cell row = 5 µm; Cytoplasm row = 200 nm; Vacuole row = 500 nm.

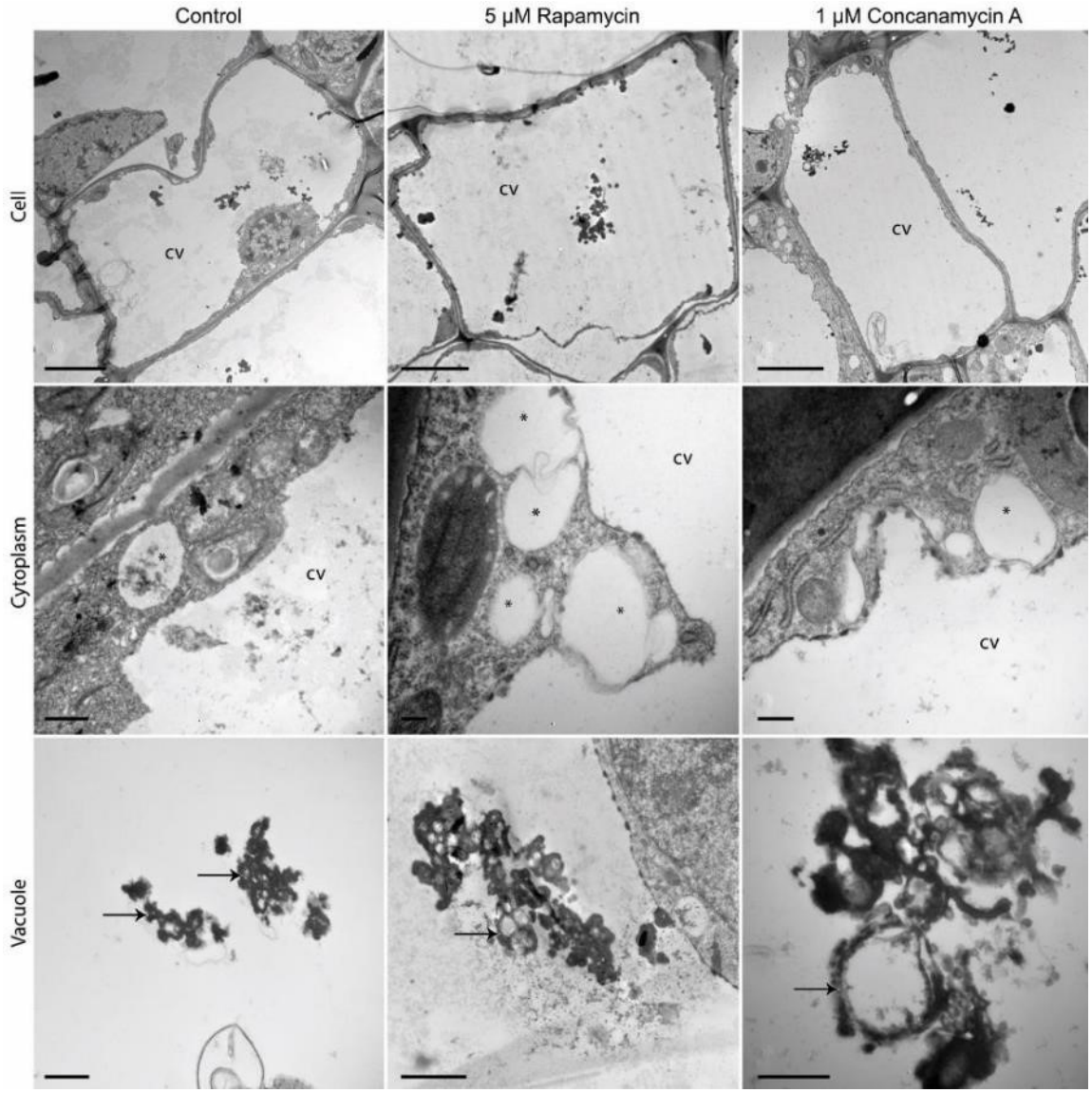

Figure 4.7. Autophagy modulation in late-programmed cell death (LPCD) cells. Transmission electron microscopy (TEM) of control, 5 µM rapamycin and 1 µM concanamycin A-treated LPCD cells from window stage leaves. Representative micrographs include cells, cytoplasm containing autophagosomes (*), and autophagic bodies (arrows) within the central vacuole (cv). Scale bars: Cell row = 5 µm; Cytoplasm row = 200 nm; Vacuole row = 500 nm.

4.4.6. Origins of Autophagosomes and Chloroplast Degradation

Rapamycin-treated samples with a high number of autophagosomes (asterisks, Figure 4.8A-C) were examined closely to explore their possible origins within the cell. Autophagosomes regularly appeared in close association with ER-like membranes (arrows, Figure 4.8A-C). The ER-like membranes proximal to autophagosomes share a similar form (Inset, Figure 4.8C). Throughout the course of PCD, organelle degradation was observed including the breakdown of chloroplasts (Figure 4.8D-F). Chloroplasts with a high number of plastoglobuli (dark spherical bodies) and disrupted thylakoid membranes (Figure 4.8D) were present in dying cells. Heavily degraded chloroplasts were commonly observed at the boundary of, or within the central vacuole (Figure 4.8E). Less frequently, chloroplasts that were not highly degraded were found within the vacuole (Figure 4.8F). Autophagosomes containing highly degraded chloroplasts with unravelling thylakoid membranes were also seen in the cytoplasm (Figure 4.8G), fusing with the tonoplast (Figure 4.8H), or within the central vacuole (Figure 4.8I).

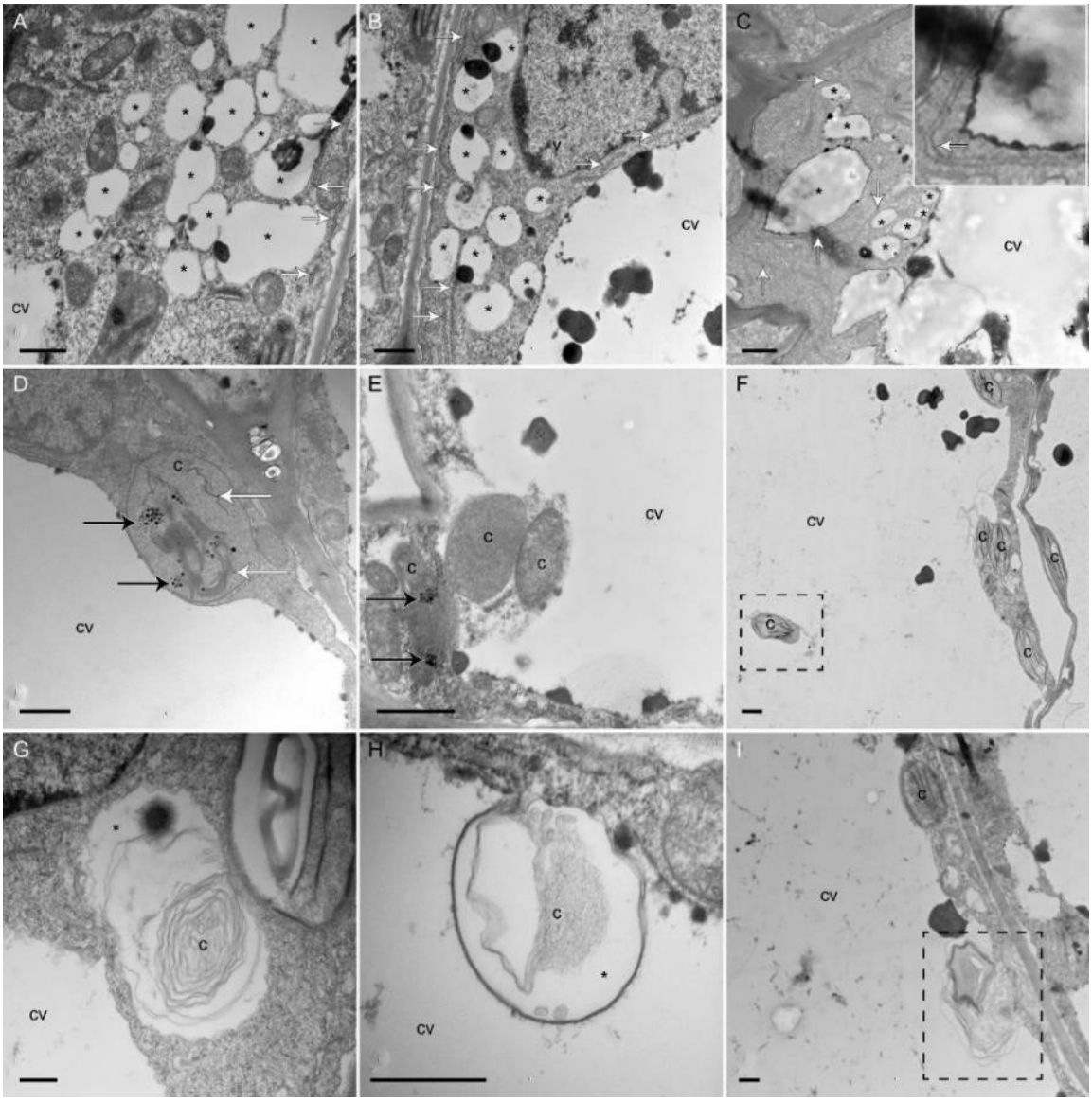

Figure 4.8. ER – autophagosome associations and chlorophagy. (A-C) Autophagosomes (*) associated with ER-like membranes (white arrows). (C-inset) An autophagosome and ER-like membrane with similar morphology and a close association. (D) Degrading chloroplast (c) near the central vacuole (cv) containing plastoglobuli (black arrows) and unorganized thylakoid membranes (white arrows). (E) Degraded chloroplasts (c) within the central vacuole (cv). (F) Mainly intact chloroplasts (c; dashed-box) were also observed within the central vacuole (cv). (G-I) Autophagosomes containing degrading chloroplasts with many unraveled membranes. (H) Autophagosome containing a degrading organelle invaginating into the central vacuole. (I) Autophagic body (dashed-box) within the vacuole containing a partially degraded organelle Scale Bars: A-F = 1 μm; G-I = 500 nm.

4.4.7. Ultrastructure of Induced Cell Death

The high degree of vesicle formation in leaves exposed to a 30 mM NaOH treatment (Dauphinee et al. 2014) warranted further ultrastructural investigation. The cells had a high degree of vacuolization and chloroplasts were localized in narrow cytoplasmic regions between vacuoles. Chloroplasts were also visible as green bodies within the central vacuole and the numerous vesicles that formed in response to the high pH stress condition (boxes, Figure 4.9A-C). TEM observations also revealed chloroplasts located between vacuoles and vesicles (Figure 4.9D). Intact chloroplasts with little degradation were also observed near the vacuolar boundary and within the vacuole (Figure 4.9E). Chloroplasts were observed being engulfed into the vacuole, and a chloroplast was found with its outer membrane fusing with the vacuole (Figure 4.9F).

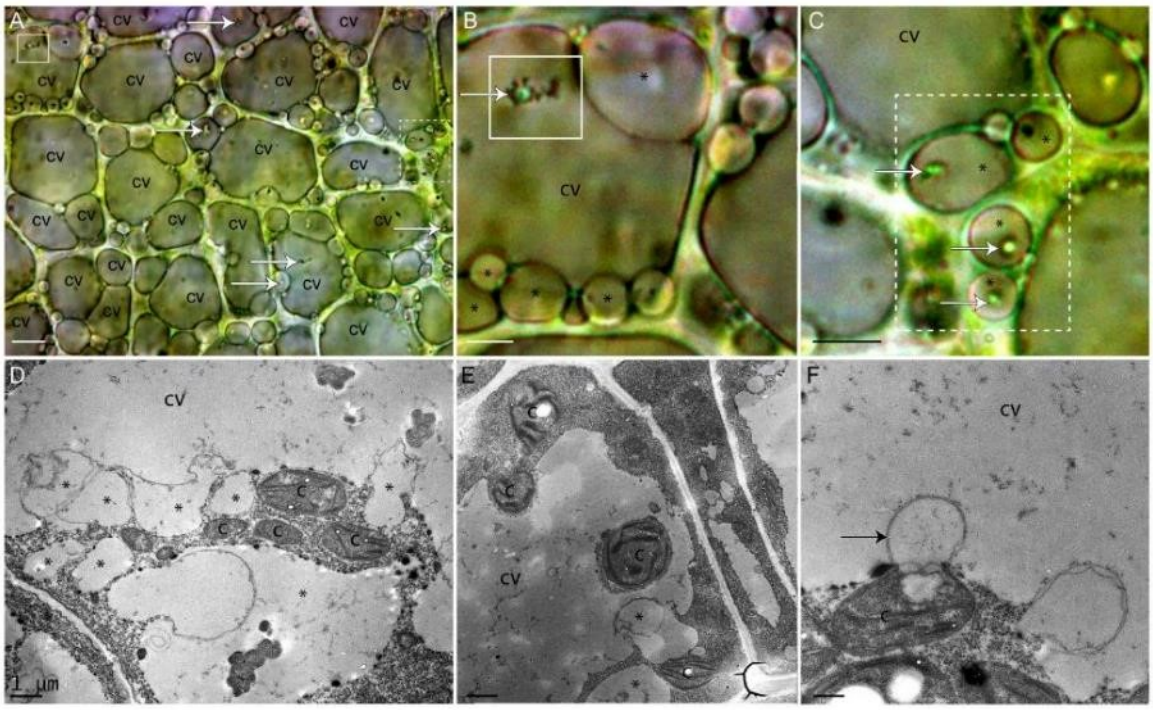

Figure 4.9. Vesiculation and chlorophagy induced by 30 mM NaOH. (A-C) Lace plant leaf sheaths treated with 30 mM NaOH, which induced cell death with a high degree of vacuolization and formation of vesicles (*). Chloroplasts were found in central vacuoles (cv) and vesicles (white arrows). The boxes (solid and dashed lines) in panel A represent panels B and C. (D-F) Transmission electron micrographs of window stage leaves exposed to 30 mM NaOH. (D) Vesicle formation (*) and chloroplasts (c) were seen in the cytoplasm between vesicles and the central vacuole (cv). (E) Whole chloroplasts (c) in the vacuole or near the tonoplast boundary. (F) Invagination of the vacuole and protrusion of the chloroplast membrane (black arrow) into the vacuole. Scale Bars: A = 10 µm; B-C = 5 µm; D-F = 1 µm.

4.4.8. Effects of Autophagy Modulation on Perforation Formation

Lace plants grown in axenic cultures were treated with either rapamycin or wortmannin and compared to the control group in order to determine the effects of autophagy modulation on the formation of perforations (Figure 4.10). Control plants (Figure 4.10A) produced leaves with an average length of 9.93 ± 0.57 cm (Figure 4.10D) and developed 75.38 ± 5.44 perforations (Figure 4.10E). The length of leaves of rapamycin treated

plants (Figure 4.10B) was not significantly different (8.08 ± 0.57 cm), but the leaves had significantly fewer perforations (39.14 ± 7.41) than the control group. Wortmannin-treated plants had significantly more perforations (100.8 ± 9.89) per leaf compared to the control but did not differ in length (9.65 ± 0.53 cm).

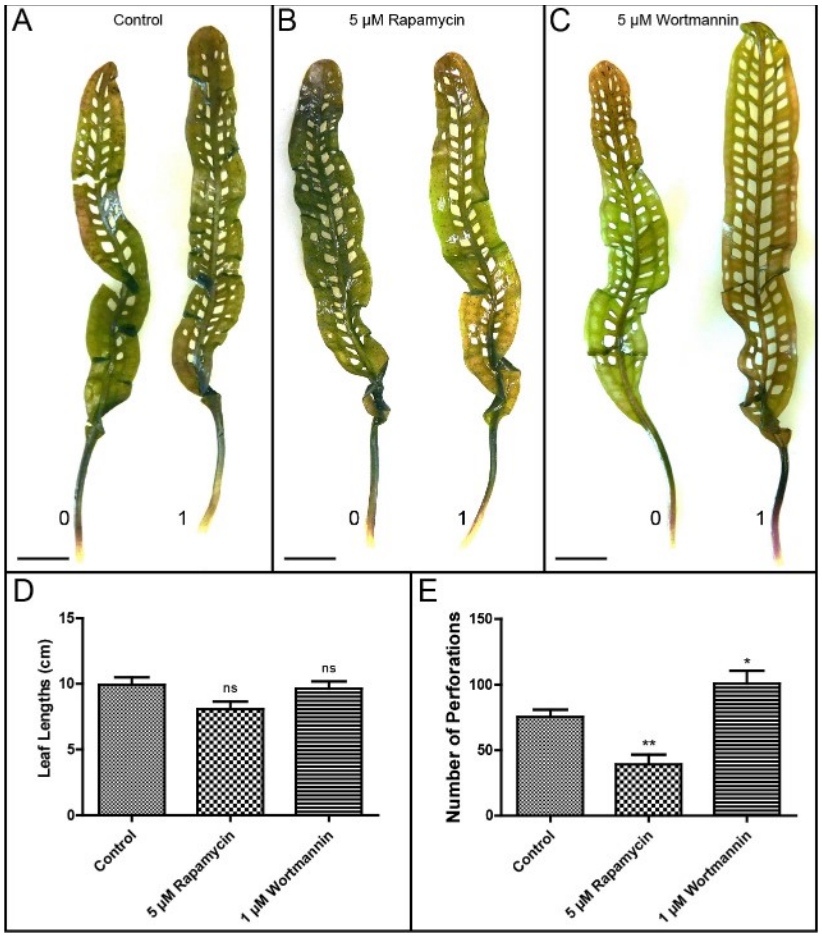

Figure 4.10. Whole plant experimentation. Representative leaves for the control (A), 5 µM rapamycin (B), and 5 µM wortmannin (C) treatment groups. Leaf 0 represents the last structure to develop prior to treatment and leaf 1 is the first to develop following treatment. (D) Mean leaf lengths of mature leaves after treatment. (E) The average number of perforations in mature leaves following treatment. (One-way ANOVA, Dunnett's multiple comparison test, $n \geq 7$; **, $P < 0.01$; *, $P < 0.05$; ns = non-significant). Error bars represent standard error. Scale Bars: 1 cm.

4.4.9. Atg8 Immunolocalization

Atg8 immunolocalization was performed in window stage leaves to determine the effects of autophagy in NPCD (Figure 4.11A; Appendix A: Online Resource 4.3) and PCD cells (Figure 4.11A, B). Modulation of autophagy (Figure 4.11B) was also achieved through treatment with: 5 μM rapamycin, 1 μM concanamycin A, and 5 μM wortmannin. Confocal laser scanning microscopy revealed that NPCD controls had 1.29 ± 0.15 puncta per cell, which was significantly fewer than PCD cells (2.52 ± 0.47; Figure 4.11A). Leaves exposed to the various autophagy modulators also appeared to have more puncta in LPCD compared to NPCD cells (Figure 4.11B).

Immunoblotting for Atg8 was carried out using leaf samples from whole plant experiments for the control and two of the chemical modulators of autophagy (rapamycin and wortmannin). The relative protein band intensities (normalized to the control mean) showed that there was a significant increase in Atg8 protein levels in rapamycin-treated leaves and a significant decrease in response to wortmannin treatment compared to the control (Figure 4.12A, B).

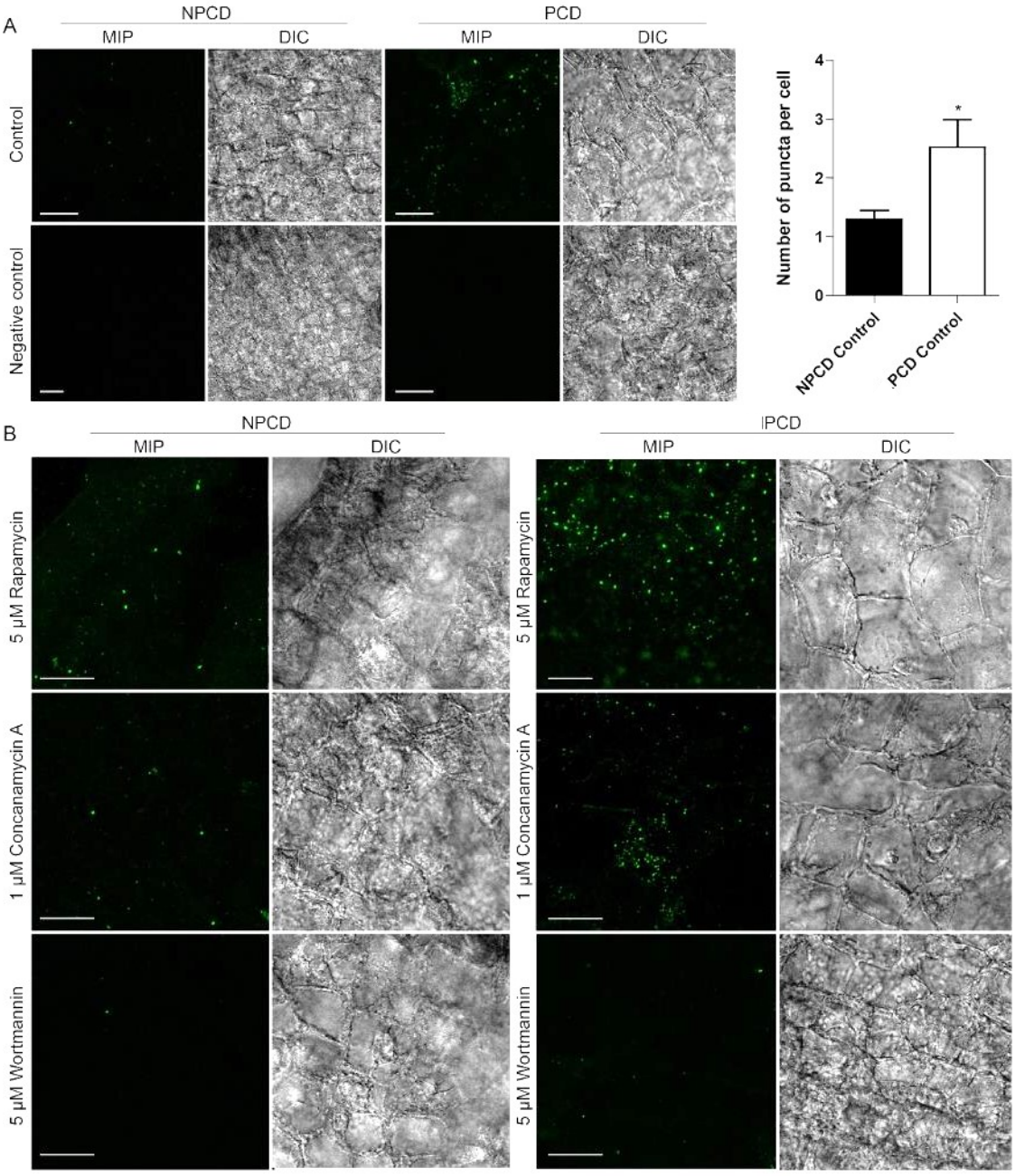

Figure 4.11. Atg8 immunolocalization. (A) Control and negative control non-programmed cell death (NPCD) and PCD cells (Student's t-test, n = 4 ± SE, *, $P < 0.05$). (B) NPCD and PCD cells of window stage leaves exposed to autophagy modulation treatments. Treatment groups included: 5 µM rapamycin, 1 µM concanamycin A, and 5 µM wortmannin. MIP = Maximum intensity projection, DIC = differential interference contrast. Scale Bars: 10 µm.

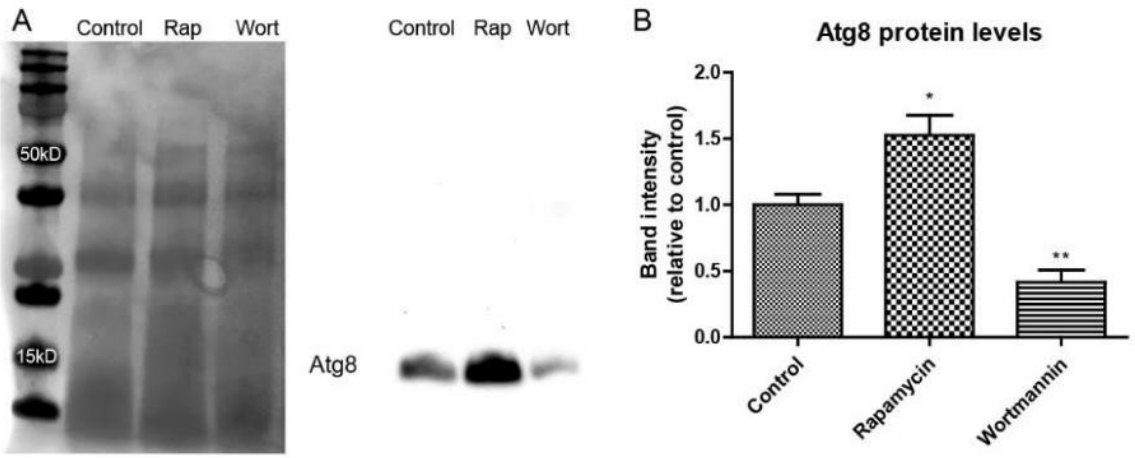

Figure 4.12. Atg8 immunoblotting. (A) Ponceau-stained membrane and corresponding Atg8 bands for control, 5 µM rapamycin (Rap), and 5 µM wortmannin (Wort) treated leaves from whole plant experiments. (B). Atg8 protein band intensities normalized to the mean value of the control group. (One-way ANOVA, Dunnett's multiple comparison test, $n = 4$). **, $P < 0.01$; *, $P < 0.05$. Error bars represent standard error.

4.5. DISCUSSION

4.5.1. Autophagy and its Role in Lace Plant PCD

Autophagy is a critical life process that allows for the degradation and repurposing of cytoplasmic constituents (Feng et al. 2014). In eukaryotes, autophagy plays a central role in development and is implicated in numerous human diseases including but not limited to cancer, diabetes, and neurodegeneration (Tsujimoto and Shimizu 2005). There is a considerable interplay between the autophagy and PCD signaling pathways (Mariño et al. 2014) and the modulation of autophagy has a wide range of outcomes on PCD depending on the experimental conditions (Minina et al. 2014). In plants, autophagy can be induced by exposure to various abiotic stresses such as starvation, exposure to saline conditions, drought, and hydrogen peroxide (Liu and Bassham 2012). Autophagy has also been implicated in PCD in response to pathogens during the hypersensitive response (HR) as

well as developmental processes ranging from embryogenesis to senescence (Liu and Bassham 2012). Here, we investigated the role of autophagy to determine whether or not it is contributing to cell survival and/or PCD signaling during lace plant perforation development. Our data indicate that autophagy primarily acts as a survival mechanism in the lace plant, but also contributes to cellular degradation during developmental PCD.

4.5.2. Ultrastructure of Lace Plant Autophagy

Autophagy was observed during lace plant leaf development using TEM. Double-membrane bound autophagosomes were observed in NPCD and PCD cells, along with single-membrane bound vesicles with a similar appearance to those found during cellular degradation in the embryos of Norway Spruce (*Picea abies*; Filonova et al., 2000; Minina et al. 2013). A general increase in the size of the vacuole was observed as cellular degradation advanced (Figure 4.3), which is a common feature observed during developmental PCD in plants (Liu and Bassham 2012). Vacuolar aggregates comprised of electron dense degraded organelle material were also seen to increase in size as PCD progressed, which is consistent with the initial lace plant observations made by Wertman et al (2012). The 5 μM rapamycin treatment generated a noticeable increase in cytoplasmic vesicles and double-membrane bound autophagosomes, and appeared to have more electron dense material within the vacuole compared to the control. Concanamycin A-treated specimens also had autophagosomes and cytoplasmic vesicles, however the high number of inclusion in the vacuole was most noticeable in this group. In both the rapamycin and wortmannin treatments, larger aggregates with a number of

membranous bodies were observed along with the typical aggregates seen in developmental PCD (Wertman et al. 2012). The membranous vacuolar aggregates were most frequently observed in concanamycin A-treated leaves in cells undergoing PCD (Vacuole, Figures 4.5 and 4.6). Autophagic bodies found within the vacuoles of Arabidopsis roots (Merkulova et al. 2014) have a similar appearance at the light microscopy level to the aggregates detailed here in the lace plant.

4.5.3. Autophagosome Origins

In yeast and mammalian systems, Atg proteins are recruited to the pre-autophagosomal structure (PAS; also known as the phagophore assembly site) prior to the formation of the isolation membrane and autophagosome (Suzuki et al. 2001; Suzuki and Ohsumi 2007; Mizushima et al. 2011). Although the process of autophagy is well understood, the source of autophagosome membranes has been controversial (Bernard and Klionsky 2013). Membranes believed to contribute to the PAS include PM-derived vesicles, (Ravikumar et al. 2010) the golgi complex (Geng and Klionsky 2010), mitochondria (Hailey et al. 2011) and the ER (Suzuki and Ohsumi 2007; Mizushima et al. 2011; Tooze 2013). Recently, ER-mitochondria contact sites have been linked to phagophore assembly, with the ER acting as a platform for autophagosome formation (Hamasaki et al. 2013). An association between the ER and autophagosomes was recently detailed in Arabidopsis, in the first study to unveil phagophore assembly and autophagosome formation in plants (Le Bars et al. 2014). Atg5 proteins are necessary for phagophore assembly — they localize to the cortical surface of the ER, recruit Atg8, and leave the structure after the

phagophore membrane is sealed (Le Bars et al. 2014). In addition, Atg9 has recently been identified as a protein necessary for ER-derived autophagosome formation (Zhuang et al. 2017). Our TEM results show ER-autophagosome associations, suggesting that the ER is involved in lace plant autophagosome formation.

4.5.4. Chlorophagy and Selective Autophagy

The breakdown of chloroplasts during PCD is a commonly observed phenomenon in plants (Bassham 2007). Selective autophagy targeting specific cellular constituents has been researched in plants more intensively in recent years, and it appears to play a role in stress tolerance and development along with normal housekeeping functions (Floyd et al. 2012; Michaeli et al. 2016). Examples of selective autophagy include pexophagy (Kim et al. 2013), mitophagy (Li et al. 2014), and chlorophagy (Michaeli et al. 2014) for peroxisomes, mitochondria, and chloroplasts, respectively. TEM of lace plant leaves revealed several levels of chloroplast degradation (Figure 4.8D-F), along with some evidence for chlorophagy. Intact or degraded plastids were found within autophagosomes as well as the vacuole. The highly degraded membranous organelles (Figure 4.8G-I) bear a resemblance to degrading chloroplasts in tobacco (Urquhart et al. 2007) and Arabidopsis (El-Kafafi et al. 2007). Furthermore, TEM images of cell death induced by 30 mM NaOH provide additional support that entire chloroplasts can enter the vacuole under certain conditions. Although there have been scattered reports and TEM observations of chlorophagy in the past (Van Doorn and Papini 2013), it has only recently been determined that autophagy plays a role in chloroplast degradation during

senescence (Wada et al. 2009), where it serves an important function in reclaiming nitrogen that is primarily stored in photosynthetic proteins (Wada et al. 2015). Chloroplast degradation is thought to occur via multiple pathways (Ishida et al. 2014). One pathway includes the piecemeal degradation of chloroplasts into vesicles called rubisco-containing bodies (RBCs) and the other represents chlorophagy where the entire organelle is engulfed (Wada et al. 2009). In fact, a recent report shows that autophagy is required for the delivery of photodamaged chloroplasts to the vacuole (Izumi et al. 2017). Our results from cell death induced by 30 mM NaOH suggest that a similar process may be occurring in response to stressful conditions, however further research is necessary to determine whether or not chloroplast degradation in developmental PCD or induced cell death in the lace plant requires Atg proteins.

4.5.5. Effects of Autophagy Modulation on PCD

Immunolocalization of Atg8 proteins was performed to determine the effects of autophagy modulators in NPCD and PCD cells. The DyLight® 488-Atg8 immunolocalization protocol employed here provide the means to compare the relative number of puncta per cell in various treatment groups. Qualitative assessment of autophagy modulators in NPCD cells produced similar results as shown by Mishra et al. (2017). Rapamycin and concanamycin A treatment increased the number of puncta observed and wortmannin had an opposite effect, which is consistent with their known effects (Klionsky et al. 2016). Although concanamycin A is an inhibitor of autophagy, it blocks the sorting and breakdown of autophagic bodies resulting in their accumulation

within the vacuole (Klionsky et al. 2016). The application of concanamycin A and detection of autophagy using GFP-Atg protein markers have shown vacuolar accumulation of autophagic bodies in the roots of transgenic Arabidopsis seedlings (Yoshimoto et al. 2004). Wortmannin effectively inhibited autophagy which was consistent with its known applications (Klionsky et al. 2016). Western blot analysis revealed a similar trend to the immunolocalization results; Atg8 protein levels were higher in rapamycin and lower in wortmannin treated leaves compared to the control.

There was a significant increase in the number of puncta in control PCD cells compared to the NPCD stage providing support to TEM results that suggest autophagic processes are involved in cellular degradation during lace plant PCD. Further study is necessary however to determine if LPCD cells have significantly more puncta than NPCD cells for the various autophagy modulator treatment groups. The live cell imaging assay developed as part of this study provided a tractable system to further test the effects that chemical modulators of autophagy have on cell death in the lace plant. Our results indicate that autophagy enhancement leads to lower cell death rates, and its inhibition will increase the rate of cell death (Figure 4.3). Furthermore, whole plant experiments using rapamycin and wortmannin revealed that the promotion or enhancement of autophagy has an inhibitory effect on the formation of perforations in the lace plant. Wortmannin effectively inhibited autophagy in the lace plant (Figures 4.11 and 4.12, and significantly increased the rate of formation of perforations. Inhibition of autophagy with wortmannin in Arabidopsis root hairs increases PCD induced by salicylic acid and Fumonisin B1 exposure, suggesting autophagy acts as a survival mechanism under these conditions

(Kacprzyk et al. 2014). In contrast, wortmannin has been shown to inhibit caspase-induced ROS accumulation and lead to more cell death in L929 mouse cells (Yu et al. 2006).

Autophagy and PCD are two intertwined degradation pathways that ultimately allow for nutrient recycling and homeostasis within eukaryotes (Mariño et al. 2014). It had long been thought that autophagy was a driver of non-apoptotic PCD (Levine and Yuan 2005) perhaps due to the conspicuous pattern of vacuolization observed in autophagic, or type II cell death that is mainly found in nematodes and insects (Mariño et al. 2014). More recently however, this notion has been challenged as there is little evidence suggesting that autophagy causes cell death (Floyd et al. 2015) and it appears as though autophagic cell death may a misnomer (Kroemer and Levine 2008). In terms of its role in PCD, autophagy has been described as an 'innocent convict' (Levine and Yuan 2005). It has also been proposed that autophagy can act as an effector of PCD signaling in the HR, and a contributor to the downstream degradation phases in developmental PCD (Minina et al. 2014). Our results support the notion that autophagy has a dual function in the lace plant. Through TEM observations and Atg8 immunolocalization, we showed that autophagy is active during developmental PCD. Increasing the incidence of autophagy with rapamycin had the effect of significantly reducing the number of perforations and the rate of cell death in the live cell imaging assays. In contrast, the inhibition of autophagy with wortmannin and concanamycin A increased cell death rates in the live cell imaging assays and wortmannin significantly increased the number of perforations compared to the control in whole plant experiments (For a summary, see Figure 4.13).

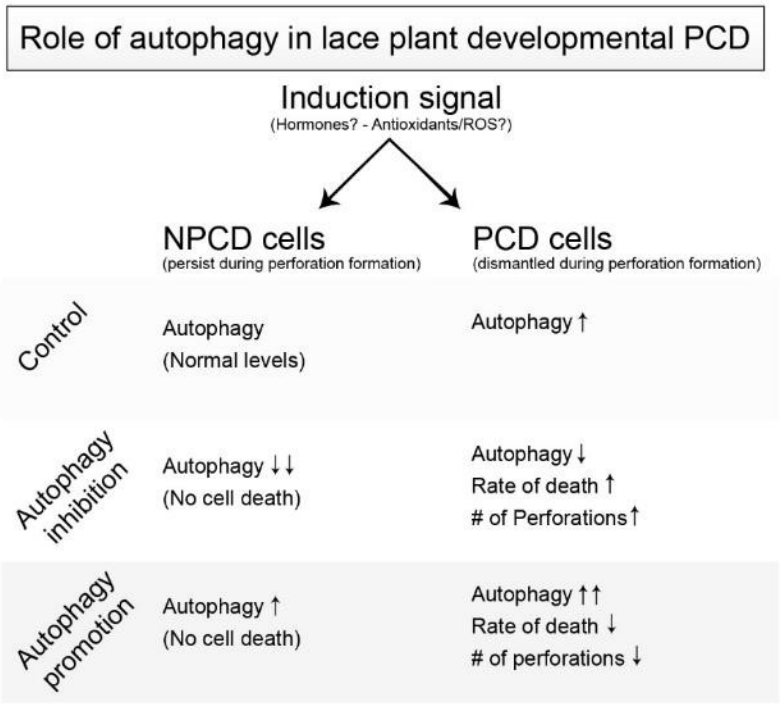

Figure 4.13. Autophagy in lace plant developmental programmed cell death (PCD). Non-PCD (NPCD) cells do not die during the formation of perforations, have standard levels of autophagy, and maintain homeostasis. PCD cells exhibit increased levels of autophagy compared to NPCD cells. The inhibition of autophagy has little observed effects on NPCD cells, however autophagy inhibition leads to greater death rates in PCD cells and increases the number of perforations in whole leaves. The opposite effect is observed following the promotion of autophagy, where the rate of cell death rate and number of perforations are reduced.

4.5.6. Conclusions and Future Work

The lace plant provides an excellent model system for studying a unique form of developmental PCD. We developed a novel live cell imaging assay that is suitable for determining the pharmacological effects of drugs on plant cells undergoing PCD. Our results demonstrate that autophagy predominantly contributes to cell survival, but is also involved in cellular dismantling during lace plant PCD. Although research in the area has

flourished in recent years, the precise roles of autophagy and the signaling pathways controlling it, as well as PCD have yet to be fully unraveled in plants. Understanding how the core components of autophagy operate in various plant systems is necessary to close the gaps in our understanding compared to well-characterized fungi and animal systems. Shedding light on autophagy in plants will help to determine how this critical mechanism acts in all eukaryotes. Le Bars et al. (2014) recently unveiled phagophore assembly in Arabidopsis and documented the association between autophagosomes and the ER. Our data show similar TEM results and suggest the lace plant ER gives rise to autophagosomes. Future work using ER-defective cells has been proposed as a fruitful area for research (Floyd et al. 2015; Michaeli et al. 2016). The lace plant presents a tractable model for studying the core autophagy machinery *in planta* and the role of the ER as it relates to autophagy and PCD has yet to be investigated within this unique developmental system.

4.6. ACKNOWLEDGEMENTS

We thank Dr. Joanna Kacprzyk (University College Dublin) for a critical review of this manuscript. Stephen Chew for assistance with the live cell imaging assay, which was supported by a Sarah Lawson Summer Research Scholarship at Dalhousie University. The Killam Trusts and the Natural Sciences and Engineering Research Council (NSERC) of Canada for providing PhD funding to AND.

CHAPTER 5

TRANSFORMING THE LACE PLANT MODEL SYSTEM

5.1. ABSTRACT

The lace plant (*Aponogeton madagascariensis*) is a novel model system for studying developmental programmed cell death (PCD). The objective of this study was to develop a protocol for the stable transformation of the lace plant. Stable transformation experiments were performed on various explants including callus derived from corm tissue and isolated shoot apical meristems (SAMs). Transformation was mediated by *Agrobacterium tumefaciens* strain GV2260 carrying the pJLU13 plasmid, which confers GFP fluorescence and hygromycin B resistance. Inoculation media, co-cultivation with the bacteria, decontamination, and plant regeneration conditions were optimized. Transformation was determined through the detection of GFP gene insertion by PCR analysis and fluorescence microscopy. Additionally, protocols for floral dipping transformation were also established using plants grown in aquaria. The highest transformation efficiency with 21% of explants having positive GFP fluorescence was achieved using isolated SAMs. The novel method included a co-cultivation period of 1 week in inoculation media consisting of 100 µM acetosyringone, 5% sucrose, 10 µM aminoethoxyvinyl glycine, and 25 µM phloroglucinol at pH 5.5. Efficient plant regeneration can be achieved within 6 weeks from isolated SAMs and 12 weeks from callus tissues derived from corm. Genetic transformation of the lace plant will be a great

tool to assess cellular dynamics and the function of genes involved in developmental PCD processes *in planta*. The protocols developed here advance the novel lace plant model system and represent the first transformation within the Aponogetonaceae family.

5.2. INTRODUCTION

5.2.1. Genetic Transformation

The insertion of foreign genetic material into another organism is known as transformation (Griffith 1928). Genetic transformation is an invaluable biotechnology that has revolutionized plant biology and agriculture (Stewart et al. 2011). The high demand for transformation technologies stems from its importance to basic scientific research and far-reaching applications including: biofortification to address malnutrition (Naqvi et al. 2009; Wirth et al. 2009; Zhu et al. 2013), creation of bioreactors for phyto-pharmaceuticals (Sevón and Oksman-Caldentey 2002; Rao et al. 2012), biofuel production (Li and Qu 2011; Singh et al. 2016) and crop improvement to increase yields (Rivera et al. 2012). Modern plant transformation techniques have become increasingly efficient and the number of transformed species increases rapidly (Rivera et al. 2012). For example, there are transformation methods with reported success rates 90% or higher in rice (Ozawa et al. 2012), switchgrass (Li and Qu 2010) and coffee (Ribas et al. 2011).

5.2.2. Transformation Techniques

Genetic transformation methods can be divided into two broad categories: direct and indirect. Direct transformations utilize physical means to penetrate the cell wall. The most common of these techniques are electroporation and biolistics (Rivera et al. 2012). Indirect methods employ viruses, as well as several species of the *Agrobacterium* genus that have the unique ability to horizontally transfer DNA using a specialized plasmid. Unless the floral dipping method can be applied, the method to generate transgenic plants is generally broken down into three phases: (i) DNA insertion into the host genome via direct or indirect methods, (ii) regeneration of whole plants from transformed explants, and (iii) selection of transgenic plants and confirmation of successful gene insertion (Piqueras et al. 2010). Selection of the appropriate gene delivery method and the types of explants are critical for the development of efficient transformation protocols. For stable transformation and whole plant regeneration using tissue culture, a high number of cells susceptible to transformation having the ability to regenerate is preferred (Birch 1997).

5.2.3. Agrobacterium: Natural Genetic Engineers

Species of the *Agrobacterium* genus are the most commonly used agents for producing transgenic plants. *Agrobacterium tumefaciens*, which contains the tumour-inducing (Ti) plasmid is the most widely studied and used for plant transformation, followed by *A. rhizogenes*, harboring the root-hair inducing (Ri) plasmid (Lacroix et al. 2011). *Agrobacterium* species can live independently in the soil, or take on a pathogenic lifestyle upon sensing a suitable host plant within the rhizosphere. Wounded eudicot plants produce various flavonoids such as acetosyringone, which activate virulence (*vir*) genes

of the Ti plasmid (Subramoni et al. 2014). Other host factors known to induce virulence genes are monosaccharides and low pH, and inhibitors include phenolic compounds, ethylene, and auxin (Lacroix et al. 2011). The *vir* genes encode for proteins that are directly involved in the cleavage, processing and delivery of the transfer-DNA (T-DNA) sequence of the Ti plasmid (Lacroix et al. 2011; Subramoni et al. 2014). The natural host range of *A. tumefaciens* is eudicots, but advancements have led to the transformation of an ever-growing number of monocot species and with enhanced efficiency. Examples of recent monocot transformations include devil's ivy (*Epipremnum aureum*; Zhao et al. 2013), Japanese or Korean lawngrass (*Zoysia japonica*; Ge et al. 2006) and oil palm (*Elaeis guineensis*; Masani et al., 2014). In addition, transformation rates have recently been dramatically improved using a new technique with *A. tumefaciens* in several monocots including: sorghum, indica rice, and sugarcane, and this method is also effective for previously non-transformable inbred maize lines (Lowe et al. 2016).

5.2.4. The Lace Plant Model System

The lace plant (*Aponogeton madagascariensis*) is an aquatic monocot species that utilizes programmed cell death (PCD) during leaf development to form perforations resulting in a lace-like pattern, hence its common name (Gunawardena et al. 2004). The plant has a spherical corm bearing its roots and shoots (Figure 5.1). The first 3-4 leaves to develop in culture typically do not contain anthocyanins and do not form perforations; leaves that perforate emerge from the corm with anthocyanin pigmentation. The lace plant has become a model organism for studying developmentally regulated PCD for three main

reasons: (i) the spatio-temporal predictability of perforations, (ii) the nearly transparent leaves that are ideal for live cell imaging, and (iii) there are established sterile cultures facilitating plant propagation and pharmacological experimentation (Gunawardena et al. 2006; Gunawardena 2008). In addition, a protocol for callus induction from inflorescences has been developed, creating an additional option for tissue culturing (Carter and Gunawardena 2011). Recent efforts have been focused on adapting biochemical and molecular methods for studying the underlying processes regulating lace plant PCD (Rantong et al. 2015). Factors currently limiting the lace plant model system from reaching its full potential include a lack of genetic data, mutants, and an efficient protocol for genetic transformation. The purpose of this study is to develop a stable transformation protocol for the lace plant system.

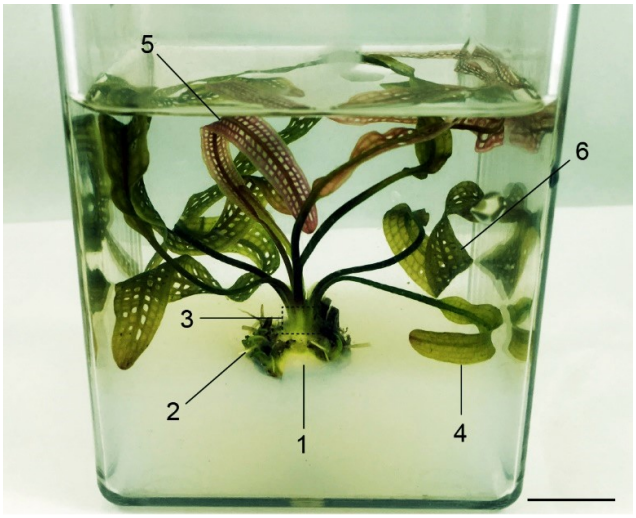

Figure 5.1. Lace plant grown in magenta box culture. The lace plant is an aquatic monocot with a spherical corm (1) that bears the roots (2) and shoots. The shoot apical meristem (3) is located near the apex of the corm. The first 3-4 leaves to develop do not form perforations (4). Young adult leaves emerge from the corm with anthocyanin pigmentation and are actively undergoing developmentally regulated programmed cell death (PCD) during the window stage (5). Perforations are complete as the leaves reach the mature stage (6). Bar = 1.5 cm.

5.3. MATERIALS AND METHODS

5.3.1. Plant Propagation and Callus Induction

Lace plant axenic cultures were prepared according to Gunawardena et al (2006). The plants were grown in half-strength Murashige and Skoog (MS) medium (30 g/L sucrose, 2.15 g/L MS basal salts, 100 mg/L myo-inositol and 0.4 mg/L thiamine, pH 5.7). The cultures were maintained at 24 ºC under fluorescent lighting (Philips Daylight Deluxe) at 125 µmol m^{-2} s^{-1} on a 12 h light/dark cycle. Callus cultures were induced from isolated corm tissues and grown in half strength MS media with various combinations of supplemental auxins such as 1-Naphthaleneacetic acid (NAA) and Picloram (PIC), as well as the cytokinins BAP (6-Benzylaminopurine) and thidiazuron (TDZ) (Table 5.1). To induce plant regeneration, 4-6 week old callus cultures were transferred to MS media with 5 mg/L BAP and 1 mg/L NAA and grown for 4 weeks under the light conditions described above. Shoot apical meristems (SAMs) were isolated according to Dauphinee et al. (2015).

Table 5.1. List of the plant growth regulator combinations tested. Cytokinin sources included BAP (6-Benzylaminopurine) and TDZ (thidiazuron) and auxins tested included NAA (1-Naphthaleneacetic acid) and PIC (Picloram).

Treatment	Cytokinin	Auxin
1	1 mg/L BAP	1 mg/L NAA
2	2 mg/L BAP	2 mg/L NAA
3	4 mg/L BAP	4 mg/L NAA
4	1 mg/L BAP	5 mg/L NAA
5	5 mg/L BAP	5 mg/L NAA
6	0 mg/L BAP	5 mg/L NAA
7	1 mg/L TDZ	5 mg/L PIC
8	1 mg/L TDZ	4 mg/L PIC
9	1 mg/L TDZ	2 mg/L PIC

5.3.2. Bacterial Strain and Plasmid

Agrobacterium tumefaciens strain GV2260 was utilized for this study. Cells transformed by *A. tumefaciens* using the pJLU13 plasmid express green fluorescent protein (GFP) and hygromycin B resistance (*hpt)* driven by the rice ubiquitin promoter *rubi3* (Lu et al. 2008). The pJLU13 plasmid was amplified using competent DH5α *Escherichia coli* cells, and purified using the EZ-10 Spin Column Plasmid DNA Kit according to the manufacturer's instructions (Bio Basic Inc.). The plasmid was introduced to *A. tumefaciens* GV2260 using heat-shock. Transformed bacterial colonies were identified on Kanamycin/Rifampicin selection plates and confirmed using PCR analysis as described below.

5.3.3. Stable Transformations

Preliminary experiments aimed towards whole plant regeneration tested a range of parameters for protocol development (summarized in Figure 5.2). In brief, several explants were utilized including corm, callus, and isolated SAMs from axenic cultures (Figure 5.3). Inoculation media were optimized primarily for: sugar source, surfactants and pH. Additionally, ethylene suppression using aminothoxyvinyl glycine (AVG) was achieved using concentrations optimized by Dauphinee et al. (2012). 1-N-Naphthylphthalamic acid (NPA) and phloroglucinol were also tested as additives to the inoculation media for the inhibition of auxins and phenolic compounds, respectively (Figure 5.2). The *A. tumefaciens* and explant co-cultivation conditions focused on the following variables: duration, temperature, pre-treatment, and vacuum infiltration. The regeneration phase tested light conditions, several media recipes, and schedules for tissue transfer to fresh media. Detection of GFP gene insertion was performed by PCR analysis or fluorescence microscopy as described below.

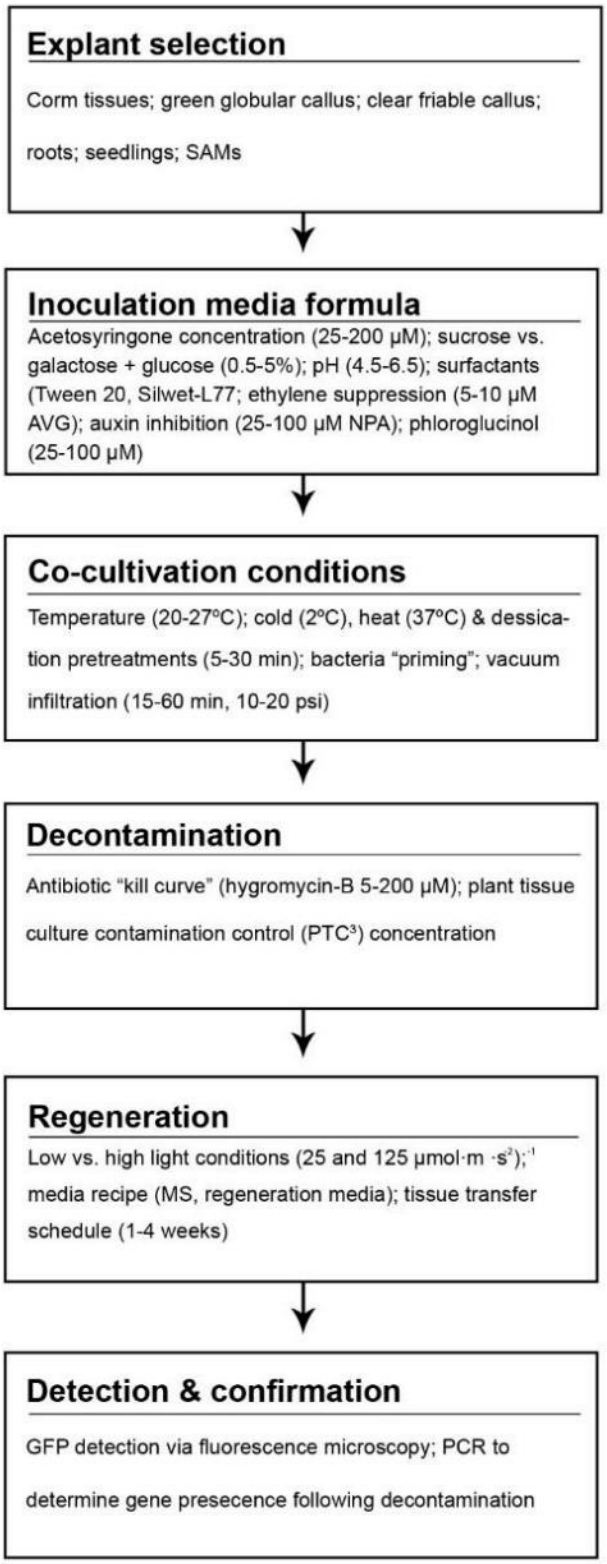

Figure 5.2. Parameters tested and optimized for lace plant transformation protocol development.

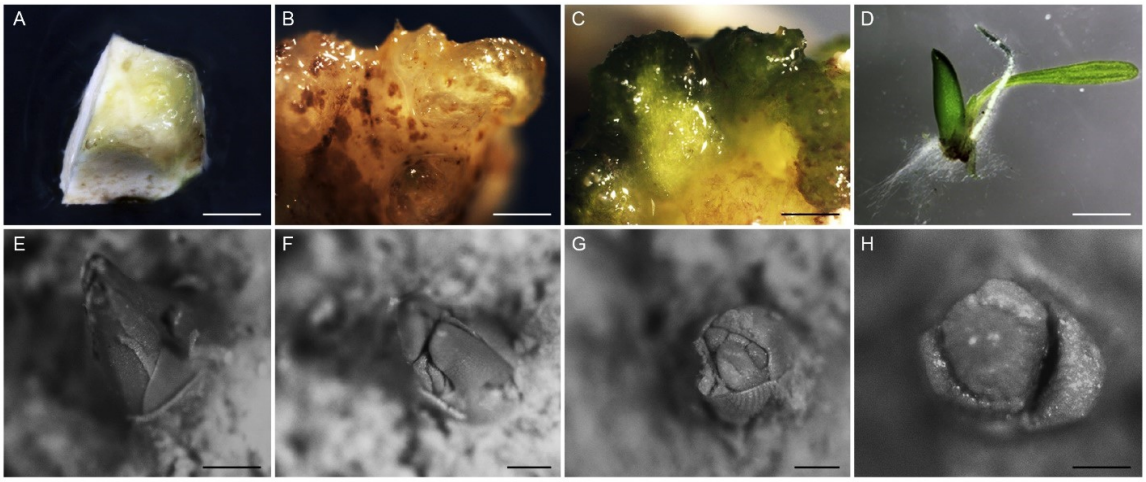

Figure 5.3. Explants used for lace plant transformation. Newly cleaned corm tissue from axenic lace plant cultures (A). Clear globular (B) and green globular (C) callus induced from corm tissues. Seedlings from aquarium-grown lace plants (D). The stages of shoot apical meristem (SAM) isolation (E-H). Bars: A = 0.5 cm, B-D = 1 mm, E = 750 µm; F-G = 500 µm; H = 100 µm.

5.3.4. Floral Dip Transformations

Plants grown in aquaria according to Dauphinee et al. (2012) were used for a floral dip protocol modified from Clough and Bent (1998). Mature inflorescences were dipped in the inoculation media containing *A. tumefaciens* for 5 min and left to air-dry. The following 3 days, the inflorescence was hand-pollinated using a Q-tip. After fertilization and seed dispersal (approximately 6 weeks later), germinated seedlings were collected and rinsed thoroughly with distilled water. The seedlings were then surface sterilized for 5 min. in 50% ethanol, brought into a laminar flow hood and then soaked in 20% bleach for 5 min. The seedlings were then rinsed 3 times in distilled water, for 5 min and then transferred to MS media and maintained as the cultures above.

5.3.5. PCR Analysis of Callus Tissues

Callus explants that were positive for GFP fluorescence were exposed to cefotaxime to remove *A. tumefaciens* in a stepwise fashion, by transferring explants to new media while reducing cefotaxime every 2 weeks from 500, 250, 125 and 0 mg/L. If no contamination was observed following 2 weeks with 0 mg/L cefotaxime (i.e. 8 weeks after the co-cultivation period), DNA extraction was performed for control and pJLU13 transformation group specimens with a DNeasy Plant Mini Kit according to the manufacturer's instructions (Qiagen Inc). GFP gene detection (715 bp expected fragment size) was achieved using a pair of primers (GTCTA-GACCATGGGATCGATGCATCATC; ACGAGCTCTTACTGTA-CAGC). Standard PCR was carried out with a 35-cycle reaction and annealing temperature of 58ºC. The positive control sample included the pJLU13 plasmid purified from DH5α *E. coli* (Invitrogen) using the EZ-10 Spin Column Plasmid DNA Kit according to the manufacturer's instructions (Bio Basic Inc.).

5.3.6. Microscopy, Image and Figure Preparations

Confocal laser scanning microscopy was performed using Nikon's C1 system on an Eclipse *Ti* inverted microscope (Nikon Instruments Inc). A Nikon AZ100 microscope with a FITC filter set was used to scan for GFP in SAMs and callus tissues. Micrographs were captured using NIS Elements Advanced Research software. Images were prepared for publication using Adobe Illustrator and Photoshop (Creative Cloud, Adobe Systems

Inc). Videos were made using Adobe Premiere Pro. When necessary to improve image clarity, adjustments were made to brightness and contrast evenly using Photoshop.

5.4. RESULTS

5.4.1. Callus Induction, SAM Isolation and Plant Regeneration

Of the various combinations of plant growth regulators (PGRs) tested to induce callus from corm tissues, the addition of 1 mg/L BAP and 5 mg/L NAA to MS media was most effective for callus induction and regeneration (Figure 5.4A). Within 4 weeks, the majority of the exposed corm tissue contained either clear, or green globular callus. Limiting exposure to light greatly reduced the proportion of green globular callus that developed (data not shown). Leaves with a narrow lamina were also commonly observed after 4 weeks, and appeared all over the exposed surface as regeneration progressed. Leaves containing anthocyanins and a low number of perforations developed within 10-12 weeks. Isolated SAMs grown in MS media without the addition of PGRs also led to callus induction and plant regeneration (Figure 5.4B). Within two weeks several narrow shoots were observed and adult leaves containing anthocyanins and perforations were obtained within 4-6 weeks.

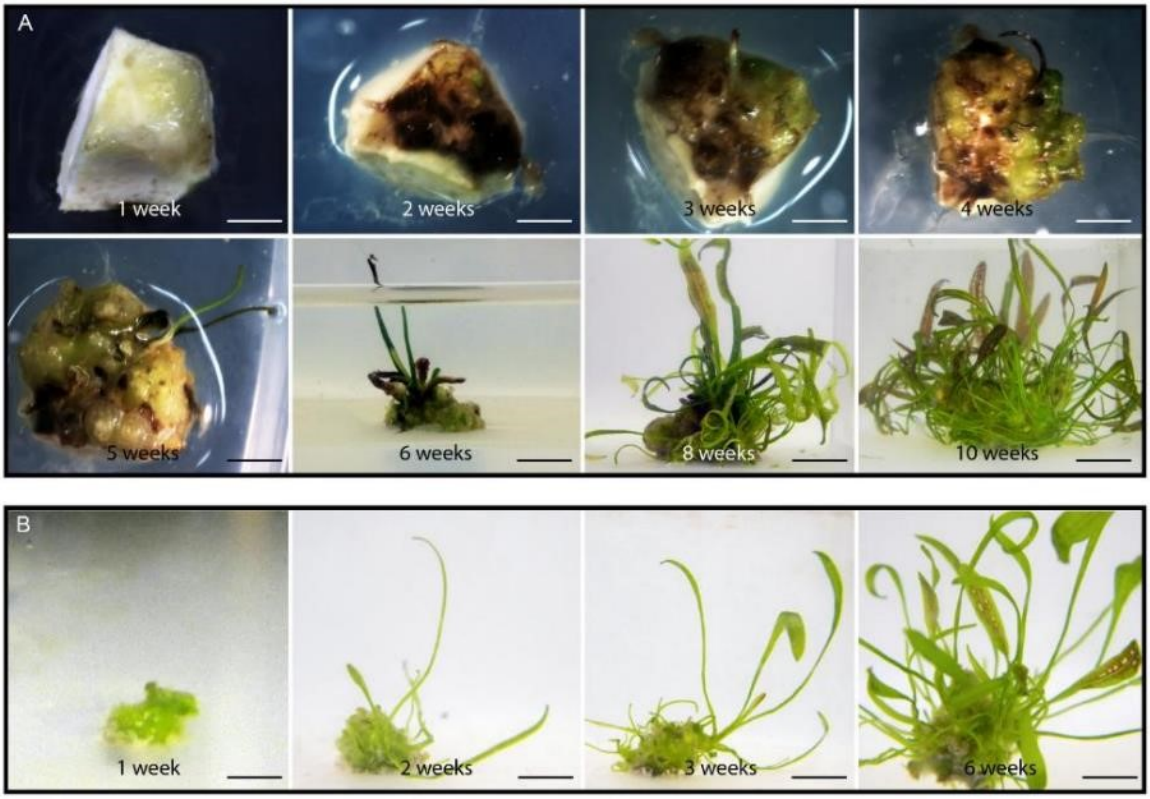

Figure 5.4. Callus induction and plant regeneration. Progression of callus induction and plant regeneration from corm tissue (A) and isolated shoot apical meristem SAM culture (B). Bars = 2mm.

5.4.2. Transformation of Callus Explants

Callus explants generated from corm tissues were tested for their susceptibility to *Agrobacterium*-mediated transformation utilizing the pJLU13 plasmid (Figure 5.5). Callus grown under dark conditions for a minimum of 4 weeks provided the best results combined with a 1 week co-cultivation with *A. tumefaciens* suspended in inoculation medium [100 µM acetosyringone, 5% (w/v) sucrose, 10 µM aminoethoxyvinyl glycine (AVG) set to pH 5.5, 0.8-1.2 OD_{600}]. After two weeks from the onset of experiments, control explants had low autofluoresence (control, Figure 5.5A). Callus explants exposed to *A. tumefaciens* carrying pJLU13 had scattered GFP on the surface (pJLU13, Figure

5.5A). After 8 weeks, control tissues still had little to no fluorescence detected and pJLU13 transformation group explants were observed with strong fluorescence throughout (Figure 5.5B). In addition, young shoots developing during the co-cultivation period also contained areas with green fluorescence (Figure 5.5C). Following decontamination (8 weeks after the onset on experimentation), PCR was used to detect the presence of the GFP gene in specimens that exhibited green fluorescence (Figure 5.6).

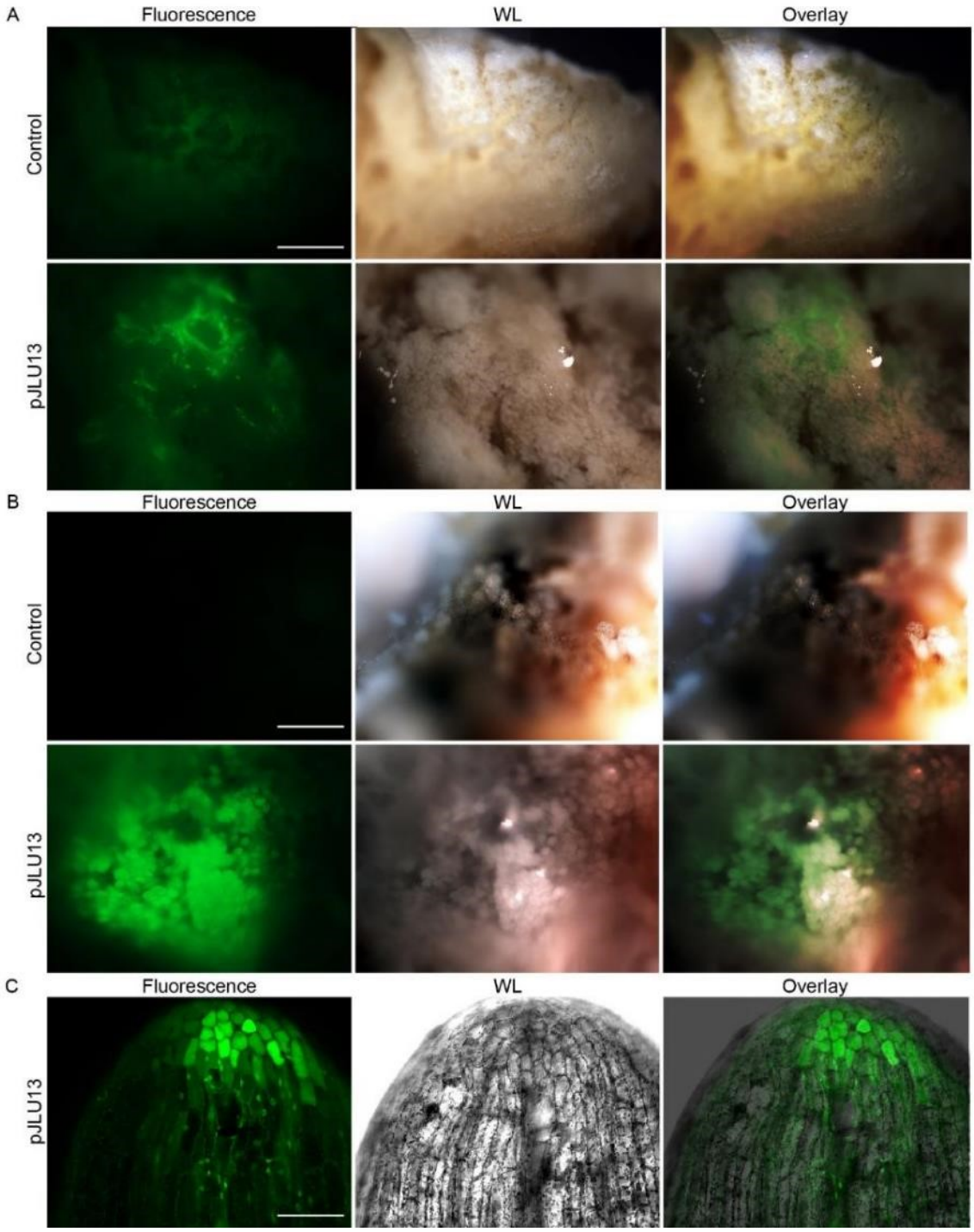

Figure 5.5. Transformation of clear globular callus. Control and pJLU13 transformation group explants positive for green fluorescence protein (GFP) expression after 2 weeks (A) and 8 weeks (B). Chimeric GFP expression was detected in callus tissues producing shoots during co-cultivation (C). WL = white light. Bars: A-B = 250 µm, C = 100 µm.

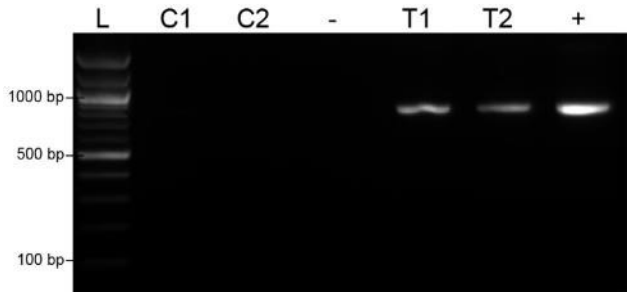

Figure 5.6. PCR analysis of GFP gene. Callus tissues that showed no signs of contaminations 8 weeks after the initial co-culture were tested for GFP gene. Groups included: control (C1 and C2), negative control (-), transformed tissues (T1 and T2) and a positive control (+) pJLU13 plasmid.

5.4.3. Transformation of SAMs

Individual plants from axenic cultures were used to obtain isolated shoot apical meristems explants. The most successful method was a 1 week co-cultivation immediately following SAM isolation under axenic conditions. The *A. tumefaciens* inoculation media consisted of 100 µM acetosyringone, 5% (w/v) sucrose, 10 µM AVG, and 25 µM phloroglucinol (pH 5.5, 0.8-1.2 OD_{600}). Two weeks after the experiment began, control and the pJLU13 transformation group explants had healthy clear globular callus developing (Figure 5.7A). Control explants (control, Figure 5.7A) had little fluorescence compared to the pJLU13 transformation group (pJLU13, Figure 7A), which had intense areas of GFP fluorescence that was observed in approximately 21% of explants (4/19 replicates from 3 independent experiments). Within 6-8 weeks, large clusters of fluorescence were detected in explants from the pJLU13 transformation group (Figure 5.7B). Shoot regeneration in MS media supplemented with PTC^3 occurred from the isolated SAM within the first 1-2 weeks, and by 8 weeks there were shoots emerging from callus tissues induced elsewhere on the surface of the corm (arrows, Figure 5.7C).

Tissues remained healthy and growth was similar between the control and transformation treatment groups.

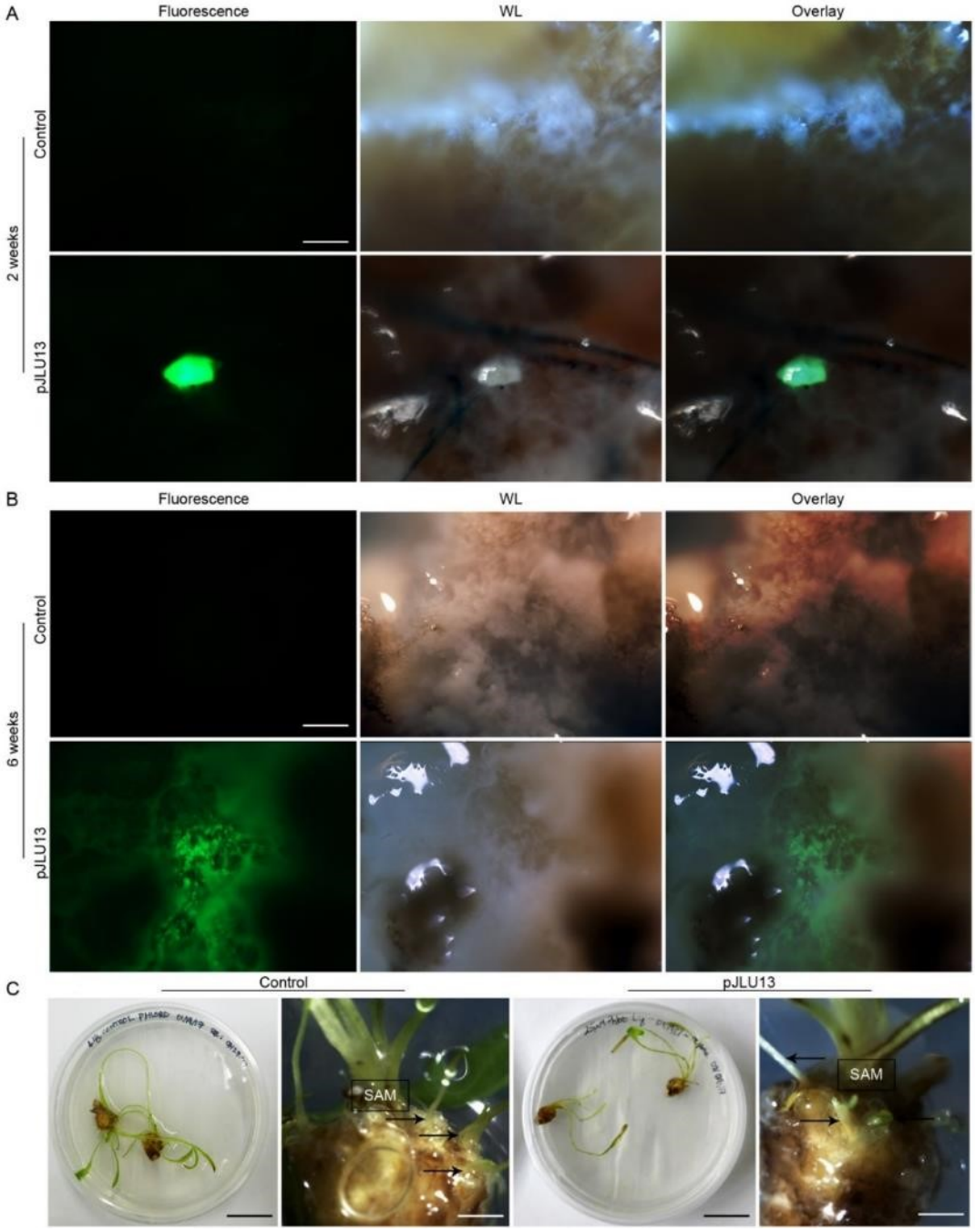

Figure 5.7. Transformation of isolated shoot apical meristem (SAM) cultures. Control and pJLU13 transformation group explants positive for green fluorescence protein (GFP) expression after 2 weeks (A) and 6 weeks (B). After 8 weeks the explants remained uncontaminated and additional shoots developed (arrows) away from the initial isolated SAM area (C). WL = white light. Bars: A, B = 50 µm, C (plates) = 1 cm, (plant) = 2 mm.

5.4.4. Floral Dip Transformation

Aquarium-grown lace plants (Figure 8A) produce inflorescences that emerge from the water (Figure 5.8B) following the rapid growth of the peduncle (arrows, Figure 5.8A). A single 5 min floral dip (Figure 8C) in inoculation media (100 µM acetosyringone, 5% (w/v) sucrose, 10 µM AVG, pH 5.5, 0.8-1.2 OD_{600}), followed by daily pollination for 3 days resulted in a high degree of fertilization (Figure 5.8D). Multiple floral dips were lethal or dramatically reduced the number of seeds that were produced (data not shown). Seedlings were collected with a meshed strainer (Figure 5.8E), rinsed thoroughly with distilled water and then surface sterilized. Effective decontamination that was non-lethal included washes of 5 min in 50% ethanol, 5 min in 20% bleach, followed by flushing the samples with sterile distilled water. The seedlings were grown in distilled water and then transferred to MS + PTC^3 media (Figure 5.8F). The seedlings' surfaces turn a brown color following the sterilization procedure, however new leaves emerged after 2-4 weeks. In the most successful experiment, 2/18 seedlings producing healthy shoots were positive for GFP fluorescence (Figure 5.8G-I).

Figure 5.8. Floral dip transformations. Aquarium-grown lace plant producing inflorescences (A) that emerge from the water at maturity (B). Floral dipping is performed on mature inflorescences (C) followed by pollination. Fertilization leads to fruit maturation and seed development (D) and release of the young seedlings (E) from the mature fruit. Seedlings are surface sterilized and transferred into culture (F). Leaves that developed in culture had green fluorescence (G) and were healthy (H = white light; I = overlay). Bars: A-C = 1.5cm, D-F = 3 mm, G = 1 mm, H = 3 mm and I = 0.5 mm.

5.5. DISCUSSION

5.5.1. Overview

The lace plant has emerged as a model for studying developmental PCD (Gunawardena et al. 2004). In order to advance our understanding of this unique example of plant PCD, biochemical and molecular techniques need to be developed. Genetic transformation is an invaluable technique in the plant biologist's toolkit. The purpose of this work was to develop a protocol for genetic transformation. In order to develop a protocol for stable transformation, explants susceptible to gene insertion with the ability to regenerate are essential. Callus tissues have the ability to regenerate whole plants and a protocol for its induction from immature inflorescences has been established (Carter and Gunawardena 2011). However, inflorescences are rarely produced in culture and therefore alternate protocols for the efficient callus induction and plant regeneration are necessary.

5.5.2. Callus Induction and Regeneration

The lace plant corm is readily available from established sterile cultures and proved to be a good candidate explant for the induction of callus tissue and subsequent regeneration of whole lace plants. Several PGR combinations added to MS media were successful in inducing callus tissue from the corm, the most effective being 1 mg/L BAP and 5 mg/L NAA. After 4 weeks the majority of the exposed corm tissue had globular callus. Globular and compact callus has embryogenic cells that possess the ability to regenerate whole plants when exposed to high levels of cytokinin (Nabors 2004). This was revealed

when the globular callus induced on the lace plant corm was transferred to a medium with higher levels of cytokinin, which led to plant regeneration and the development of adult leaves within 10-12 weeks. The isolation of SAMs and cultivation in MS medium without additional hormones was also effective for regeneration from this small population of cells. Additionally, callus induction and shoot regeneration occurred over the surface of the surrounding corm tissue that was damaged during SAM isolation and whole plant regeneration occurred within 6 weeks. A common feature within monocot species is the development of immature, or daughter corms (Bell 2008), which may have contributed to the promotion of callus formation when the SAM of the mother corm was intact.

5.5.3. *Agrobacterium tumefaciens* pJLU13 Transformations

Agrobacterium tumefaciens strain GV2260 has been employed to transform eudicot and monocot species and it was recently found to be an effective gene-delivery vector for the phytopathogenic fungus *Colletotrichum sansevieriae* (Nakamura et al., 2012). The GV2260 strain was effective for lace plant transformation and the highest success rate (25% of explants) was obtained from a week-long cultivation period with isolated SAM explants. The inoculation medium consisted of 100 µM acetosyringone, 5% sucrose, 10 µM AVG, and 25 µM phloroglucinol at a pH of 5.5. The addition of acetosyringone, sucrose, and the low pH are all known contributors to *vir* gene activation (Lacroix et al., 2011). The inclusion of AVG was to suppress ethylene biosynthesis, and treatments using a concentration of 5-10 µM are effective in lace plant cultures (Dauphinee et al., 2012).

Phloroglucinol is commonly used in plant tissue culture and was added due to its ability to reduce phenolic compounds that also inhibit *vir* gene activation (Lacroix et al. 2011). Although transformation was achieved in callus tissues, the induction time and poor regeneration make this explant a less viable option compared to the isolated SAM cultures. SAM cultures offer advantages over callus tissues as they can be obtained the day of the transformation experiment and have a population of continuously dividing cells that are organized (Traas and Bohn-Courseau 2005). Additionally, SAM isolation can be achieved relatively quickly and the high number of daughter corms that are produced in magenta box cultures provides a reliable source.

5.5.4. Floral Dip Transformation Protocol and Culturing Seedlings

Inflorescences have been documented to rarely develop under cultivation in aquaria (Sergueff, 1907). Under our aquarium conditions, we had several opportunities to develop a floral dip transformation method throughout the course of this study. Results indicate that floral dipping can be performed without killing the inflorescence or inhibiting fertilization, and seedlings can be introduced to axenic culture. This method provides an alternate route for genetic transformations without a dependence on clonal propagation and somatic embryogenesis.

5.5.5. Conclusions and Future Work

The current work provides a template for stable gene insertions into the lace plant using

an *A. tumefaciens* vector. Aquatic monocots that have been transformed include duckweed (Yamamoto et al. 2010) and water trumpet (Wong et al. 2010) of the Araceae, however the transformation of the lace plant represents the first transformation within the Aponogetonaceae family. Applications of lace plant transformation includes the creation of the transgenic lines that are overexpressing genes that may be involved in PCD regulation and the creation of the transgenic lines carrying various fluorescence organelle markers to understand their dynamics and responses to PCD modulation. The use of fluorescent protein markers would be particularly advantageous in the lace plant due to its suitability for live cell imaging and established systems to observe PCD throughout the formation of perforations. For example, fluorescent proteins targeted to mitochondria (Logan and Leaver 2000), the endoplasmic reticulum (Costantini and Snapp 2014), and peroxisomes (Jedd and Chua 2002) can be used in conjunction with the live cell imaging assay developed by Wertman et al. (2012) to better understand lace plant PCD. The use of isolated SAM cultures presents efficient conditions for globular callus formation and shoot regeneration. Based on our results, in order to obtain whole plant transformants going forward, we plan on using the isolated SAM protocol described here combined with the appropriate selective pressure during the regeneration phase. Upon successful regeneration of whole plants, transformation will be confirmed using Southern-blotting.

CHAPTER 6

DISCUSSION

6.1. PCD SIGNIFICANCE AND OVERVIEW

Programmed cell death (PCD) is a vital mechanism for multicellular organisms due to its roles in development and homeostasis (Greenberg 1996; Green 2011; Kacprzyk et al. 2011). The pathways controlling forms of animal PCD such as apoptosis are well defined compared to plants despite the significance of PCD in a wide array of processes essential to their life (Mignolet-Spryut et al. 2016). Plant PCD is observed throughout reproductive and vegetative development; examples include deletion of the embryonic suspensor, anther dehiscence, as well as xylem and aerenchyma formation to name a few (Mignolet-Spryut et al. 2016). Plant PCD also provides resistance to harmful abiotic and biotic stimuli, playing significant roles in homeostasis and the plant immune system thereby fulfilling critical roles necessary for a sessile lifestyle (Bozhkov and Lam 2011). Research into the complex networks controlling PCD has intensified in recent years in a diverse range of plant model systems (Dauphinee and Gunawardena 2015). The lace plant has been recognized as a unique model system to study the development of perforations, which is a rare manifestation of PCD *in planta* (Gunawardena 2008; Kacpryzk et al. 2011). This thesis confirmed the regulatory roles of ethylene, antioxidants and ROS, as well as autophagy in lace plant developmental PCD during the formation of perforations. This chapter reviews the key regulators identified in this thesis, along with

their known interactions in other plant systems and based on these data, a model for PCD signaling in the lace plant is proposed. Additionally, future work and applications for the novel genetic transformation will be discussed.

6.2. ETHYLENE SIGNALLING

Chapter 2 revealed the association between ethylene production and lace plant PCD during perforation formation. Additionally, a climacteric-like pattern of ethylene and CO_2 production was correlated to window stage and senescent leaves, where PCD is actively occurring. Among the plant hormones, the gaseous phytohormone ethylene is the smallest and is most often associated with cell death (Mattoo and Handa 2004). Ethylene is perhaps best known for its roles in fruit ripening, senescence and abscission (Mattoo and Handa 2004; Noodén 2004; Trobacher 2009). Ethylene perception and signal transduction begins at the endoplasmic reticulum (ER)-bound receptors that negatively regulate ethylene responses (Trobacher 2009). The ethylene signaling pathway is highly conserved in plants (Zhang et al. 2016). In Arabidopsis there are five receptor genes: *EIN4, ERS1, ERS2, ETR1, and ETR2* (Trobacher 2009; Ju and Chang 2015; Zhang et al. 2016)). After ethylene binds to the receptors, their negative regulation of the pathway is inhibited, which ultimately leads to the activation of nuclear transcription factors EIN3 and EIL1 and then a transcriptional cascades controlled by ethylene response factor (*ERF*) genes. A recent lace plant study by Rantong et al. (2015) employed quantitative PCR and laser capture microdissection to determine that ethylene receptor AmERS (a

homologue of Arabidopsis ERS1) levels are high in NPCD stage cells and lower in PCD cells thereby further implicating ethylene in lace plant PCD signaling.

6.3. ANTIOXIDANTS AND ROS

The roles of antioxidants and ROS in lace plant PCD were elucidated in chapter 3. Anthocyanin disappearance is the first visible sign that PCD is occurring in window stage leaves, and it was determined that there is a concomitant accumulation of ROS, specifically superoxide, as PCD progressed. The redox state of the cell must be kept in balance in order to maintain homeostasis (Schieber and Chandel 2014). Developmental signals and perturbation from stress can shift this balance in favor of ROS and lead to the initiation of PCD (van Brusegem and Dat 2006). Through the application of exogenous antioxidants, we showed that PCD could be inhibited significantly and appeared to shift the balance of antioxidants and ROS toward the former. Conversely, the application of exogenous ROS (i.e. H_2O_2) reversed the PCD-inhibitory effect of the antioxidants and increased cell death rates. Plant cells are constantly challenged to mitigate ROS damage with its antioxidant systems that are regulated both spatially and temporally (Gadjev et al. 2008b). Data indicate that cells within lace plant window stage leaves control their antioxidant systems in order to cope with ROS; the relative proportions of ROS and antioxidants therefore play a significant role in the fate of the cell.

6.4. AUTOPHAGY

Autophagy is a survival mechanism that allows for the sequestration, breakdown and repurposing of cytoplasmic constituents (Bassham et al. 2006; Mizushima et al. 2008). Autophagic cell death is one of the two classic forms of animal PCD, however there are only a handful of examples within eukaryotes suggesting that autophagy is essential for cell death to occur (Minina et al. 2014; Mariño et al. 2014). The function of autophagy in lace plant PCD was investigated in chapter 4 and results suggest that it is primarily a survival mechanism, but also contributes to cellular breakdown. Autophagy was active in both NPCD and PCD cells, and likely aiding cellular homeostasis. In PCD stage cells however, autophagy is upregulated suggesting it also plays a role in cellular degradation. Our study showed that ER-like bodies were associated to autophagosomes suggesting that the ER may be their point of origin in the lace plant. Le Bars et al. (2015) recently determined that the ER is the membrane source for autophagosomes and that phagophore assembly is Atg5 dependent in Arabidopsis.

6.5. INTERACTIONS

Ethylene and ROS play important roles during development and stress responses (Steffens 2014). For instance, during climacteric fruit ripening tomatoes produce ethylene, which coincides with increased H_2O_2, lipid peroxidation, and protein oxidation (Jimenez et al. 2002). Throughout ripening the antioxidant system responds through a general increase in antioxidant enzymes and activity (Jimenez et al. 2002). Similarly, the application of exogenous ethylene in detached mangos leads to an increase in ROS, H_2O_2 specifically, and a decrease in ascorbic acid, whereas inhibition of ethylene perception by

1-methycyclopropene (1-MCP) had an opposite effect and inhibited CAT, SOD1 and APX activity (Wang et al. 2009). Ethylene is also known to induce ROS production by NADPH oxidases during aerenchyma formation in wheat roots (Yamauchi et al. 2014). Additionally, ethylene has been linked to several cases of ROS-burst induced cell death (Overmyer 2000; Tuominen et al. 2004; Mersmann et al. 2010). ROS produced in response to stress can also increase ethylene biosynthesis suggesting that there is reciprocal regulation between these two plant signaling mediators (Zhang et al., 2016).

Although ethylene is best known for inducing ROS production, it has also been shown to stimulate an increase in antioxidants. For example, in Arabidopsis guard cells, exogenous application of ethylene increased chalcone synthase (Watkins et al., 2014), a key enzyme responsible for the biosynthesis of flavonoids (Dao et al 2011). The tomato ethylene response gene *ERF1* (*TERF1*) is responsible for increased expression of several antioxidants including CAT, GPX and GDP-D-mannose pyrophosphorylase, which catalyze ascorbic acid biosynthesis (Zhang et al. 2016). Overexpression of *TERF1* in tobacco seedlings also led to greater resistance to H_2O_2 exposure (Zhang et al. 2016).

Autophagy has also been shown to be influenced by ethylene signaling. In soybean seedlings grown under starvation conditions, the upregulation of autophagosome formation genes *ATG8* and *ATG4* coincides with *ACC synthase* (ethylene biosynthesis precursor) and *ERF* (Okuda et al. 2011). Soybean seedlings grown under extreme starvation conditions also had increased levels of the ethylene signaling nuclear transcription factor EIN3 (Okuda et al. 2011). Similarly, ethylene appears to play an

important role in regulating autophagy during Petunia petal senescence following pollination. Ethylene inhibition with 1-MCP delays *PhATG8* induction, while the application of exogenous ethylene stimulated autophagy (Shibuya et al. 2013). Furthermore, Arabidopsis *atg8* mutants have reduced levels of ethylene-response genes (Chen et al. 2015).

ROS and autophagy also interact; both are commonly observed during stress responses and PCD. In general, autophagy and antioxidants mitigate damage from oxidative-damaged cellular components and ROS, respectively, and excessive ROS production will stimulate autophagy and antioxidant production (Perez-Perez et al. 2012). Increasing evidence suggests that ROS are necessary for autophagy activation. However the mechanisms underlying this pathway remain unclear and target of rapamycin (TOR)-independent pathways have been hypothesized (Scherz-Shouval and Elazar 2011; Perez-Perez et al. 2012).

6.6. PROPOSED MODEL FOR LACE PLANT PCD SIGNALING

The results highlighted in the previous chapters indicate that ethylene, the balance between antioxidants and ROS, as well as autophagy all contribute within the lace plant developmental PCD pathway. Based on our data and the literature, a pathway for PCD regulation and cell fate determination during the formation of perforations in lace plant leaves is hypothesized (Figure 6.1). In young leaves there is an upregulation of ethylene, which is self-promoted through a positive feedback loop. In the preperforation stage

ethylene continues to increase, leading to increases ROS, antioxidants (including anthocyanins), and autophagy. ROS are also generated through positive feedback and are known to increase ethylene, autophagy, and antioxidants. Antioxidants and autophagy act as inhibitors of ROS and therefore aid in maintaining cellular homeostasis. The stage of leaf development (preperforation or window) where cell fate is determined remains unknown. Compared to the resilient NPCD cells, PCD cells are susceptible to the death signals. PCD cells are also farther from the veins, have higher ROS and autophagy levels and are more sensitive to ethylene signaling due to their lower receptor levels (Rantong et al. 2015). NPCD cells differ from PCD cells in that they are near the leaf veins, have high antioxidant vs ROS levels, basal autophagy and are resistant to ethylene signaling as they have a higher number of receptors (Rantong et al. 2015). Once cell fate is determined and the threshold for PCD induction is crossed, cellular degradation occurs as described by Wertman et al. (2012). By the time leaves reach maturity, all PCD cells are deleted but NPCD cells persist, maintaining homeostasis beyond perforation formation.

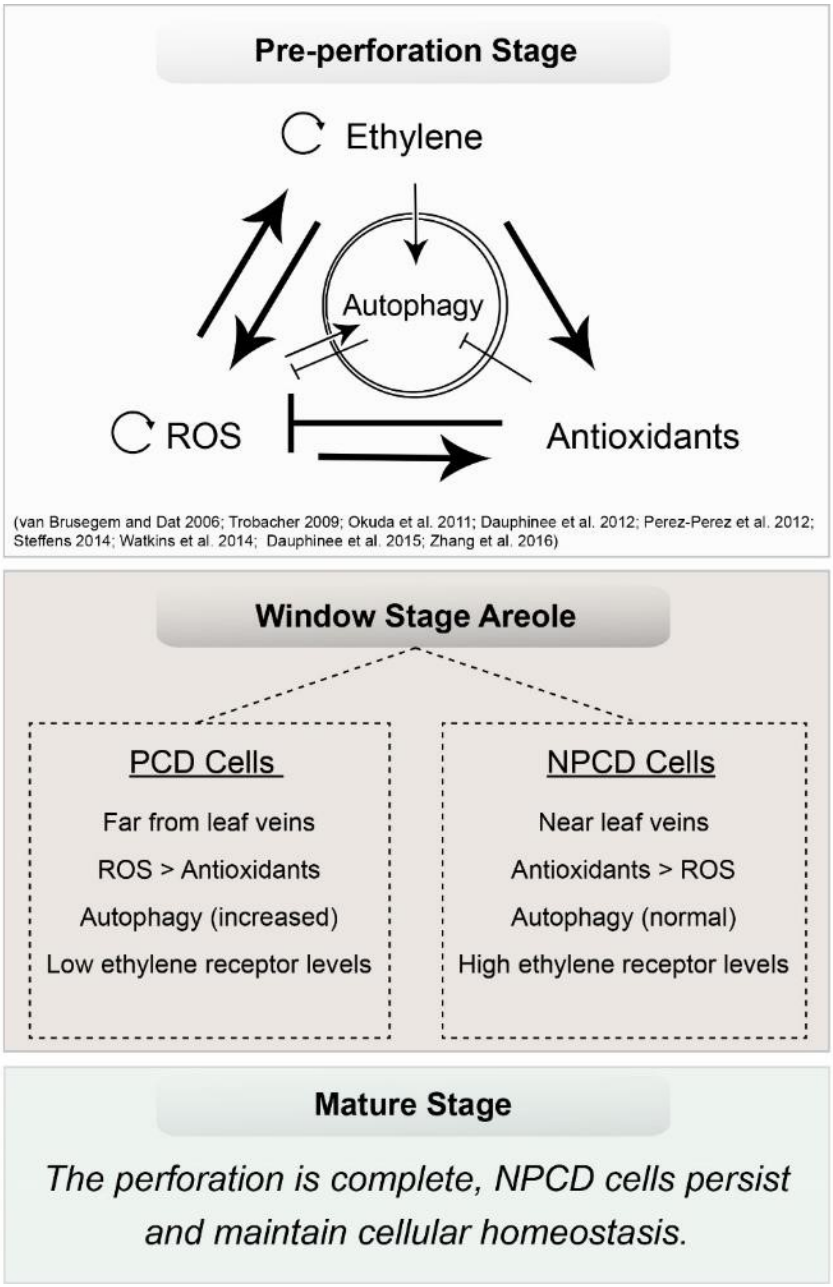

Figure 6.1. A proposed model for lace plant PCD signaling. During the preperforation stage of development, as the leaf emerges from the corm, ethylene production leads to an increase in ROS (reactive oxygen species), autophagy and antioxidants. Ethylene and ROS levels increase through positive feedback. Higher levels of ROS lead to greater anthocyanin production as well. Antioxidants inhibit ROS and autophagy, and autophagy inhibits ROS. In the window stage, PCD cells and non-PCD (NPCD) cells are distinguishable. PCD cells are distant from leaf veins, have greater ROS than antioxidants, higher autophagy and lower ethylene receptor levels compared to NPCD cells. NPCD cells are near the leaf veins, have high antioxidants compared to ROS, normal autophagy and higher ethylene receptor levels than PCD cells. Perforation formation is complete in the mature stage, NPCD cells persist.

6.7. TRANSFORMATION

The protocol for lace plant transformation detailed in chapter 5 can be used going forward to gain greater insight into the mechanistic control of lace plant developmental PCD. For example, developing an ethylene receptor overexpression mutant could be used to understand if ethylene production and perception affects the gradient of PCD observed in the window stage. Fluorescent protein markers targeted to specific organelles would be a valuable application of genetic transformation for the study of PCD in the lace plant because fluorescent stains are not ideal for long-term live cell imaging. Priorities for the lace plant system include markers for the ER due to its significance in ethylene signaling and autophagosome formation, mitochondria as they have been linked to lace plant PCD induction, and peroxisomes since they generate ROS and are unexplored in the lace plant.

6.8. CONCLUSIONS

In this thesis, ethylene, antioxidants, ROS, and autophagy were identified as key regulators of lace plant developmental PCD during the formation of perforations. Identification of signaling molecules that regulate PCD and the development of a novel transformation technique further advance our understanding of cell death regulation in the lace plant model system. The formation of perforations in the lace plant represents a rare example of PCD during plant development that warrants investigation and will contribute significantly to the unraveling of plant PCD signaling pathways. The

importance of understanding PCD in plants cannot be overstated due to its involvement in plant development, defense, and homeostasis.

REFERENCES

Adams DO, Yang SF (1979) Ethylene biosynthesis: Identification of 1-aminocyclopropane-1-carboxylic acid as an intermediate in the conversion of methionine to ethylene. Proc Natl Acad Sci U S A 76:170–174. doi: 10.1073/pnas.76.1.170

Aharoni N, Lieberman M (1979a) Patterns of Ethylene Production in Senescing Leaves. Plant Physiol 64:796–800

Aharoni N, Lieberman M (1979b) Ethylene as a regulator of senescence in tobacco leaf discs. Plant Physiol 64:801–4. doi: 10.1104/pp.64.5.801

Ahmad P, Jaleel CA, Salem MA, et al (2010) Roles of enzymatic and nonenzymatic antioxidants in plants during abiotic stress. Crit Rev Biotechnol 30:161–175. doi: 10.3109/07388550903524243

Allocati N, Masulli M, Di Ilio C, De Laurenzi V (2015) Die for the community: an overview of programmed cell death in bacteria. Cell Death Dis 6:e1609. doi: 10.1038/cddis.2014.570

Arrigoni O, De Tullio MC (2002) Ascorbic acid: much more than just an antioxidant. Biochim Biophys Acta 1569:1–9. doi: 10.1016/S0304-4165(01)00235-5

Bae GY, Nakajima N, Ishizuka K, Kondo N (1996) The role in ozone phytotoxicity of the evolution of ethylene upon induction of 1-aminocydopropane-l-carboxylic acid synthase by ozone fumigation in tomato plants. Plant Cell 37:129–134

Baehrecke EH (2003) Autophagic programmed cell death in *Drosophila*. Cell Death Differ 10:940–5. doi: 10.1038/sj.cdd.4401280

Ballou LM, Lin RZ (2008) Rapamycin and mTOR kinase inhibitors. J Chem Biol 1:27–36. doi: 10.1007/s12154-008-0003-5

Bassham DC (2007) Plant autophagy-more than a starvation response. Curr Opin Plant Biol 10:587–593. doi: 10.1016/j.pbi.2007.06.006

Bassham DC, Laporte M, Marty F, et al (2006) Autophagy in development and stress responses of plants. Autophagy 2:2–11. doi: 10.4161/auto.2092

Baxter A, Mittler R, Suzuki N (2014) ROS as key players in plant stress signalling. J Exp Bot 65:1229–1240. doi: 10.1093/jxb/ert375

Bayles KW (2014) Bacterial programmed cell death: making sense of a paradox. Nat Rev Microbiol 12:63–9. doi: 10.1038/nrmicro3136

Bell AD (2008) Plant Form: an illistrated guide to flowering plant morphology, 2nd edn. Timber Press, Portland, Oregon, USA

Bernard A, Klionsky D (2013) Autophagosome formation: tracing the source. Dev Cell 25:116–117. doi: 10.1016/j.devcel.2013.04.004

Biale JB (1950) Postharvest physiology and biochemistry of fruits. Annu Rev Plant Physiol 1: 183–206

Birch RG (1997) Plant transformation: problems and strategies for practical application. Annu Rev Plant Physiol Plant Mol Biol 48:297–326. doi: 10.1146/annurev.arplant.48.1.297

Bouchez O, Huard C, Lorrain S, et al (2007) Ethylene is one of the key elements for cell death and defense response control in the Arabidopsis lesion mimic mutant vad1. Plant Physiol 145:465–477. doi: 10.1104/pp.107.106302

Bowler C, Montagu M Van, Inze D (1992) Superoxide dismutase and stress tolerance. Annu Rev Plant Physiol Plant Mol Bioi 43:83–116

Bozhkov P, Jansson C (2007) Autophagy and cell-death proteases in plants: two wheels of a funeral cart. Autophagy 3:136–138. doi: 10.4161/auto.3600

Bozhkov PV, Lam E (2011) Green death: revealing programmed cell death in plants. Cell Death Differ 18:1239–40. doi: 10.1038/cdd.2011.86

Bradford MM (1976) A rapid and sensitive method for the quantitation of microgram quantities of protein utilizing the principle of protein-dye binding. Anal Biochem 72:248–254. doi: http://dx.doi.org/10.1016/0003-2697(76)90527-3

Brady CJ (1987) Fruit ripening. Annu Rev Plant Physiol 38:155–178

Buer CS, Muday GK, Djordjevic MA (2007) Flavonoids are differentially taken up and transported long distances in Arabidopsis. Plant Physiol 145:478–490. doi: 10.1104/pp.107.101824

Carter J, Gunawardena AHLAN (2011) Regeneration of the aquatic monocot *Aponogeton madagascariensis* (lace plant) through callus induction. Aquat Bot 94:143–149. doi: 10.1016/j.aquabot.2011.01.005

Chalker-Scott L (1999) Environmental significance of anthocyanins in plant stress responses. Photochem Photobiol 70:1–9. doi: 10.1111/j.1751-1097.1999.tb01944.x

Chen L, Liao B, Qi H, et al (2015) Autophagy contributes to regulation of the hypoxia response during submergence in *Arabidopsis thaliana*. Autophagy 11:2233–2246. doi: 10.1080/15548627.2015.1112483

Clough SJ, Bent AF (1998) Floral dip: a simplified method for Agrobacterium-mediated transformation of A*rabidopsis thaliana*. Plant J 16:735–743. doi: 10.1046/j.1365-313X.1998.00343.x

Coll NS, Epple P, Dangl JL (2011) Programmed cell death in the plant immune system. Cell Death Differ 18:1247–56. doi: 10.1038/cdd.2011.37

Costantini L, Snapp E (2014) Probing endoplasmic reticulum dynamics using fluorescence imaging and photobleaching techniques. Curr Protoc Cell Biol 60:1–32. doi: 10.1002/0471143030.cb2107s60

Daneva A, Gao Z, Durme M Van, et al (2016) Functions and regulation of programmed cell death in plant development. Annu Rev Cell Dev Biol 32:1–7. doi: 10.1146/annurev-cellbio-111315-124915

Dao TTH, Linthorst HJM, Verpoorte R (2011) Chalcone synthase and its functions in plant resistance. Phytochem Rev 10(3):397-412. doi: 10.1007/s11101-011-9211-7

Dauphinee AN, Wright H, Rantong G, Gunawardena AHLAN (2012) The involvement of ethylene in programmed cell death and climacteric-like behaviour during the remodelling of lace plant (*Aponogeton madagascariensis*) leaves. Botany 90:1237–1244. doi: 10.1139/b2012-093

Dauphinee AN, Gunawardena AH (2015) An overview of programmed cell death: from canonical to emerging model species. In: Gunawardena AHLAN, McCabe PF (eds). pp 1–31

Dauphinee AN, Warner TS, Gunawardena AHLAN (2014) A comparison of induced and developmental cell death morphologies in lace plant (*Aponogeton madagascariensis*) leaves. BMC Plant Biol 14:1–13. doi: 10.1186/s12870-014-0389-x

Davisons AJ, Kettle AJ, Fatur DJ (1986) Mechanism of the inhibition of catalase by ascorbate. J Biol Chem 261:1193–1200

Deponte M (2008) Programmed cell death in protists. Biochim Biophys Acta 1783:1396–405. doi: 10.1016/j.bbamcr.2008.01.018

Dhillon WS, Mahajan BVC (2011) Ethylene and ethephon induced fruit ripening in pear. J Stored Prod Postharvest Res 2(3):45–51

Din FVN, Valanciute A, House VP, et al (2012) Aspirin inhibits mTOR signaling , activates AMP-activated protein kinase , and induces autophagy in colorectal cancer. Gastroenterology 142:1504–1524. doi: 10.1053/j.gastro.2012.02.050

Doyle SM, Diamond M, McCabe PF (2010) Chloroplast and reactive oxygen species involvement in apoptotic-like programmed cell death in Arabidopsis suspension cultures. J Exp Bot 61:473–82. doi: 10.1093/jxb/erp320

Edinger AL, Thompson CB (2004) Death by design: apoptosis, necrosis and autophagy. Curr Opin Cell Biol 16:663–669. doi: 10.1016/j.ceb.2004.09.011

El-Kafafi E-S, Karamoko M, Pignot-Paintrand I, et al (2007) Developmentally regulated association of plastid division protein FtsZ1 with thylakoid membranes in *Arabidopsis thaliana*. Biochem J 409:87–94. doi: 10.1042/BJ20070543

Feng Y, He D, Yao Z, Klionsky DJ (2014) The machinery of macroautophagy. Cell Res 24:24–41. doi: 10.1038/cr.2013.168

Filonova LH, Bozhkov P V, Brukhin VB, et al (2000) Two waves of programmed cell death occur during formation and development of somatic embryos in the gymnosperm, Norway spruce. J Cell Sci 113 Pt 24:4399–411

Floyd BE, Morriss SC, Macintosh GC, Bassham DC (2012) What to eat: evidence for selective autophagy in plants. J Integr Plant Biol 54:907–920. doi: 10.1111/j.1744-7909.2012.01178.x

Floyd BE, Soto-Burgos J, Bassham DC (2015) To live or die: autophagy in plants. In: Gunawardena AHLAN, McCabe PF (eds) Plant Programmed Cell Death, 1st edn. Springer International, Switzerland pp 269–300. doi: 10.1007/978-3-319-21033-9_11

Foulkes EC, Lemberg R (1948) The inhibition of catalase by ascorbic acid. Aust J Exp Biol Med Sci 26:307–313

Fuchs Y, Steller H (2011) Programmed cell death in animal development and disease. Cell 147:742–58. doi: 10.1016/j.cell.2011.10.033

Gadjev I, Stone JM, Gechev TS (2008) Programmed cell death in plants. New insights into redox regulation and the role of hydrogen peroxide. In: International Review of Cell and Molecular Biology 270:87–144. doi: 10.1016/S1937-6448(08)01403-2

Galluzzi L, Vitale I, Abrams JM, et al (2012) Molecular definitions of cell death subroutines: recommendations of the Nomenclature Committee on Cell Death 2012. Cell Death Differ 19:107–20. doi: 10.1038/cdd.2011.96

Galluzzi L, Bravo-San Pedro, Vitale I, et al (2015) Essential versus accesory aspects of cell death: reccomendations of the NCCD 2015. Cell Death Differ 22:58-73. doi: 10.1038/cdd.2014.137

Ge Y, Norton T, Wang ZY (2006) Transgenic zoysiagrass (*Zoysia japonica*) plants obtained by Agrobacterium-mediated transformation. Plant Cell Rep 25:792–798. doi: 10.1007/s00299-006-0123-8

Gechev TS, Hille J (2005) Hydrogen peroxide as a signal controlling plant programmed cell death. J Cell Biol 168:17–20. doi: 10.1083/jcb.200409170

Gechev TS, Van Breusegem F, Stone JM, et al (2006) Reactive oxygen species as signals that modulate plant stress responses and programmed cell death. Bioessays 28:1091–101. doi: 10.1002/bies.20493

Geng J, Klionsky DJ (2010) The golgi as a potential membrane source for autophagy. Autophagy 6:950–951. doi: 10.4161/auto.6.7.13009

Gill SS, Tuteja N (2010) Reactive oxygen species and antioxidant machinery in abiotic stress tolerance in crop plants. Plant Physiol Biochem 48:909–930. doi: 10.1016/j.plaphy.2010.08.016

Gladish DK, Niki T (2008) Ethylene is involved in vascular cavity formation in pea (*Pisum sativum*) primary roots. Plant Root 2:38–45. doi: 10.3117/plantroot.2.38

Gould KS (2004) Nature's swiss army knife: the diverse protective roles of anthocyanins in leaves. J Biomed Biotechnol 5:314–320. doi: 10.1155/S1110724304406147

Gray J (2004) Paradigms of the evolution of programmed cell death. In: Gray J (ed) Programmed Cell Death in Plants. Blackwell Publishing Ltd, Oxford, pp 1–20

Green DR (2011) Means to an end: apoptosis and other cell death mechanisms. Cold Spring Harbor Laboratory Press pp 220

Greenberg JT (1996) Review programmed cell death : a way of life for plants. Proc Nat Acadademy Sci USA 93:12094–12097

Grellet Bournonville CF, Díaz-Ricci JC (2011) Quantitative determination of superoxide in plant leaves using a modified NBT staining method. Phytochem Anal 22:268–271. doi: 10.1002/pca.1275

Griffith F (1928) The significance of pneumococcal types. J Hyg 27(2):113–159

Gunawardena AHLAN (2008) Programmed cell death and tissue remodelling in plants. J Exp Bot 59:445–51. doi: 10.1093/jxb/erm189

Gunawardena AHLAN, Dengler NG (2006) Alternative modes of leaf dissection in monocotyledons. Bot J Linn Soc 25–44

Gunawardena AHLAN, Greenwood JS, Dengler N (2007) Cell wall degreadation and modification during programmed cell death in lace plant, *Aponogeton madagascariensis* (Aponogetonaceae). Am J Bot 94:1116–1128

Gunawardena AHLAN, Greenwood JS, Dengler NG (2004) Programmed cell death remodels lace plant leaf shape during development. Plant Cell 16:60–73. doi: 10.1105/tpc.016188.ous

Gunawardena AHLAN, Navachandrabala C, Kane M, Dengler NG (2006) Lace plant: a novel system for studying developmental programmed cell death. In: Teixeira da Silva JA (ed) Floriculture, ornamental and plant biotechnology: advances and tropical issues. Global Science Books, Middlesex, pp 157–162

Chae H, Lee W (2001) Ethylene- and enzyme-mediated superoxide production and cell death in carrot cells grown under carbon starvation. Plant Cell Rep 20:256–261. doi: 10.1007/s002990000307

Hadfield KA, Rose JKC, Bennett AB (1995) The respiratory climacteric is present in Charentais (*Cucumis melo* cv . reticulatus F1 alpha) melons ripened on or off the plant. Communication 46:1923–1925.

Hailey DW, Rambold AS, Satpute-Krishnan P, et al (2011) Mitochondria supply membranes for autophagosome biogenesis during starvation. 141:656–667. doi: 10.1016/j.cell.2010.04.009

Hamasaki M, Furuta N, Matsuda A, et al (2013) Autophagosomes form at ER-mitochondria contact sites. Nature 495:389–393. doi: 10.1038/nature11910

Hansen E (1965) Postharvest physiology of fruits. Annu Rev Plant Physiol 17:459–480.

Hara-Nishimura I, Hatsugai N, Nakaune S, et al (2005) Vacuolar processing enzyme: an executor of plant cell death. Curr Opin Plant Biol 8:404–8. doi: 10.1016/j.pbi.2005.05.016

Hedrich R, Neher E (1987) Cytoplasmic calcium regulates voltage-dependent ion channels in plant vacuoles. Nature 329:833–836. doi: 10.1038/329833a0

Heras-Sandoval D, Pérez-Rojas JM, Hernández-Damián J, Pedraza-Chaverri J (2014) The role of PI3K/AKT/mTOR pathway in the modulation of autophagy and the clearance of protein aggregates in neurodegeneration. Cell Signal 26:2694–2701. doi: 10.1016/j.cellsig.2014.08.019

Hoeberichts FA, Woltering EJ (2003) Multiple mediators of plant programmed cell death: interplay of conserved cell death mechanisms and plant-specific regulators. Bioessays 25:47–57. doi: 10.1002/bies.10175

Huss M, Ingenhorst G, König S, et al (2002) Concanamycin A, the specific inhibitor of V-ATPases, binds to the VO subunit c. J Biol Chem 277:40544–40548. doi: 10.1074/jbc.M207345200

Ishida H, Izumi M, Wada S, Makino A (2014) Roles of autophagy in chloroplast recycling. Biochim Biophys Acta - Bioenerg 1837:512–521. doi: 10.1016/j.bbabio.2013.11.009

Izumi M, Ishida H, Nakamura S, Hidema J (2017) Entire photodamaged dhloroplasts are transported to the central vacuole by autophagy. Plant Cell tpc.00637.2016. doi: 10.1105/tpc.16.00637

Jedd G, Chua N-HN (2002) Visualization of peroxisomes in living plant cells reveals acto-myosin-dependent cytoplasmic streaming and peroxisome budding. Plant Cell Physiol 43:384–392. doi: 10.1093/pcp/pcf045

Jiang P, Mizushima N (2014) Autophagy and human disease. Cell Cycle 6:1837–1849. doi: 10.1038/cr.2013.161

Jimenez A, Creissen G, Kular B, et al (2002) Changes in oxidative processes and components of the antioxidant system during tomato fruit ripening. Planta 214:751–758. doi: 10.1007/s004250100667

Jing HC, Schippers JHM, Hille J, Dijkwel PP (2005) Ethylene-induced leaf senescence depends on age-related changes and OLD genes in Arabidopsis. J Exp Bot 56:2915–2923. doi: 10.1093/jxb/eri287

Ju C, Chang C (2015) Mechanistic insights in ethylene perception and signal transduction. Plant Physiol 169:85–95. doi: 10.1104/pp.15.00845

Kacprzyk J, Daly CT, McCabe PF (2011) The botanical dance of death: programmed cell death in plants. In: Kader J-C, Delseny M (eds) Advances in Botanical Research, Vol. 60. Elsevier Ltd., pp 169–261

Kacprzyk J, Dauphinee AN, Gallois P, et al (2015) Methods to study plant programmed cell death. Methods Mol Biol 1419:145–160. doi: 10.1007/978-1-4939-3581-9

Kacprzyk J, Devine A, McCabe PF (2014) The root hair assay facilitates the use of genetic and pharmacological tools in order to dissect multiple signalling pathways that lead to programmed cell death. PLoS One. doi: 10.1371/journal.pone.0094898

Katz E, Riov J, Weiss D, Goldschmidt EE (2005) The climacteric-like behaviour of young, mature and wounded citrus leaves. J Exp Bot 56:1359–67. doi: 10.1093/jxb/eri137

Kerr JFR, Wyllie AH, Currie AR (1972) Apoptosis: a basic biological phenomenon with wide-ranging implications in tissue kinetics. Br J Cancer 26:239–257

Kim J, Lee H, Lee HN, et al (2013) Autophagy-related proteins are required for degradation of peroxisomes in Arabidopsis hypocotyls during seedling growth. Plant Cell 25:4956–66. doi: 10.1105/tpc.113.117960

Klener P (2006) Cell death signalling pathways in the pathogenesis and therapy of haematologic malignancies : overview of apoptotic pathways. 44:34–44

Klionsky DJ, Abdelmohsen K, Abe A, et al (2016) Guidelines for use and interpretation of assays for monitoring autophagy (3rd edition). Autophagy 12:1–222. doi: 10.1080/15548627.2015.1100356

Kroemer G, El-Deiry WS, Golstein P, et al (2005) Classification of cell death: recommendations of the Nomenclature Committee on Cell Death. Cell Death Differ 12(2):1463–7. doi: 10.1038/sj.cdd.4401724

Kroemer G, Galluzzi L, Vandenabeele P, et al (2009) Classification of cell death - recommendations of the Nomenclature Committee on Cell Death. Cell Death Differ 16:3–11. doi: 10.1038/cdd.2008.150

Kroemer G, Levine B (2008) Autophagic cell death: the story of a misnomer. Nat Rev Mol Cell Biol 9:1004–10. doi: 10.1038/nrm2529

Kroemer G, Reed J (2000) Mitochondrial control of cell death. Nat Med 6:513–519

Kwak D, Choi S, Jeong H, et al (2012) Osmotic stress regulates mammalian target of rapamycin (mTOR) complex 1 via c-Jun N-terminal kinase (JNK)-mediated raptor protein phosphorylation. J Biol Chem 287:18398–18407. doi: 10.1074/jbc.M111.326538

Lacroix B, Zaltsman A, Citovsky V (2011) Host factors involved in genetic transformation of plant cells by Agrobacterium. In: Stewart NC, Touraev A, Citovsky V, Tzfira T (eds) Plant Transformation Technologies. Wiley-Blackwell, pp 3–29

Lam E (2004) Controlled cell death, plant survival and development. Nat Rev Mol Cell Biol 5:305–15. doi: 10.1038/nrm1358

Landi M, Tattini M, Gould KS (2015) Multiple functional roles of anthocyanins in plant-environment interactions. Environ Exp Bot 119:4–17. doi: 10.1016/j.envexpbot.2015.05.012

Le Bars R, Marion J, Le Borgne R, et al (2014) ATG5 defines a phagophore domain connected to the endoplasmic reticulum during autophagosome formation in plants. Nat Commun 5:4121. doi: 10.1038/ncomms5121

Lee DW (2002) Anthocyanins in autumn leaf senescence. Adv Bot Res 37:147–165. doi: 10.1016/S0065-2296(02)37048-4

Les DH, Tippery NP (2013) In time and with water... the systematics of alismatid monocotyledons. In: Wilkin P, Mayo SJ (eds) Early Events in Monocot Evolution. Cambridge University Press, pp 119–164

Levine B, Yuan J (2005) Review series autophagy in cell death: an innocent convict? J Clin Invest 115:2679–2688. doi: 10.1172/JCI26390

Li F, Chung T, Vierstra RD (2014) AUTOPHAGY-RELATED11 plays a critical role in general autophagy- and senescence-induced mitophagy in Arabidopsis. Plant Cell 26:788–807. doi: 10.1105/tpc.113.120014

Li R, Qu R (2011) High throughput Agrobacterium-mediated switchgrass transformation. Biomass and Bioenergy 35:1046–1054. doi: 10.1016/j.biombioe.2010.11.025

Li Z, Pan Q, Cui X, Duan C (2010) Optimization on anthocyanins extraction from wine grape skins using orthogonal test design. Food Sci Biotechnol 19:1047–1053. doi: 10.1007/s10068-010-0147-2

Liakopoulos G, Nikolopoulos D, Klouvatou A, et al (2006) The photoprotective role of epidermal anthocyanins and surface pubescence in young leaves of grapevine (Vitis vinifera). Ann Bot 98:257–65. doi: 10.1093/aob/mcl097

Lin MT, Beal MFF (2006) Mitochondrial dysfunction and oxidative stress in neurodegenerative diseases. Nature 443:787–795. doi: 10.1038/nature05292

Liu Y, Bassham DC (2012) Autophagy: pathways for self-eating in plant cells. Annu Rev Plant Biol 63:215–237. doi: 10.1146/annurev-arplant-042811-105441

Logan DC, Leaver CJ (2000) Mitochondria-targeted GFP highlights the heterogeneity of mitochondrial shape, size and movement within living plant cells. J Exp Bot 51:865–871. doi: 10.1093/jexbot/51.346.865

Lombardi L, Mariotti L, Picciarelli P, et al (2012) Ethylene produced by the endosperm is involved in the regulation of nucellus programmed cell death in Sechium edule Sw. Plant Sci 187:31–38. doi: 10.1016/j.plantsci.2012.01.011

Lord C, Gunawardena AHLAN (2010) Isolation of leaf protoplasts from the submerged aquatic monocot *Aponogeton madagascariensis*. Am J Plant Sci Biotechnol 4:6–11

Lord CEN, Gunawardena AHLAN (2012) The lace plant: a novel model system to study plant proteases during developmental programmed cell death in vivo. Physiol Plant 145:114–20. doi: 10.1111/j.1399-3054.2012.01570.x

Lord CEN, Wertman JN, Lane S, Gunawardena AHLAN (2011) Do mitochondria play a role in remodelling lace plant leaves during programmed cell death? BMC Plant Biol 11:102. doi: 10.1186/1471-2229-11-102

Lowe K, Wu E, Wang N, et al (2016) Morphogenic regulators baby boom and wuschel improve monocot transformation. Plant Cell 28:tpc.00124.2016. doi: 10.1105/tpc.16.00124

Lu J, Sivamani E, Li X, Qu R (2008) Activity of the 5' regulatory regions of the rice polyubiquitin rubi3 gene in transgenic rice plants as analyzed by both GUS and GFP reporter genes. Plant Cell Rep 27:1587. doi: 10.1007/s00299-008-0577-y

Lu SC (2013) Glutathione synthesis. Biochim Biophys Acta 1830:3143–3153. doi: 10.1016/j.bbagen.2012.09.008

Macnish AJ, Jiang C-Z, Negre-Zakharov F, Reid MS (2010) Physiological and molecular changes during opening and senescence of *Nicotiana mutabilis* flowers. Plant Sci 179:267–272. doi: 10.1016/j.plantsci.2010.05.011

Mariño G, Niso-Santano M, Baehrecke EH, Kroemer G (2014) Self-consumption: the interplay of autophagy and apoptosis. Nat Rev Mol Cell Biol 15:81–94. doi: 10.1038/nrm3735

Marty (1999) Plant vacuoles. Plant Cell 11:587–600. doi: 10.1105/tpc.11.4.587

Masani MYA, Noll GA, Parveez GKA, et al (2014) Efficient transformation of oil palm protoplasts by PEG-mediated transfection and DNA microinjection. PLoS One 9:1–11. doi: 10.1371/journal.pone.0096831

Mattoo A, Handa A (2004) Ethylene signaling in plant cell death. In: Nooden L (ed) Plant Cell Death Processes. Elsevier Inc., New York, pp 125–142

McGlasson WB, Pratt HK (1964) Effects of ethylene on cantaloupe fruits harvested. Plant Physiol 39:120–127

Mergemann H, Sauter M (2000) Ethylene induces epidermal cell death at the site of adventitious root emergence in rice. Plant Physiol 124:609–14

Merkulova EA, Guiboileau A, Naya L, et al (2014) Assessment and optimization of autophagy monitoring methods in arabidopsis roots indicate direct fusion of autophagosomes with vacuoles. Plant Cell Physiol 55:715–726. doi: 10.1093/pcp/pcu041

Mersmann S, Bourdais G, Rietz S, Robatzek S (2010) Ethylene signaling regulates accumulation of the FLS2 receptor and is required for the oxidative burst contributing to plant immunity. Plant Physiol 154:391–400. doi: 10.1104/pp.110.154567

Michaeli S, Galili G, Genschik P, et al (2016) Autophagy in plants - what's new on the menu? Trends Plant Sci 21:134–144. doi: 10.1016/j.tplants.2015.10.008

Michaeli S, Honig A, Levanony H, et al (2014) Arabidopsis ATG8-INTERACTING PROTEIN1 is involved in autophagy-dependent vesicular trafficking of plastid proteins to the vacuole. Plant Cell 26:4084–4101. doi: 10.1105/tpc.114.129999

Mignolet-Spruyt L, Xu E, Idänheimo N, et al (2016) Spreading the news: subcellular and organellar reactive oxygen species production and signalling. J Exp Bot 67:3831–3844. doi: 10.1093/jxb/erw080

Minina EA, Bozhkov PV, Hofius D (2014) Autophagy as initiator or executioner of cell death. Trends Plant Sci 19:692–697. doi: 10.1016/j.tplants.2014.07.007

Minina EA, Filonova LH, Fukada K, et al (2013) Autophagy and metacaspase determine the mode of cell death in plants. J Cell Biol 203:917–927. doi: 10.1083/jcb.201307082

Mishra P, Dauphinee AN, Gunawardena AH, Manjithaya R (In Press) Discovery of pan autophagy inhibitors through a highthroughput screen highlights macroautophagy as an evolutionarily conserved process across three kingdoms- fungi, animals and plants. Autophagy.

Mizushima N, Levine B, Cuervo AM, Klionsky DJ (2008) Autophagy fights disease through cellular self-digestion. Nature 451:1069–75. doi: 10.1038/nature06639

Mizushima N, Yoshimori T, Ohsumi Y (2011) The role of Atg proteins in autophagosome formation. Annu Rev Cell Dev Biol 27:107–132. doi: 10.1146/annurev-cellbio-092910-154005

Morgan PW, He CJ, Drew MC (1992) Intact leaves exhibit a climacteric-like rise in ethylene production before abscission. Plant Physiol 100:1587–90

Nabors MW (2004) Introduction to botany, 1st edn. Pearson Benjamin Cummings, San Francisco pp 626

Naqvi S, Zhu C, Farre G, et al (2009) Transgenic multivitamin corn through biofortification of endosperm with three vitamins representing three distinct metabolic pathways. Proc Natl Acad Sci U S A 106:7762–7767. doi: 10.1073/pnas.0901412106

Noodén, L.D. 2004. Introduction. In: Plant cell death processes. Noodén, LD (ed). Elsevier Academic Press, San Diego pp 1-18

Nowak JS, Bolduc N, Dengler NG, Posluszny U (2011) Compound leaf development in the palm *Chamaedorea elegans* is KNOX-independent. Am J Bot 98:1575–1582. doi: 10.3732/ajb.1100101

Oberst A, Bender C, Green DR (2008) Living with death: the evolution of the mitochondrial pathway of apoptosis in animals. Cell Death Differ 15:1139–1146. doi: 10.1038/cdd.2008.65

Oeticker JH, Yang SF (1995) The role of ethylene in fruit ripening. Acta Hort 398:167-178. doi: 10.17660/ActaHortic.1995.398.17

Okuda M, Nang MPSH, Oshima K, et al (2011) The ethylene signal mediates induction of GmATG8i in soybean plants under starvation stress. Biosci Biotechnol Biochem 75:1408–1412. doi: 10.1271/bbb.110086

Olvera-Carrillo Y, Van Bel M, Van Hautegem T, et al (2015) A conserved core of PCD indicator genes discriminates developmentally and environmentally induced programmed cell death in plants. Plant Physiol 169:pp.00769.2015. doi: 10.1104/pp.15.00769

Ondrej V, Navrátilová B, Protivánková I, et al (2010) Recondensation level of repetitive sequences in the plant protoplast nucleus is limited by oxidative stress. J Exp Bot 61:2395–401. doi: 10.1093/jxb/erq067

Overmyer K (2000) Ozone-sensitive Arabidopsis rcd1 mutant reveals opposite roles for ethylene and jasmonate signaling pathways in regulating superoxide-dependent cell death. Plant Cell 12:1849–1862. doi: 10.1105/tpc.12.10.1849

Ozawa K, Wakasa Y, Ogo Y, et al (2012) Development of an efficient agrobacterium-mediated gene targeting system for rice and analysis of rice knockouts lacking granule-bound starch synthase (Waxy) and β1,2-xylosyltransferase. Plant Cell Physiol 53:755–761. doi: 10.1093/pcp/pcs016

Pandhair V, Sekhon B (2006) Reactive oxygen species and antioxidants in plants: an overview. J Plant Biochem Biotechnol 15:71–78

Pasternak T, Tietz O, Rapp K, et al (2015) Protocol: an improved and universal procedure for whole-mount immunolocalization in plants. Plant Methods 11:50. doi: 10.1186/s13007-015-0094-2

Pavet V, Olmos E, Kiddle G, et al (2005) Ascorbic acid deficiency activates cell death and disease resistance responses in Arabidopsis. Plant Physiol 139:1291–1303. doi: 10.1104/pp.105.067686

Perez-Perez ME, Lemaire SD, Crespo JL (2012) Reactive oxygen species and autophagy in plants and algae. Plant Physiol 160:156–164. doi: 10.1104/pp.112.199992

Petrov V, Hille J, Mueller-Roeber B, Gechev TS (2015) ROS-mediated abiotic stress-induced programmed cell death in plants. Front Plant Sci 6:1–16. doi: 10.3389/fpls.2015.00069

Piqueras A, Alburquerque N, Folta KM (2010) Transgenic crop plants. In: Kole C, Michler CH, Abbott AG, Hall TC (eds) Transgenic Crop Plants. Springer, Berlin Heidelberg, pp 31–56

Rantong G, Evans R, Gunawardena AHLAN (2015) Lace plant ethylene receptors, AmERS1a and AmERS1c, regulate ethylene-induced programmed cell death during leaf morphogenesis. Plant Mol Biol 89:215–227. doi: 10.1007/s11103-015-0356-4

Rao K, Chodisetti B, Mangamoori LN, Giri A (2012) Agrobacterium-mediated transformation in alpinia galanga (Linn.) willd. for enhanced acetoxychavicol acetate production. Appl Biochem Biotechnol 168:339–347. doi: 10.1007/s12010-012-9777-6

Ravikumar B, Moreau K, Jahreiss L, et al (2010) Plasma membrane contributes to the formation of pre-autophagosomal structures. Nat Cell Biol 12:747–757. doi: 10.1038/ncb2078\rncb2078

Reape TJ, McCabe PF (2008) Apoptotic-like programmed cell death in plants. New Phytol 180:13–26. doi: 10.1111/j.1469-8137.2008.02549.x

Reape TJ, McCabe PF (2013) Commentary: the cellular condensation of dying plant cells: programmed retraction or necrotic collapse? Plant Sci 207:135–9. doi: 10.1016/j.plantsci.2013.03.001

Rees D (2012) Introduction. In: Rees D, Farrell G, Orchard J (eds) Crop Post-Harvest: Science and Technology, 1st edn. New Jersey, pp 1–4

Ribas AF, Dechamp E, Champion A, et al (2011) Agrobacterium-mediated genetic transformation of *Coffea arabica* (L.) is greatly enhanced by using established embryogenic callus cultures. BMC Plant Biol 11:92. doi: 10.1186/1471-2229-11-92

Rice KC, Bayles KW (2003) Death's toolbox : examining the molecular components of bacterial programmed cell death 50:729–738. doi: 10.1046/j.1365-2958.2003.03720.x

Rivera AL, Gómez-Lim M, Fernández F, Loske AM (2012) Physical methods for genetic plant transformation. Phys Life Rev 9:308–345. doi: 10.1016/j.plrev.2012.06.002

Scherz-Shouval R, Elazar Z (2011) Regulation of autophagy by ROS: physiology and pathology. Trends Biochem Sci 36:30–38. doi: 10.1016/j.tibs.2010.07.007

Schieber M, Chandel NS (2014) ROS function in redox signaling and oxidative stress. Curr Biol 24:R453–R462. doi: 10.1016/j.cub.2014.03.034

Sergueff M (1907) Contribution á la morphologie et la biologie des aponogetonacèes. University of Geneva

Serrano M, Romojaro F, Casas JL, Acosta M (1991) Ethylene and polyamine metabolism in climacteric and nonclimacteric carnation flowers. Hort Sci 26(7):894–896

Sevón N, Oksman-Caldentey KM (2002) Agrobacterium rhizogenes-mediated transformation: root cultures as a source of alkaloids. Planta Med 68:859–868. doi: 10.1055/s-2002-34924

Shalata A, Neumann PM (2001) Exogenous ascorbic acid (vitamin C) increases resistance to salt stress and reduces lipid peroxidation. J Exp Bot 52:2207–2211. doi: 10.1093/jexbot/52.364.2207

Shen S, Kepp O, Kroemer G (2012) The end of autophagic cell death? Autophagy 8:1–3.

Shibuya K, Niki T, Ichimura K (2013) Pollination induces autophagy in petunia petals via ethylene. J Exp Bot 64:1111–1120. doi: 10.1093/jxb/ers395

Shpilka T, Weidberg H, Pietrokovski S, Elazar Z (2011) Atg8: an autophagy-related ubiquitin-like protein family. Genome Biol 12:226. doi: 10.1186/gb-2011-12-7-226\rgb-2011-12-7-226

Sies H (1997) Oxidative stress: oxidants and antioxidants. Exp Physiol 82:291–295. doi: 10.1113/expphysiol.1997.sp004024

Singh S, Grover A, Nasim M (2016) Biofuel potential of plants transformed genetically with NAC family genes. Front Plant Sci 7:1–5. doi: 10.3389/fpls.2016.00022

Smirnoff N, Wheeler GL (2000) Ascorbic acid in plants: biosynthesis and function. Crit Rev Biochem Mol Biol 35:291–314. doi: 10.1080/07352680091139231

Steffens B (2014) The role of ethylene and ROS in salinity, heavy metal, and flooding responses in rice. Front Plant Sci 5:685. doi: 10.3389/fpls.2014.00685

Stewart CN, Touraev A, Citovsky V, Tzfira T (2011) Introduction. In: Plant Transformation Technologies

Subramoni S, Nathoo N, Klimov E, Yuan Z-C (2014) *Agrobacterium tumefaciens* responses to plant-derived signaling molecules. Front Plant Sci 5:322. doi: 10.3389/fpls.2014.00322

Suzuki K, Kirisako T, Kamada Y, et al (2001) The pre-autophagosomal structure organized by concerted functions of APG genes is essential for autophagosome formation. EMBO J 20:5971–5981. doi: 10.1093/emboj/20.21.5971

Suzuki K, Ohsumi Y (2007) Molecular machinery of autophagosome formation in yeast, *Saccharomyces cerevisiae*. FEBS Lett 581:2156–2161. doi: 10.1016/j.febslet.2007.01.096

Szalai G, Kellős T, Galiba G, Kocsy G (2009) Glutathione as an antioxidant and regulatory molecule in plants under abiotic stress conditions. J Plant Growth Regul 28:66–80. doi: 10.1007/s00344-008-9075-2

Tanaka Y, Sasaki N, Ohmiya A (2008) Biosynthesis of plant pigments: anthocyanins, betalains and carotenoids. Plant J 54:733–49. doi: 10.1111/j.1365-313X.2008.03447.x

Thomas H, Ougham HJ, Wagstaff C, Stead AD (2003) Defining senescence and death. J Exp Bot 54:1127–1132. doi: 10.1093/jxb/erg133

Tooze SA (2013) Current views on the source of the autophagosome membrane. Essays Biochem 55:29–38. doi: bse0550029 [pii]\n10.1042/bse0550029

Touitou E, Alkabes M, Memoli A, Alhaique F (1996) Glutathione stabilizes ascorbic acid in aqueous solution. Int J Pharm 133:85–88. doi: 10.1016/0378-5173(95)04419-1

Traas J, Bohn-Courseau I (2005) Cell proliferation patterns at the shoot apical meristem. Curr Opin Plant Biol 8:587–92. doi: 10.1016/j.pbi.2005.09.004

Trobacher CP (2009) Ethylene and programmed cell death in plants. Botany 87:757–769. doi: 10.1139/B09-041

Trobacher CP, Senatore A, Holley C, Greenwood JS (2013) Induction of a ricinosomal-protease and programmed cell death in tomato endosperm by gibberellic acid. Planta 237:665–679. doi: 10.1007/s00425-012-1780-1

Tsiatsiani L, Van Breusegem F, Gallois P, et al (2011) Metacaspases. Cell Death Differ 18:1279–88. doi: 10.1038/cdd.2011.66

Tsujimoto Y, Shimizu S (2005) Another way to die: autophagic programmed cell death. Cell Death Differ 12:1528–1534. doi: 10.1038/sj.cdd.4401777

Tucker GA (1993) Introduction. In Biochemistry of fruit ripening. Seymour GB, Taylor JE, Tucker GA (eds). Chapman & Hall, London, UK. pp. 3-43

Tuominen H, Overmyer K, Keinänen M, et al (2004) Mutual antagonism of ethylene and jasmonic acid regulates ozone-induced spreading cell death in Arabidopsis. Plant J 39:59–69. doi: 10.1111/j.1365-313X.2004.02107.x

Urquhart W, Gunawardena AHLAN, Moeder W, et al (2007) The chimeric cyclic nucleotide-gated ion channel ATCNGC11/12 constitutively induces programmed cell death in a Ca2+ dependent manner. Plant Mol Biol 65:747–761. doi: 10.1007/s11103-007-9239-7

Van Breusegem F, Dat JF (2006) Reactive oxygen species in plant cell death. Plant Physiol 141:384–390. doi: 10.1104/pp.106.078295.384

van Bruggen HWE (1985) Monograph of the genus Aponogeton (Aponogetonaceae). Bibl Bot 8:76

van Doorn WG (2011) Classes of programmed cell death in plants, compared to those in animals. J Exp Bot 62:4749–61. doi: 10.1093/jxb/err196

van Doorn WG, Beers EP, Dangl JL, et al (2011) Morphological classification of plant cell deaths. Cell Death Differ 18:1241–6. doi: 10.1038/cdd.2011.36

van Doorn WG, Papini A (2013) Ultrastructure of autophagy in plant cells: a review. Autophagy 9:1922–1936. doi: 10.4161/auto.26275

van Doorn WG, Woltering EJ (2005) Many ways to exit? Cell death categories in plants. Trends Plant Sci 10:117–22. doi: 10.1016/j.tplants.2005.01.006

Van Durme M, Nowack MK (2016) Mechanisms of developmentally controlled cell death in plants. Curr Opin Plant Biol 29:29–37. doi: 10.1016/j.pbi.2015.10.013

Vandenabeele P, Galluzzi L, Vanden Berghe T, Kroemer G (2010) Molecular mechanisms of necroptosis: an ordered cellular explosion. Nat Rev Mol Cell Biol 11:700–14. doi: 10.1038/nrm2970

Wada S, Hayashida Y, Izumi M, et al (2015) Autophagy supports biomass production and nitrogen use efficiency at the vegetative stage in rice. Plant Physiol 168:60–73. doi: 10.1104/pp.15.00242

Wada S, Ishida H, Izumi M, et al (2009) Autophagy plays a role in chloroplast degradation during senescence in individually darkened leaves. Plant Physiol 149:885–893. doi: 10.1104/pp.108.130013

Wang B, Wang J, Feng X, et al (2009) Effects of 1-MCP and exogenous ethylene on fruit ripening and antioxidants in stored mango. Plant Growth Regul 57:185–192. doi: 10.1007/s10725-008-9335-y

Wang H, Cao G, Prior RL (1997) Oxygen radical absorbing capacity of anthocyanins. J Agric Food Chem 45:304–309. doi: 10.1021/jf960421t

Wertman J, Lord CEN, Dauphinee AN, Gunawardena AHLAN (2012) The pathway of cell dismantling during programmed cell death in lace plant (*Aponogeton madagascariensis*) leaves. BMC Plant Biol 12:115

Wirth J, Poletti S, Aeschlimann B, et al (2009) Rice endosperm iron biofortification by targeted and synergistic action of nicotianamine synthase and ferritin. Plant Biotechnol J 7:631–644. doi: 10.1111/j.1467-7652.2009.00430.x

Wong SM, Sahidin N, Khalid N (2010) Agrobacterium-mediated transformation of the aquarium plant *Cryptocoryne willisii* with gus and gfp genes. J Trop Agric 48:11–16

Wright H, van Doorn WG, Gunawardena AHLAN (2009) In vivo study of developmental programmed cell death using the lace plant (*Aponogeton madagascariensis; Aponogetonaceae*) leaf model system. Am J Bot 96:865–76. doi: 10.3732/ajb.0800343

Yakimova ET, Kapchina-Toteva VM, Laarhoven L-J, et al (2006) Involvement of ethylene and lipid signalling in cadmium-induced programmed cell death in tomato suspension cells. Plant Physiol Biochem 44:581–9. doi: 10.1016/j.plaphy.2006.09.003

Yamamoto YT, Rajbhandari N, Lin X, et al (2010) Genetic transformation of duckweed *Lemna gibba* and *Lemna minor*. In Vitro Cell Dev Biol 37:349–353. doi: 10.1079/IVP2001171

Yamauchi T, Watanabe K, Fukazawa A, et al (2014) Ethylene and reactive oxygen species are involved in root aerenchyma formation and adaptation of wheat seedlings to oxygen-deficient conditions. J Exp Bot 65:261–273. doi: 10.1093/jxb/ert371

Yang X, Srivastava R, Howell SH, Bassham DC (2016) Activation of autophagy by unfolded proteins during endoplasmic reticulum stress. Plant J 85:83–95. doi: 10.1111/tpj.13091

Yang Y-P, Hu L-F, Zheng H-F, et al (2013) Application and interpretation of current autophagy inhibitors and activators. Acta Pharmacol Sin 345:625–635. doi: 10.1038/aps.2013.5

Yoshimoto K, Hanaoka H, Sato S, et al (2004) Processing of ATG8s, ubiquitin-like proteins, and their deconjugation by ATG4s are essential for plant autophagy. Plant Cell 16:2967–2983. doi: 10.1105/tpc.104.025395

Young TE, Gallie DR (1999) Analysis of programmed cell death in wheat endosperm reveals differences in endosperm development between cereals. Plant Mol Biol 39:915–26.

Yu L, Wan F, Dutta S, et al (2006) Autophagic programmed cell death by selective catalase degradation. Proc Natl Acad Sci U S A 103:4952–7. doi: 10.1073/pnas.0511288103

Yu YB, Yang SF (1979) Auxin-induced ethylene production and its inhibition by aminoethyoxyvinylglycine and cobalt ion. Plant Physiol 64:1074–7

Zhang H, Li A, Zhang Z, et al (2016) Ethylene Response Factor TERF1, Regulated by ETHYLENE-INSENSITIVE3-like factors, functions in reactive oxygen species (ROS) scavenging in tobacco (*Nicotiana tabacum L.*). Sci Rep 6:29948. doi: 10.1038/srep29948

Zhao J, Li ZT, Cui J, et al (2013) Efficient somatic embryogenesis and Agrobacterium-mediated transformation of pothos (*Epipremnum aureum*). Plant Cell Tissue Organ Cult 114:237–247. doi: 10.1007/s11240-013-0319-x

Zhu C, Sanahuja G, Yuan D, et al (2013) Biofortification of plants with altered antioxidant content and composition: Genetic engineering strategies. Plant Biotechnol J 11:129–141. doi: 10.1111/j.1467-7652.2012.00740.x

Zhuang X, Chung KP, Cui Y, et al (2017) ATG9 regulates autophagosome progression from the endoplasmic reticulum in *Arabidopsis*. Proc Natl Acad Sci 201616299. doi: 10.1073/pnas.1616299114

Zong W-X, Thompson CB (2006) Necrotic death as a cell fate. Genes Dev 20:1–15. doi: 10.1101/gad.1376506

APPENDIX A: ONLINE RESOURCES

Online Resource 1.1. Compilation of videos from a lace plant window stage leaf. (A) There is a visible gradient of PCD, which shows various features of PCD across N-, E-, and LPCD stage cells. (B) NPCD stage cells have anthocyanin (in the mesophyll), as well as chlorophyll pigmentation, and illustrate typical cellular dynamics as they persist throughout leaf morphogenesis. (C) EPCD stage cells have lost anthocyanin pigmentation and are fated to die. As PCD advances, aggregates of organelles are collected in the central vacuole and can be seen undergoing Brownian motion. There is an increase in transvacuolar strands in this early phase of PCD. (D) LPCD stage cells that are on the brink of collapse are nearly devoid of pigmentation and have large aggregates within the vacuole. In the very late stages of PCD, there is nuclear displacement; cessation of aggregate movement, which precedes the collapse of the tonoplast, and plasma membrane shrinkage. Scale bars: 30 μm. ~25× playback speed.

Online Resource 1.2. Developmental vs. induced death in lace plant. (A) Cells in the later stages of developmental PCD (LPCD) exhibit little to no pigmentation. Aggregates undergoing Brownian motion in the central vacuole are visible. As the cell is terminated, nuclear displacement occurs, followed by the collapse of the tonoplast and the plasma membrane, leaving a condensed corpse. (B) NPCD stage cells (which do not undergo PCD during leaf development) treated with a 2 M NaCl solution, which causes a reduction in cellular volume due to plasmolysis. As the cells die, the color shifts to green, and there is swelling which occurs prior to tonoplast collapse. Finally, there is further shrinkage of the corpse which bears a resemblance to developmental PCD (A). Scale bars: (A) = 10 μm; (B) = 15 μm. ~25× and 250× playback speeds, respectively.

Online Resource 3.1. Long-term live cell imaging of lace plant window stage leaf areoles. Leaves from the control, antioxidant, 1 mM H_2O_2 and 5 mM H_2O_2 treatment groups were recorded for 12 h daily until the termination of PCD cells. The sequence shown here reveals the views of entire areoles as cell death advanced over time (T). *Bar* = 100μm.

Online Resource 3.2. Long-term live cell imaging of lace plant window stage gradients. Leaves from the control, antioxidant, 1 mM H_2O_2 and 5 mM H_2O_2 treatment groups were recorded for 12 h daily until the termination of all PCD cells. The sequence shown here reveals the progressions of cell death in window stage programmed cell death (PCD) gradient over time (T). *Bar* = 50μm.

Online Resource 4.1. Developmental programmed cell death. Control group window stage leaf displaying PCD and high magnification view of cellular collapse.

Online Resource 4.2. Live cell imaging assay. Control, 5 μM rapamycin, 1 μM concanamycin and 5 μM wortmannin treated detached window stage leaves. Scale bar = 100 μm.

Online Resource 4.3. 3D Confocal microscopy of leaves following autophagy modulation. Treatment groups include control, 5 μM rapamycin, 1 μM concanamycin and 5 μM wortmannin.

APPENDIX B: COPYRIGHT RELEASE LETTERS

B.1. COPYRIGHT RELEASE FOR CHAPTER 1

01_03

Springer

PERMISSION LETTER

January 27, 2017

Springer reference

Plant Programmed Cell Death
pp. 1-31
An Overview of Programmed Cell Death Research: From Canonical to Emerging Model Species
Authors: Adrian N. Dauphinee, Arunika N. Gunawardena
© Springer International Publishing Switzerland 2015
DOI 10.1007/978-3-319-21033-9_1
Print ISBN 978-3-319-21032-2
Online ISBN 978-3-319-21033-9

Your project

Requestor: Adrian Dauphinee
PhD Candidate
Programmed Cell Death Lab
Biology Dept. Dalhousie University
1355 Oxford Street, B3H 4R2
adrian@Dal.Ca
University: Dalhousie University
Purpose: Dissertation/Thesis

With reference to your request to reuse material in which Springer controls the copyright, our permission is granted free of charge under the following conditions:

Springer material

- represents original material which does not carry references to other sources (if material in question refers with a credit to another source, authorization from that source is required as well);
- requires full credit (Springer book/journal title, chapter/article title, volume, year of publication, page, name(s) of author(s), original copyright notice) to the publication in which the material was originally published by adding: "With permission of Springer";
- may not be altered in any manner. Abbreviations, additions, deletions and/or any other alterations shall be made only with prior written authorization of the author;
- Springer does not supply original artwork or content.

This permission

- is non-exclusive;
- is valid for one-time use only for the purpose of defending your thesis and with a maximum of 100 extra copies in paper. If the thesis is going to be published, permission needs to be reobtained.
- includes use in an electronic form, provided it is an author-created version of the thesis on his/her own website and his/her university's repository, including UMI (according to the definition on the Sherpa website: http://www.sherpa.ac.uk/romeo/);
- is subject to courtesy information to the co-author or corresponding author;
- is personal to you and may not be sublicensed, assigned, or transferred by you to any other person without Springer's written permission;
- is only valid if no personal rights, trademarks, or competitive products are infringed.

This license is valid only when the conditions noted above are met.

B.2. COPYRIGHT RELEASE FOR CHAPTER 2

NRC RESEARCH PRESS LICENSE TERMS AND CONDITIONS

Apr 06, 2017

This Agreement between Adrian N Dauphinee ("You") and NRC Research Press ("NRC Research Press") consists of your license details and the terms and conditions provided by NRC Research Press and Copyright Clearance Center.

License Number	4083111398555
License date	Apr 06, 2017
Licensed Content Publisher	NRC Research Press
Licensed Content Publication	Botany
Licensed Content Title	The involvement of ethylene in programmed cell death and climacteric-like behaviour during the remodelling of lace plant (Aponogeton madagascariensis) leaves
Licensed Content Author	A.N. Dauphinee, H. Wright, G. Rantong, et al
Licensed Content Date	Dec 1, 2012
Licensed Content Volume	90
Licensed Content Issue	12
Type of Use	Thesis/Dissertation
Requestor type	Author (original work)
Format	Print and electronic
Portion	Full article
Order reference number	
Title of your thesis / dissertation	IDENTIFICATION AND MANIPULATION OF CRITICAL PROGRAMMED CELL DEATH REGULATORS IN THE LACE PLANT
Expected completion date	May 2017
Estimated size(pages)	185
Requestor Location	Adrian N Dauphinee Dalhousie University Biology Department, Life Sciences Centre 1355 Oxford Street Halifax, NS B3H4R2 Canada Attn: Adrian N Dauphinee
Billing Type	Invoice
Billing Address	Adrian N Dauphinee Dalhousie University Biology Department, Life Sciences Centre 1355 Oxford Street Halifax, NS B3H4R2 Canada Attn: Adrian N Dauphinee
Total	0.00 CAD
Terms and Conditions	

General Terms & Conditions

B.3. COPYRIGHT RELEASE FOR CHAPTER 3

Copyright Clearance Center RightsLink®

Home | Account Info | Help

Title: Remodelling of lace plant leaves: antioxidants and ROS are key regulators of programmed cell death
Author: Adrian N. Dauphinee
Publication: Planta
Publisher: Springer
Date: Jan 1, 2017

Logged in as:
Adrian Dauphinee
Account #:
3001106966
LOGOUT

Permissions Request